Structural and Functional Characterization of the Putative Pineal ATPase PINA

A Thesis Submitted to the College of
Graduate Studies and Research
in Partial Fulfillment of the Requirements
for the Degree of Master of Science
in the Department of Biochemistry
University of Saskatchewan
Saskatoon

By

Dzmitriy Turavets

Permission to Use

In presenting this thesis/dissertation in partial fulfillment of the requirements for a Post-graduate degree from the University of Saskatchewan, I agree that the Libraries of this University may make it freely available for inspection. I further agree that permission for copying of this thesis/dissertation in any manner, in whole or in part, for scholarly purposes may be granted by the professor or professors who supervised my thesis/dissertation work or, in their absence, by the Head of the Department or the Dean of the College in which my thesis work was done. It is understood that any copying or publication or use of this thesis/dissertation or parts thereof for financial gain shall not be allowed without my written permission. It is also understood that due recognition shall be given to me and to the University of Saskatchewan in any scholarly use which may be made of any material in my thesis/dissertation.

Requests for permission to copy or to make other uses of materials in this thesis/dissertation in whole or part should be addressed to:

Head of the Department of Biochemistry

107 Wiggins Road

University of Saskatchewan

Saskatoon, Saskatchewan S7N 5E5 Canada

Abstract

Copper plays a crucial role in human metabolism as a cofactor of enzymes responsible for respiration, iron metabolism, free radical disposal, and many other functions. Copper ATPases (Cu-ATPases) are a family of enzymes facilitating copper transport in the body. ATP7B is one of them, and it belongs to a P-type class of ATPases. In 1999, an mRNA of a splice variant (PINA) has been discovered in rat pineal gland and retina. Transcription levels of the mRNA increase during the night and decrease during the day. Homologous mRNA (ATP7B.K) was also reported in humans.

The goals of this study were to confirm the expression of PINA in rat pineal gland, as well as to verify the temporal expression pattern. We also aimed to express and investigate the enzymatic activity of a recombinant putative PINA homologue from human, and compare its properties to the full-length ATP7B.

We have successfully expressed the full-length ATP7B and two putative isoforms of human PINA homologue in *K. lactis* expression system. We have established a purification procedure that enabled us to get active enzymes and study their ATPase activity. This is the first successful purification of the active full-length human ATP7B reported. The activity of the full-length protein produced according to our procedure is comparable to previously reported by other groups, who studied either the full-length protein in the membrane or its purified truncated variants. The putative PINA homologues showed much higher ATPase activity than the full-length enzyme.

We could not detect the putative PINA protein in pineal gland extracts and membrane preparations due to low sensitivity of the available antibodies. Further investigations are needed for establishing copper transport rates of the full-length ATP7B and the PINA homologues, as our new protocol for copper transport quantification needs further optimizations.

Acknowledgements

I would like to express my gratitude to my scientific adviser, Dr. Oleg Dmitriev, for guidance and support throughout the duration of the project. I would like to thank Dr. Nataliya Dolgova for her invaluable help. I would like to thank all members of Dmitriev lab for their advice and support, including but not limited to Chris O'Grady, Sergiy Nokhrin, Eva Uhlemann, Daryna Kulik, and Corey Yu. I would also like to thank my advisory committee members: Dr. Scot Leary, Dr. Miroslaw Cygler, and Dr. Scot Stone – for their advice and support. I would like to thank our collaborators and colleagues: Dr. Christopher Chang (California) for providing CS-1 fluorescent copper sensor, Dr. Hugh Goldie for help with large-scale yeast growth, Dr. George Katselis for help with mass spectrometry analysis.

Table of Contents

List of Tables

List of Figures

List of Abbreviations

BCA – bicinchoninic acid

BCS – bathocuproinedisulfonic acid

cAMP – cyclic adenosine monophosphate

CCG – clock-controlled gene

CHAPS – 3-[(3-Cholamidopropyl)dimethylammonio]-1-propanesulfonate

CHO – Chinese hamster ovary cells

COS – CV-1 (simian) origin SV-40-immortalized cells

COX – cytochrome *c* oxidase

CREB – *cis*-response element binding protein

DDM – dodecyl maltoside

DMSO – dimethyl sulfoxide

CRX – cone-rod homeobox

CV – column volume

DTT – dithiothreitol

GABA – γ-aminobutyric acid

GFP – green fluorescent protein

HEPES – 4-(2-hydroxyethyl)-1-piperazineethanesulfonic acid

HIOMT – acetylserotonin *O*-methyltransferase

HRP – horseradish peroxidase

HSP – heat shock protein

ICER – inducible cAMP early repressor

LMPG – 1-myristoyl-2-hydroxy-*sn*-glycero-3-phosphocholine (lyso-myristoyl phosphatidyl glycerol)

MBD – metal-binding domain

MES – 2-(*N*-morpholino)ethanesulfonic acid

NAT – *N*-acetyltransferase

Ni-NTA – nickel-nitriloacetic acid

NMR – nuclear maginetic resonance

ORF – open reading frame

PBS – phosphate buffered saline

PrP^C – prion protein cellular isoform

PVN – paraventricular nucleus

PINA – pineal night-specific ATPase

ROS – reactive oxygen species

SCN – suprachiasmatic nucleus (nuclei)

SDS – sodium dodecyl sulfate

SDS-PAGE – sodium dodecyl sulfate polyacrylamide gel electrophoresis

SOD – Superoxide dismutase

TCEP – tris(2-carboxyethyl)phosphine

TGN – *trans*-Golgi network

TM – transmembrane helix

UTR – untranslated region

1. Introduction

Copper plays a crucial role in human metabolism. It is involved in many crucial processes, such as cell growth, angiogenesis, oxidation stress protection, and tumour growth. It works primarily as a cofactor of various enzymes, providing many physiological functions, such as respiration, iron metabolism, free radical disposal, and connective tissue formation (Festa and Thiele, 2011).

A number of proteins is responsible for maintaining copper homoeostasis. Copper ATPases (Cu-ATPases) are a family of enzymes facilitating copper transport. They are membrane proteins that transport copper from cytosol to secretory pathways and enzymes (Steveson *et al.*, 2003; Guo *et al.*, 2005).

One of two known copper ATPases in human body, ATP7B, plays the major role in copper regulation in the liver, where it is responsible for excretion of excess copper from the body into the bile (Linder *et al.*, 1998). Another major function of the enzyme in all tissues where it's present is incorporation of copper into certain enzymes, such as superoxide dismutase (SOD) (Culotta *et al.*, 2006), as well as into ferroxidase ceruloplasmin (Punter and Glerum, 2003; Prohazka and Gybina, 2004; Barnes *et al.*, 2005; Horng *et al.*, 2008).

The genetic deficiency in ATP7B leads to a condition known as Wilson's disease. It is characterized by an excessive accumulation of copper in the tissues, especially in the liver and the brain. It manifests in liver malfunction and neurological symptoms, and is fatal if untreated.

Several alternative splicing variants of the *ATP7B* gene are known (Bull *et al.*, 1993; Petrukhin *et al.*, 1994; Borjigin *et al.*, 1999; "AceView", 2015; "Entrez", 2015), with PINA (Pineal Night-Specific ATPase) seeming the most interesting in terms of its structure and functions. It is expressed primarily in the pineal gland (hence its name) and in the retina. The expression has a strong diurnal dependence both in the retina and in the pineal, with a 100-fold increase in transcription levels during the night compared to daytime (Borjigin *et al.*, 1999). Structurally, PINA is peculiar: it misses a significant part of the N-terminus in comparison with ATP7B, but it retains

elements of structure essential for copper transport. An mRNA of putative human homologue of PINA, ATP7B.K has also been reported (Totoki *et al*., 2005).

We propose that PINA represents a novel splice variant of P-type ATPases with yet unknown function and novel catalytic mechanism, which is involved in circadian regulation of copper metabolism.

Because copper is involved in many important processes, understanding the properties of PINA protein could shed light on interaction between circadian rhythms and biochemical processes in the organism. Recent research has shown that disruption of circadian rhythms caused by technological development of modern civilization (for example, ability to have light 24 hours a day, jet-lags, shift work, etc.) leads to development of many serious disorders, from constant fatigue to diabetes and cancer. Currently mechanisms of circadian rhythm regulations and their interaction with functions of other organs and processes in the organisms are not very well understood.

In this study, we aimed to confirm presence of the protein product of PINA mRNA in rat pineal gland and check whether or not protein expression also shows circadian rhythm dependence, as well as to express, purify and characterize enzymatic activity of putative human homologue of PINA in comparison with ATP7B.

2. Background Information

2.1. Heavy Metals and Copper Homoeostasis

Heavy metals are those metals and metalloids which have a relatively high density and are toxic at low concentrations (Srivastava and Goyal, 2010). Among these are chromium, cobalt, nickel, copper, zinc, arsenic, mercury, lead, platinum group of elements, and other metals and metalloids.

Despite being toxic, many of these elements play important biological functions. Zinc, for example, is a very important trace element for humans and animals, plants and microorganisms (Stipanuk, 2006; Nakashima and Dyck, 2009). The major role of cobalt is in vitamin B12 (cobalamin). Arsenic is a highly toxic metalloid. Nevertheless, it has been shown to have an unknown essential role in metabolism of higher animals (Uthus, 1992). Some bacteria are capable of oxidation of arsenic compounds to produce energy (Mukhopadhyay *et al.*, 2002). Cadmium is renowned for its environmental toxicity; however, it was recently shown to play a biological function in carbonic anhydrase in some marine diatoms (Lane *et al.*, 2005). Copper also follows the pattern, being both beneficial and harmful, depending on the amounts.

Copper is 26th most abundant element in the Earth crust. Only small part of that copper is present in soils in form available to living organisms. In fact, it's the observations on poor plant growth and animals' health issues in regions with low soil copper content that led to understanding of an importance of copper for living organisms (Linder, 2013).

Copper is very important for energy metabolism, being a cofactor in cytochrome *c* oxidase, an enzyme common for all aerobic organisms. It also plays an important role in connective tissue, where extracellular cuproenzyme lysyl oxidase cross-links elastin and collagen. Other roles include reactive oxygen species (ROS) detoxification (superoxide dismutase, SOD), production of melanin (tyrosinase), nerve functions and metabolism (dopamine β-hydroxylase). Ceruloplasmin, a ferroxidase, also relies on copper for its functions (Linder, 2013).

The ability of copper to shift between two oxidation states – Cu^{+} and Cu^{2+} – allows it to facilitate redox reactions by the enzymes. The same ability is also a reason for copper toxicity:

redox conversion of copper in tissues and cells starts free radicals chains following Fenton and Harber-Weiss mechanism in aerobic conditions:

$$O_2^{\bullet-} + Cu^{2+} \rightarrow O_2 + Cu^{+}$$

$$Cu^{+} + H_2O_2 \rightarrow Cu^{2+} + HO^{\bullet} + OH^{-}$$

$$Cu^{2+} + H_2O_2 \rightarrow Cu^{+} + HOO^{\bullet} + H^{+}$$

Hydroxyl and hydroxyperoxyl radicals are very powerful oxidants, and are capable of causing a lot of damage to proteins, lipids and DNA, ultimately leading to cell death. For this reason, copper is not present in the cell as a free ion. It is usually bound to copper chaperons and small molecules. Another way of exhibiting toxicity for copper is by acting as a high affinity ligand for methionine, cysteine and histidine residues in proteins, which leads to displacement of other metal ions from active sites and to protein misfolding (Banci *et al.*, 2010).

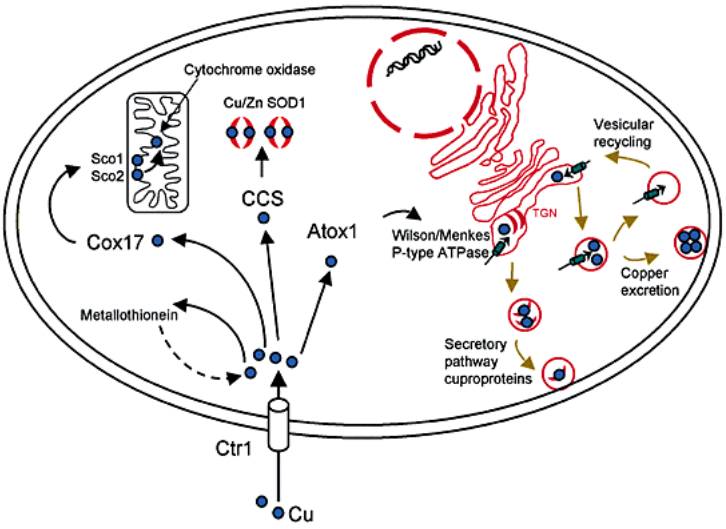

Figure 2.1: A scheme of copper transport in a mammalian cell. Reprinted by permission from Macmillan Publishers: Nature (Bartnikas and Gitlin, 2001), copyright 2001.

Copper transport in the cell is regulated by a network of copper-transporting proteins (Fig. 2.1). Copper uptake by the cell is facilitated by CTR1, a copper importer located in the plasma membrane. Cellular localization of the importer depends on the extracellular copper content: CTR1

is internalized to prevent excessive copper uptake when there's too much copper in the extracellular space, while low levels of copper lead to redistribution of the importer back to the plasma membrane (Molloy and Kaplan, 2009). Requirements of the cell itself also play a role: an increased demand for copper intake or release up- or downregulates the protein, as well as rearranges its localization.

When copper is inside the cell, it is taken from CTR1 by copper chaperones, like ATOX1 (7.4 kDa protein which delivers copper to *trans*-Golgi network, TGN) and CCS (54 kDa cytosolic protein which delivers copper to Cu,Zn-SOD). There are probably other unknown intermediate carriers, which aid delivery of copper to mitochondria.

ATOX1 is a small cytosolic protein which binds Cu^{+} ion with 1:1 stoichiometry. Its first discovered role was protection of cells from oxidative stress, hence the name, Antioxidant protein 1. Later it was discovered that it plays an essential role in copper trafficking in a cell, in particular, shuttling of copper to TGN to ATP7A and ATP7B copper ATPases, which then facilitate copper integration into cuproenzymes or copper excretion from the cell (Lutsenko *et al.*, 2007). Another recently discovered role of ATOX1 is a copper-dependent cyclin D1 transcription activator, playing a role in cell proliferation (Itoh *et al.*, 2008).

Copper ATPases ATP7A and ATP7B which receive copper from ATOX1 are generally localised in TGN or plasma membrane. ATP7B protein is co-expressed in many tissues together with ATP7A; however these two proteins seem to have different roles and regulation (Lutsenko *et al.*, 2007). For example, in choroid plexus cells ATP7B performs removal of excess copper from brain tissue to blood, while ATP7A pumps copper from circulation to the brain cells and cerebrospinal fluid (Nevitt *et al.*, 2012).

ATP7A plays an essential role in copper uptake in the intestine, pumping copper across the basolateral membrane of intestinal epithelial cells to the peripheral blood flow, and in the brain across the blood brain barrier (Nevitt *et al.*, 2012). In other tissues, for example in kidneys, it removes excess copper from the cells and supplies certain enzymes with copper, namely, peptidyl-α-monooxygenase, tyrosinase, and lysyl oxidase (Lutsenko *et al.*, 2008). The gene encoding

ATP7A is located on the X chromosome. The defects in *ATP7A* result in Menkes disease, a fatal copper uptake disorder, which leads to death at a very young age (Menkes *et al.*, 1962).

ATP7B is a sole copper ATPase in the liver, where it plays both biosynthetic and export roles (Tanzi *et al.*, 1993). Its major role is loading of cuproenzymes (for example, apo-ceruloplasmin) with copper ions in trans-Golgi network. It also secretes copper to blood plasma and excretes it into the bile. Its gene is located on the chromosome 13, and several splice variants are known ("AceView", 2015; "Entrez", 2015). Deficiency in this protein leads to Wilson's disease with symptoms of copper overloading, which manifests in very high copper content mostly in liver and brain. This, if untreated, leads to liver failure and severe neurological disorders.

Storage of copper is carried out mostly by metallothioneins (MTs) – small cysteine rich polypeptides, which can bind up to 12 copper ions, sequestering them from cytoplasm (Nevitt *et al.*, 2012). Metallothioneins are rapidly induced in a response to elevation of level of metals (such as copper, but also other heavy metals). Not only these proteins provide protection against deleterious effects of excess heavy metals, but they can also serve as a depot for copper and release it in conditions of copper deficit (Ogra *et al.*, 2006).

Another labile pool of copper in the cell is represented by small molecules, such as glutathione (Nevitt *et al.*, 2012). Experimental depletion of GSH levels in liver showed a disruption in normal copper metabolism (Ogra *et al.*, 2010). This disruption could result from several concurrent effects, for example, decrease of copper bioavailability due to oxidative environment, or inhibition of ATP7A/B pumps by low GSH levels. GSH was found to be capable of loading SOD1 directly (Nevitt *et al*., 2012), so another reason for the disruption could be the lack of direct loading of the ATPase pumps. This complex regulation system ensures copper balance in the cell.

2.2. ATP7B as a Member of P-Type ATPase Family

Copper-transporting ATPases belong to a P-type family of ATPases. P-type ATPases comprise a vast and ubiquitous family of membrane-localized enzymes that are involved in transport of ions and lipids.

Table 2.1: Classification of P-type ATPases

Class	**Substrate**	**Features, functions and examples**
I A	K^+	Bacterial KdpB is a part of a larger K^+-transporting complex, functions as ATPase only (Kühlbrandt, 2004)
I B	Soft Lewis acids: Cu^+, Ag^+, Cu^{2+}, Zn^{2+}, Cd^{2+}, Pb^{2+}, and Co^{2+}	Provide metalloenzymes with the metal cofactors, excrete toxic metals (Nucifora *et al.*, 1989; Rensing *et at*, 1999). Single polypeptide. Members of the class: ATP7A, ATP7B, CopA, ZntA, and others. Possess metal-binding domains.
II A	Ca^{2+}	Prokaryotic (Deves and Brodie, 1989) and eukaryotic Ca^{2+}-transporters. Regulated by phospholamban and sarcolipin (Asahi *et al.*, 2003). SERCA is the best-studied P-type ATPase with solved crystal structure (Palmgren and Nissen, 2011).
II B	Ca^{2+}, Mn^{2+}	Eukaryotic plasma membrane Ca^{2+}-transporters (Brini and Carafoli, 2009) or Mn^{2+}-transporters in Golgi (Mandal *et al.*, 2003). Regulated by calmodulin (Scharff and Foder, 1978).
II C	Na^+/K^+, H^+/K^+	Na/K-ATPase is responsible for maintaining membrane potential, H/K-ATPase acidifies gastric lumen. These proteins usually have at least one supporting subunit, which can prevent pumping ions in reverse (Abe *et al.*, 2009).
II D	Unknown	Unknown, found in fungi.
IIIA	H^+	Found in plants and fungi, where they help to maintain membrane potential (Kühlbrandt, 2004)
IIIB	Mg^{2+}	Found in bacteria, closely related to IIIA (Kühlbrandt, 2004)
IV	Phospholipids	Maintain lipid bilayer asymmetry by flipping lipid molecules from one side of the bilayer to another. The second proposed function of these enzymes is initiation of budding of membrane vesicles.
V A	Unknown, putatively phospolipids	Orphan transporters that have P-type ATPase signatures, otherwise uncharacterised (Sørensen *et al.*, 2010)
V B	Unknown	

These intricate molecular machines perform a variety of roles, which are very important for metabolism: they mediate cellular signalling, build electrochemical gradients, initiate vesicle

budding, detoxify cellular environment, load metalloenzymes with metal ions, and regulate membrane composition. P-type ATPases can be found in all living organisms.

The classification of P-type ATPases is based on conserved core sequences found among all members of the family (Axelsen and Palmgren, 1998). They are divided into five major subfamilies, which are further subdivided into several classes (Table 2.1).

ATP7B together with other heavy metal pumps belongs to a P_{IB} class of ATPases. It's a single polypeptide (157 kDa) with a complex domain structure (Fig. 2.2). The core structure is similar to all other P-type ATPases and consists of the soluble A, P, N domains, and the transmembrane S and T domains. The ATPase activity is performed by the soluble domains. The movements caused by ATP hydrolysis induce conformation changes in the transmembrane domains, thus coupling the hydrolysis to translocation of ions.

No crystal structure of ATP7B has been solved to date. The best available model is a homology model of ATP7B created recently (Schushan *et al.*, 2012).

Homology modelling is based on the assumption that the secondary structure elements are more conserved than the primary amino acid sequence. The method of homology modelling uses known 3D-structures of homologous proteins which are used as templates for alignment. A model is built after aligning the sequences, and is assessed for geometrical validity (Nugent and Jones, 2009).

The quality of a model depends on compatibility of a template and sequence similarity. With the sequence similarity above 30% modelled membrane proteins were showed to deviate not more than 2 Å from the native structure (Forrest *et al.*, 2006). X-ray structures of several members of the family have been successfully solved, including CopA from *A. fulgidus* and *L. pneumonia*, as well as individual domains of various P-type ATPases (Toyoshima *et al.*, 2000; Pedersen *et al.*, 2007; Hakansson, 2009; Tsuda and Toyoshima, 2009; Gourdon *et al.*, 2011; Wu *et al.*, 2011; and others). The similarity of ATP7B sequence and CopA from *L. pneumonia* is around 35%, which gives quite a reliable model.

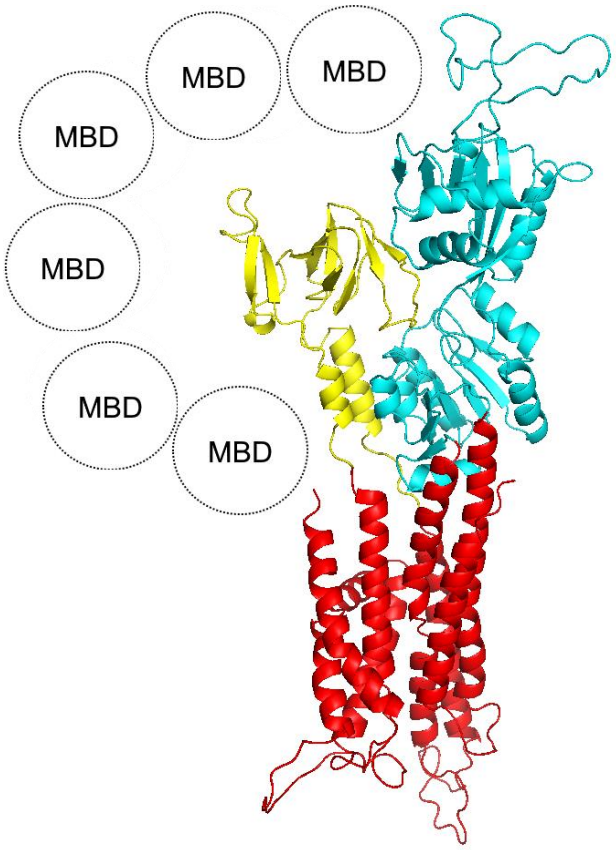

Figure 2.2: Homology model of ATP7B. Yellow – A-domain, cyan – ATP-binding domain (P- and N-domains), Red – transmembrane domain (S- and T-domains). MBDs are denoted as dotted circles for illustrative purposes (from Schushan *et al.*, 2012, with modifications)

The P-domain and the N-domain are a part of a single cytosolic loop (ATP-binding loop or domain, ATP-BD). The P-domain contains a β-sheet surrounded by three α-helices (Dmitriev *et al.*, 2006). The invariant Asp residue in the P-domain (in conserved DKTG sequence) undergoes transient phosphorylation by a phosphate from ATP molecule during the catalytic cycle. Conserved sequences TGDN and GDG play role in Mg^{2+} coordination. Overall, P-domain shows higher degree of conservation among different P-type ATPases, and shows homology with haloacid dehalogenase superfamily (Aravind *et al.*, 1998).

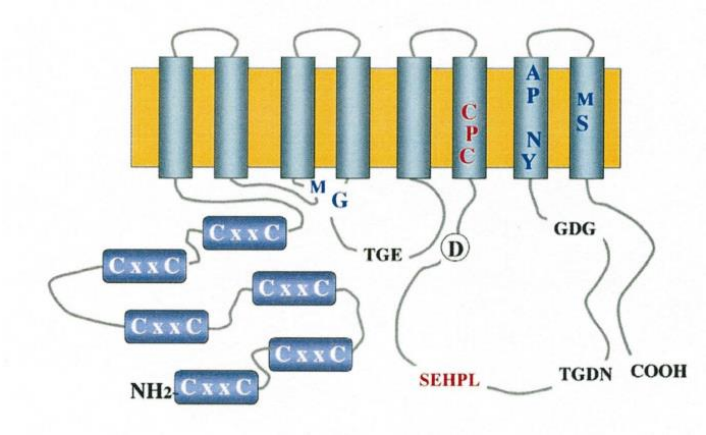

Figure 2.3: Molecular architecture of WNDP. (A) The predicted transmembrane organization of WNDP. The cylinders in the N-terminal portion with the CxxC motif represent the cytosolic copper-binding sites. TGE, TGDN, and GDG are the sequence motifs conserved in all P-type ATPases. D in a circle is an invariant Asp residue in the DKTG sequence motif that is phosphorylated during ATP hydrolysis. CPC and SEHPL are the sequence motifs characteristic of the P1-type ATPases. Other letters mark location of the amino-acid residues highly conserved in the copper-transporting ATPases. (from Lutsenko *et al.*, 2002). Reprinted with permission of Springer.

The N-domain binds the ATP molecule and phosphorylates the P-domain. It has considerable sequence variability inside the family, but the core is conserved (Kühlbrandt, 2004). The N-domain of P_{IB}-ATPases has a stronger similarity with that of P_{IA}-ATPase KdpB (Dmitriev *et al.*, 2006). The conserved SEHPL is involved in nucleotide binding. The mutation of the histidine residue impairs binding of ATP and as a result the catalytic function of the enzyme (Tsvikovskii *et al.*, 2003). This domain is the least conserved among copper ATPases between different phyla. In comparison with bacterial copper ATPases, the eukaryotic enzymes have an insert between β-strands 3 and 4, which is longer in more evolutionarily advanced species, i.e. it's very short in yeast, longer in plants and lower vertebrates, and the longest in mammals. This sequence is not involved in ATP binding, and is proposed to have a regulatory role (Gupta and Lutsenko, 2011).

The A-domain of ATP7B exhibits a protein phosphatase activity. It has been found (Xu *et al.*, 2002) to come into a close contact with the phosphorylation site in the P-domain. The main role in this process belongs to the TGE conserved sequence, which is involved in hydrolysis of the aspartate-P_i bond in the P-domain's DKTG motif: the glutamate residue orients a water molecule in a position suitable for the hydrolysis and release of the phosphate. The A-domain is attached to the membrane component of the enzyme via flexible linkers to TM2 and TM3 helices. It has been

shown that proteolytic cleavage of these linkers renders the enzyme inactive, because it breaks conformational inter-domain communications necessary to go through the stages of the catalytic cycle, at least as observed in SERCA (Møller *et al.*, 2002; Lenoir *et al.*, 2004). The movement of helices connected to the A-domain opens and closes the gate for ion translocation pathway (Kühlbrandt, 2004). The rotation of the domain also influences the rate of the enzyme turnover by controlling the rate of protein dephosphorylation (Argüello *et al.*, 2007). The A-domain of P_{IB}-type ATPases is structurally different from A-domains of P_{II}-type and P_{III}-ATPases: it is smaller and does not have a separate N-terminal subdomain formed by a preceding cytosolic loop.

The transmembrane part of the enzyme consists of eight helices. The first two belong to the more rigid S-domain, and the rest – to the more flexible T-domain (Palmgren and Nissen, 2011). Of these, the last three contain the sequences that appear to be essential for copper translocation (Fig. 2.3 and Fig. 2.4, C). The CPC motif is located in the transmembrane helix 6 (TM4). This motif is conserved in all ATPases which are involved in transition metal transport (Bissig *et al.*, 2001). The M5 contains YN residues which are conserved among all ATPases known or predicted to transport copper (Lutsenko *et al.*, 2002), and the M6 contains a conserved MxxSS fragment. The second transmembrane helix (TMB), which belongs to the S-domain, has an almost perpendicular kink, which results in part of the TMB lying on the interface of the membrane and the cytosol (Sitsel *et al.*, 2015).

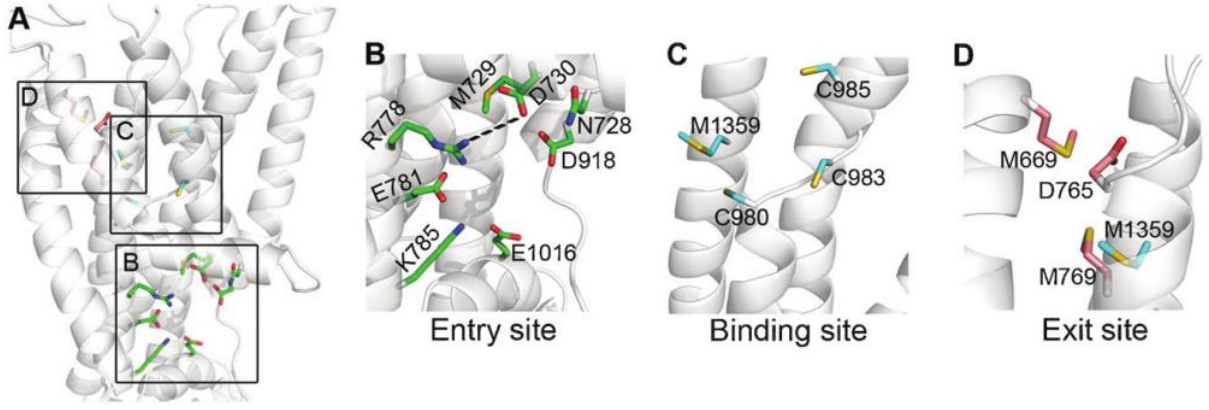

Figure 2.4: Putative copper translocation channel in ATP7B (from Schushan *et al.*, 2012). Reprinted by permission of Royal Society of Chemistry.

The homology model, as well as previous knowledge of P-type ATPase structure and function based on crystal structures of SERCA and Na/K-ATPase, helps to get an insight on copper translocation channel through the transmembrane domain. The putative entry site for Cu^+ ions is located near the kinked TMB segment, and is putatively formed by residues in TM1 (N728, M729, D730), TM2 (R778, E781, K785), TM3 (D918), and behind TM4 (E1016). The importance of these residues has been established by analyzing ATP7B from Wilson's disease patients and by comparing them with CopA. M729, E781, and D918 are conserved and are suggested as the most important in copper uptake by enzyme. Other residues were shown to be otherwise clinically important in ATP7B (Fig. 2.4, B) (Schushan *et al*., 2012).

The ion-binding site is located further inside the transmembrane domain, and is formed by residues located in TM4 (C980, C983, C985) and TM6 (M1359). C983 and C985 belong to the conserved CPC motif, and are essential for copper transport (Forbes and Cox, 1998). The two cysteines of the motif and the methionine form a trigonal coordination plane for a single Cu^+ ion. The YN motif in TM5 (Y1331, N1332) and MS in TM6 (M1359 and S1369) is also conserved between CopA and ATP7B, as well as other Cu^+-ATPases (Schushan *et al.*, 2012). Another model, based on *Archaeoglobus fulgidus* CopA studies, proposed that these residues are needed to form another trigonal planar copper binding site. The same analysis suggested that CopA transports two copper ions per one ATP molecule hydrolysed (González-Guerrero *et al.*, 2008). Transport of counter-ions is not known for Cu^+-ATPases, although it's a usual feature of other P-type ATPases, such as Na/K-ATPase and SERCA (counter-ion: H^+).

The exit site exhibits a lesser degree of conservation between CopA and ATP7B. In ATP7B, the site is comprised of residues in TMA (M669), TM2 (D765, M769), and M1359, which can also be putatively involved in formation of the second internal binding site for a copper ion. Clinically important mutations in the first three mentioned residues reduce the rate of turnover of the enzyme (Schushan *et al.*, 2012).

A distinctive feature of ATP7B, as of other P_{IB}-ATPases, is its N-terminal region, which consists of six metal binding domains (MDB1-6) which have a ferredoxin-like fold and one CXXC

metal binding motif per domain (Arnesano *et al.*,2002). The N-terminus of copper ATPases appears to have mainly regulatory functions. The first 63 amino acids of the N-terminus, which are not involved in copper binding, are important for trafficking of ATP7B to the apical membrane of polarised cells in high copper concentration (Guo *et al.*, 2005). Trafficking is also regulated by phosphorylation at several sites in the N-terminus (Vanderwerf et al., 2001). Not only phosphorylation, but also interactions between the individual MBDs of the N-terminus can induce intracellular trafficking of human ATP7B (Huang *et al.*, 2014).

MBDs can also regulate enzyme activity. It has been shown that MBDs can regulate the rate of the enzyme by interacting with the A-domain and N-domain (Tsvikovskii *et al.*, 2001; Huster and Lutsenko, 2003). The metal-binding domains in P_{IB}-ATPases are not needed for metal transport itself. Recent studies demonstrate that P_{IB}-ATPases are capable of heavy metal transport even in absence of the MBDs (Baekgaard et al., 2010; González-Guerrero and Argüello, 2008). Furthermore, it is the core of the enzyme and not MBDs that determines ion specificity of the pump (Fatemi and Sarkar, 2002). Usual number of MBDs in organisms that sit low on the evolutionary ladder – bacteria and lower eukaryotes – is two. P_{IB}-ATPases of evolutionarily higher organisms usually have more MBDs, up to six in human ATP7A and ATP7B (Gupta and Lutsenko, 2012).

The initial ideas on the function of MBDs and N-terminus regarded them as necessary for copper translocation by accepting copper from chaperones and transporting it downstream to the transmembrane domain. However, more recent evidence shows that copper chaperones, such as CopZ in bacteria or ATOX1 in mammals, are capable of delivering Cu^+ ions to the MBDs and the protein core alike, and a separate copper-loaded MBD cannot transfer ions to the core (González-Guerrero and Argüello, 2008; Fu *et al.*, 2013). The deletion of MBDs from *A. fulgidus* CopA showed to have little or no effect on ATPase activity of the enzyme in the presence of Cu^+ (González-Guerrero and Argüello, 2008). Interestingly, it has been reported, that in *E. coli* at least one metal-binding domain is needed for copper resistance *in vivo* (Fan *et al.*, 2002), but CopA from *E. coli* preserves its activity even in the absence of all domains *in vitro* (Drees *et al.*, 2015). In ATP7A, tested in enriched Golgi fraction from CHO cells, mutation of all copper-binding CXXC motifs did not alter the activity of the enzyme (Voskoboinik *et al.*, 1999). A different experiment, however,

showed that at least one copper-binding motif in either MBD5 or MBD6 of ATP7B is needed for proper functioning of the enzyme (Huster and Lutsenko, 2003).

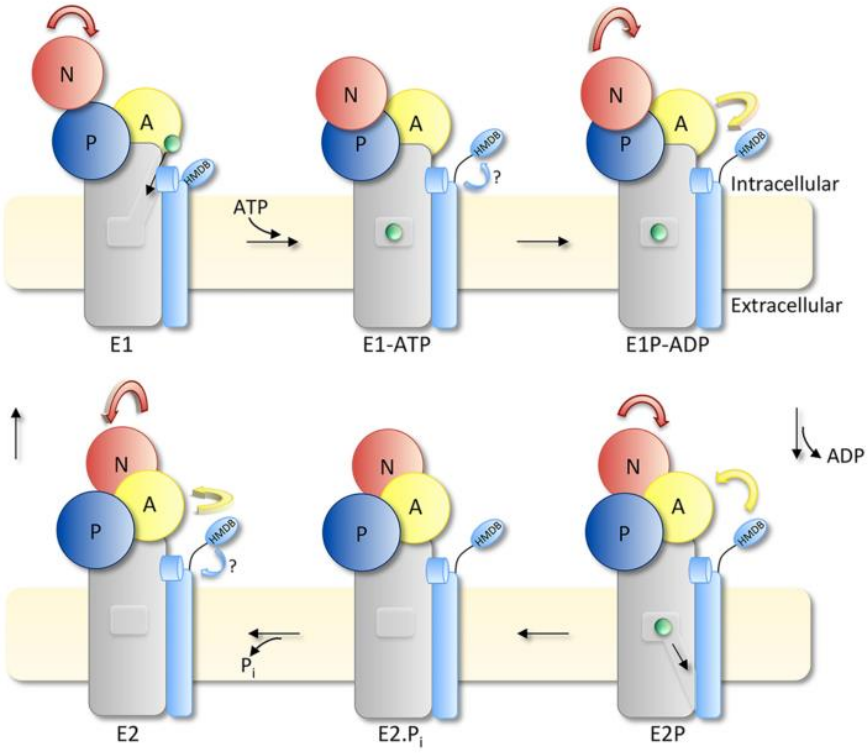

Figure 2.5: Scheme of the catalytic cycle of P_{IB}-type ATPases. Green - copper ion, light blue - S-domain, grey - T-domain. Domain movements are indicated by coloured arrows. Reprinted with permission from Sitsel *et al*., 2015. Copyright (2015) American Chemical Society.

Another distinctive feature of ATP7B is its long C-terminal tail, which resides on the cytoplasmic side together with all other soluble domains, and is 80 amino acids long. In the C-terminus, there are three conserved Leu residues. In ATP7A there're two Leu residues which are known to play role in its trafficking (Petris *et al.*, 1998). No structural data is available for this region.

The catalytic mechanism of ATP7B, as of all P-type ATPases, is described by Post-Albers cycle (Albers *et al.*, 1963; Post and Sen, 1965). The scheme originally described a mechanism of Na/K-ATPase, and defined two distinctive states: E1 (inward-open, high affinity for exported ions) and E2 (outward-open, high affinity for imported ions) (Jardetsky, 1966). Currently, more distinct conformational states, which drive ATP hydrolysis and substrate translocation, are defined (Kühlbrandt, 2004; see Fig. 2.5).

In E1 state the protein is inward-open, and the ion-binding site has high affinity for copper ions. Ion binding induces conformational changes which promote binding of ATP to the N-domain (E1-ATP). This transition occludes the ion binding site, and the P-domain gets phosphorylated at the invariant Asp residue in the DKTG motif (E1P-ADP), while β-γ phosphate bond of the ATP is broken, and the ADP is released. The protein undergoes a large conformational change, turning outward-open, the affinity for the exported ion decreases, and the ion gets released. The release of the ion leads to the binding site occlusion and phosphate release from the protein, which leads to transition to E2 state, which then transitions to E1 state (Bublitz *et al.*, 2010; Sitsel *et al.*, 2015). This mechanism is common for all P-type ATPases, with the exception that many of them also transport a counter-ion in an opposite direction.

The complete *ATP7B* gene sequence was determined in 1994. It is a large gene with a size of approximately 80 kb; it has 21 exons 77 to 1234 bp in length (Fig. 2.6) with the start codon for the initiating Met situated within exon 1 (Petrukhin *et al.*, 1994).

Figure 2.6: Genetic map of ATP7B gene. Rectangles represent exons, while jagged lines represent introns, number of supporting reads/accessions indicated (from "AceView", 2015)

Several alternative splicing variants of the gene are known (Bull *et al.*, 1993; Petrukhin *et al.*, 1994; Borjigin *et al.*, 1999, see "AceView", 2015). It was found that the alternative splicing of the ATP7B gene can be tissue-specific, and might be a form of gene regulation. Some cDNAs obtained from brain tissue were shown to sometimes exclude regions of the protein which are crucial for its functionality, for example, ATP-binding motif. Thus, some of alternative splicing events seem to play regulatory role, by decreasing quantities of an active enzyme. However, it cannot be excluded that some of splicing events produce functional variants of ATP7B with different properties than the normal protein, for example missing exons 6-7-8 in some brain-derived cDNA clones which encode for an N-terminal segment of the M-domain (Petrukhin *et al.*, 1994).

PINA (Pineal Night-Specific ATPase) is an interesting splice variant in terms of its structure and functions. It is expressed primarily in the pineal gland (hence its name) and in the retina.

The expression has a strong diurnal dependence both in the retina and in the pineal, with a 100-fold increase in transcription levels during the night compared to daytime (Borjigin *et al.*, 1999).

Interestingly, as PINA represents essentially a C-terminal half of ATP7B, it lacks all the cytosolic metal binding sites present in the intact protein, and TMA-TM2 helices. However, it retains the CPC motif which is thought to be essential for heavy metal transport (Solioz and Vulpe, 1996), and it shows at least some copper transport activity in yeasts (Borjigin *et al.*, 1999).

2.3. Circadian Rhythms in Metabolism

My research focuses on PINA, which is putatively diurnally regulated. It means, it is most probably involved in circadian metabolism. Circadian rhythm is a biological process that exhibit an endogenous entrainable oscillation which corresponds to day-night cycle. Circadian rhythms can be observed in organisms in all kingdoms of life.

The rhythms are regulated by circadian clocks – internal biochemical oscillators, which keep running independently with a cycle of approximately 24 hours and can adjust in accordance to inputs from external stimuli, such as daily changes in amount of light. It is a marvellous invention of the evolution which gave a significant advantage to living organisms by making them anticipate diurnal changes in the environment and hence helping them use all possible physical and social resources (Maronde and Stehle, 2007).

Many biological processes follow circadian rhythms. The most significant physiological landmarks of the circadian cycle in mammals are melatonin levels, core body temperature (Benloucif *et al.*, 2005) and cortisol levels in blood plasma. Other changes include heart rate, oxidative stress, cell metabolism, immune and inflammatory responses, epigenetic modification, hypoxia/hyperoxia response pathways, endoplasmic reticular stress, autophagy, and regulation of the stem cell environment (NHLBI, 2014).

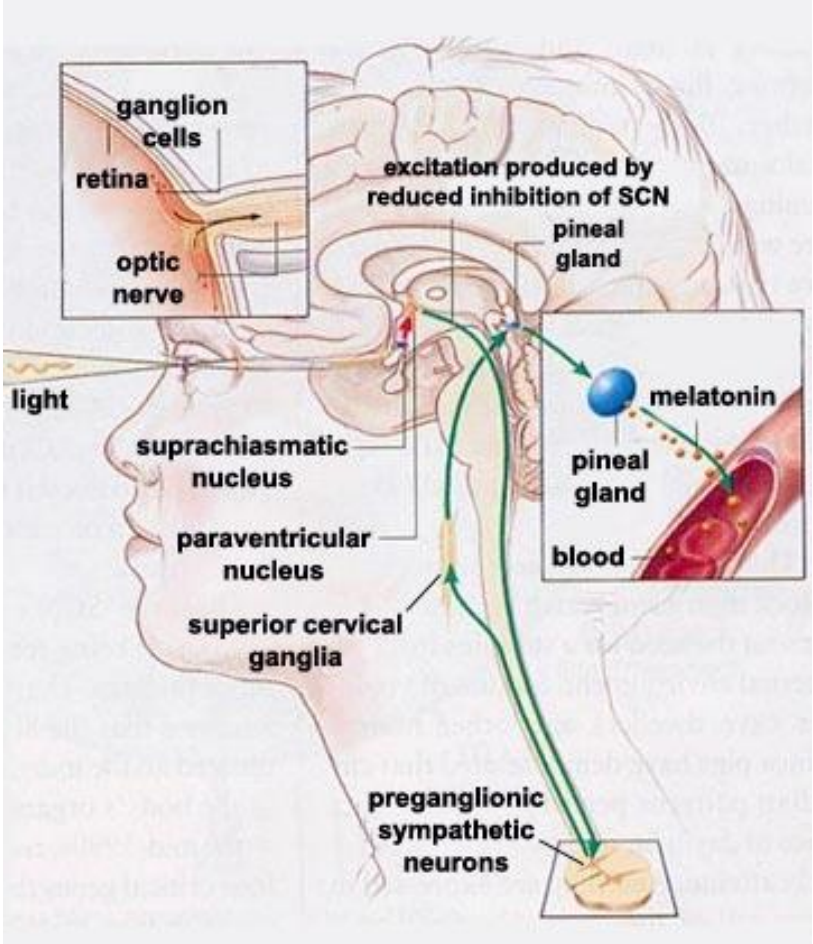

Figure 2.7: Human photoneuroendocrine system. Light information reaches suprachiasmatic nucleus (violet), which inhibits (red arrow) the paraventricular nucleus (yellow) during day time. Green arrows represent night time neuronal activity: the axons of the uninhibited paraventricular nucleus send signals to the preganglionic sympathetic neurons, which then transmit the signal to the superior cervical ganglia (light yellow), and the axons of the neurons of the latter innervate the pineal gland, which produces melatonin and releases it into blood (from "The Brain from Top to Bottom", 2015)

Interestingly, the photodetection that ultimately influences the internal clock is not connected with visual perception: experiments show that even in transgenic rats which lack any functional cones and rods in their retinas the light-dependent circadian entrainment and melatonin synthesis still occurs (Freedman, 1999; Lucas *et al.*, 1999). It was found (Sekaran *et al.*, 2003) that retina contains a population of light-sensing neurons that transmit the information on light conditions – in particular wavelength of 480 nm – downstream to the "master clock". The "master clock"

which coordinates the cycle resides in the suprachiasmatic nuclei (SCN) – a part of the brain located in the anterior hypothalamus (Ralph *et al.*, 1990). Information on light conditions reaches the suprachiasmatic nuclei via the retinohypothalamic tract coming from the retina (Fig. 2.7).

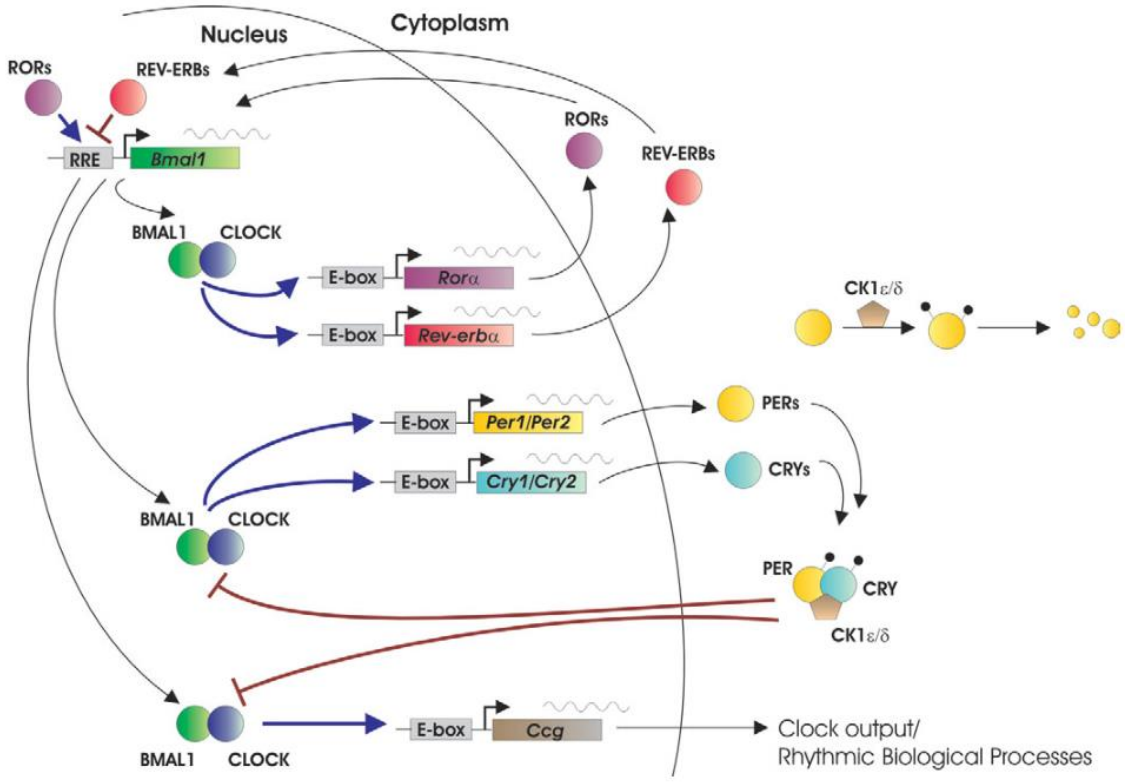

Figure 2.8: Mammalian circadian master clock components. Activating effects are represented with blue arrows, inhibition is represented by maroon barred lines. Ccg – clock controlled genes. Casein kinase 1δ (CK1δ) and casein kinase 1ε (CK1ε) are important factors that regulate core clock proteins turnover (from Ko and Takahashi, 2006). Reprinted by permission of Oxford University Press.

Suprachiasmatic nuclei send innervation to various parts of the brain; one of these pathways leads to the paraventricular nucleus (PVN), which, in turn, sends innervation to the pineal gland, a major component of circadian machinery. The suprachiasmatic nuclei receive environmental light information from eyes and then inhibit the paraventricular nucleus by GABA release. Inhibition of the paraventricular nucleus results in decreased noradrenergic output of the superior cervical ganglia to the pineal gland, which leads to downregulation of *N*-acetyltransferase (NAT), a crucial enzyme for melatonin synthesis (Kalsbeek *et al.*, 1999).

Interestingly, although all these structures lie in close proximity in the brain, the nervous path from the paraventricular nucleus to the pineal gland is somewhat convoluted: it goes down to the spinal cord to the preganglion sympathetic neurons, and then back up to the superior cervical ganglia, and the neurons of the latter finally innervate the pineal gland (Fig. 2.7).

Molecular mechanism of the circadian clock, in particular, the regulation of "master clock" genes is known. The master clock itself self-regulates in a ~24 hour fashion via a network of feed-back loops. The cells of the suprachiasmatic nuclei have a cell autonomous system of timekeeping, which consists of several genes and their products: CLOCK, BMAL1, PER and CRY (Fig. 2.8). CLOCK and BMAL1 comprise the positive component of the feedback loop and induce *Period* and *Cryptochrome* genes (Gekakis *et al.*, 1998). They upregulate PER:CRY and REV-ERBα, which act as negative component of the feedback loop and suppress CLOCK:BMAL1 (Kume et al., 1999; Okamura et al., 1999; Guillaumond *et al.*, 2005). CLOCK:BMAL1 also serves as an effector for clock-dependent genes. Examples of clock dependent (cyclically regulated) genes include *Mug2* (a protease inhibitor), *Ccr4* (chemokine receptor 4); *Dtx4* (a Notch pathway E3 ubiquitin ligase), *Atp4a* (α-subunit of gastric H/K-ATPase), and many others (Storch *et al.*, 2002; Zhang *et al.*, 2014). In fact, it was found that at least 43% of all mouse gene-coding mRNAs exhibited diurnal variability (Zhang *et al.*, 2014). Such large-scale cyclical changes are also known in plants and unicellular organisms (Liu *et al.*, 1995; Michael and McClung, 2003). So, not only the core clock components depend on circadian rhythm, but also other clock-controlled genes (CCGs). This indicates the high importance of cyclic regulation in proper functioning of a multicellular organism. Importantly, the "master clock" is responsible for cyclical signalling from SCN to PVN, which in turn controls the pineal gland function.

2.4. Pineal Gland and Melatonin

Pineal gland, or epiphysis, is a small neuroendocrine structure in vertebrate brain, which plays one of central roles in circadian system. Evolutionarily, it appeared along with lateral eyes, which became sensors for visual information, and took the role of sensing the changes of light and darkness and transform this information into hormonal signals (Peirson and Foster, 2006). In lower vertebrates, the pineal gland performs the light sensing directly, being a so-called "third eye"

(Mano and Fukada, 2006). In higher vertebrate, however, the evolution deprived the pineal gland of its light-sensing role by internalizing it into the brain. Pinealocytes of higher vertebrates underwent certain evolutionary changes as well, for example, they lost their internal clock function (Okano and Fukada, 2001; Mano and Fukada, 2006).

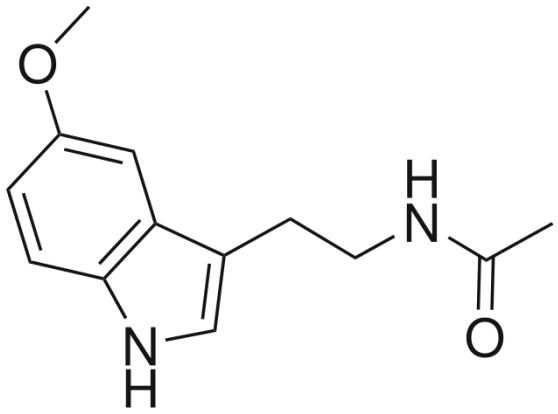

Figure 2.9: Melatonin molecule

Still, they have a considerable resemblance to photoreceptor cells: they even retain photosensory proteins of unknown function, possibly vestiges of evolution. Thus, in mammals, the pineal gland now only transduces the environmental light information coming from the suprachiasmatic nuclei into hormonal signals. Despite the fact that the pineal gland and pinealocytes underwent serious morphological changes over the course of evolution, the gland's function as a melatonin-producing body remained (Maronde and Stehle, 2007).

In animals, melatonin (Fig. 2.9) is a hormone involved in circadian rhythm regulation (Hardeland *et al.*, 2006). It is predominantly produced in the pineal gland, but also in retina, where it acts locally (Tosini and Fukuhara, 2003). The effects of the melatonin are carried out via melatonin receptors, which are found in the suprachiasmatic nuclei and pituitary gland, and also in the retinal cells. There are also reports of melatonin receptors present in gonads (Morgan *et al.*, 1994). So mainly the effects of melatonin are executed locally in the central nervous system, where melatonin helps to entrain the circadian clock in the suprachiasmatic nuclei and regulate physiological processes in the body and behaviour via the action of pituitary gland.

Melatonin is synthesized in a short biochemical pathway from serotonin by the consecutive action of two enzymes: NAT (serotonin *N*-acetyltransferase) and HIOMT (acetylserotonin *O*-methyltransferase) – which are pineal-specific (Axelrod and Wurtman, 1968). HIOMT is a rate-limiting enzyme in the biosynthesis of melatonin (Reiter *et al.*, 2007). The expression of NAT and HIOMT genes is controlled by pineal regulatory element (PIRE) sequences – conserved TAAT/C sequences in the promotors of the pineal-specific genes, which bind CRX (cone-rod homeobox) (Li *et al.*, 1998). CRX is a photoreceptor-specific transcription factor (Furukawa *et al.*, 1997) which is believed to transactivate photoreceptor-specific genes and regulate photoreceptor differentiation. In pineal gland, it is present at all times, but the level shows diurnal pattern, with the peak of expression 1-2 hours before the peak of NAT (Li *et al.*, 1998). In the research done by Borjigin and colleagues (Borjigin *et al.*, 1999), the *PINA* gene has been shown to have the PIRE regulatory sequence in its promoter, like *NAT* and *HIOMT*. Spatial distribution of transcription of both NAT and PINA mRNAs follows that of CRX exactly in the pineal gland and retina. While it seems that CRX is involved in upregulation of both melatonin synthesis pathway genes and *PINA*, the regulation is more complex and involves additional factors. Such factors, which regulates melatonin synthesis pathway genes, are CREB/ICER (CRE-binding protein and inducible cAMP early repressor). They are involved in clock genes and CCGs regulation in pineal gland and other tissues (Foulkes *et al.*, 1996; Zmrzljak *et al.*, 2013), and play important role in brain plasticity (Borlikova and Endo, 2009). In the pineal gland, CREB/ICER connect incoming ambient lighting information in form of norepinephrinergic cAMP response to the clock-controlled genes expression. Synergy of CRX and CREB/ICER is the likely mechanism that ensures both tissue specificity and diurnal behaviour of expression of melatonin pathway genes. It is possible that *PINA* transcription is regulated by both CRX and CREB/ICER in the same way.

2.5. PINA – Putative Copper Transporter from Pineal Gland

Studies of the mechanism of control of expression of NAT and HIOMT led to a discovery of the PIRE elements described above, as well as a novel transcript, which was regulated by the same mechanism. The novel mRNA was characterized as a splice variant of ATP7B, and its transcription had the same temporal behavior as that of NAT. The splice variant was designated PINA (pineal night-specific ATPase) (Borjigin *et al.*, 1999).

Two variants of PINA mRNA were detected, which differed by their polyadenylation tails. Both mRNAs have a pineal-specific 300 bp 5'-UTR. It is located in the intron region of the ATP7B gene just upstream the exon 9.

PINA expression in the pineal gland was shown to be regulated both developmentally and diurnally. In adult rats, PINA mRNA is detected only in the pineal gland and, to a lesser extent, in the retina. Its transcription pattern follows that of the NAT mRNA: it is undetectable in light period, first appears 3 hours into the dark period, peaks after 6 hours into the dark period, and abruptly disappears within 1 hour after the beginning of the light period (Borjigin *et al.*, 1999). Both genes follow a different pattern in neonatal rats: in two-days old rats the mRNAs can be detected both at daytime and nighttime, although the diurnal variation already exists. In 16-days old rats both gene products become undetectable at day. In the same age, sympathetic innervation to the gland matures. Different transcriptional patterns at different developmental stages indicate that PINA may play some role in the photoreceptor and photoreceptor-like cell lines development. According to the experiments, both PINA and NAT are regulated by circadian clock via the β-adrenergic receptors and cAMP intracellular signalling (Borjigin *et al.*, 1999).

According to its sequence (GenBank accession number: AF120492), PINA mRNA encodes the C-terminal half of the ATP7B (Fig. 2.10). The predicted polypeptide sequence is missing the metal binding domains, as well as the first four transmembrane helices.

Rat PINA has complete N- and P-domains required for ATP hydrolysis as well as copper-binding sites in the transmembrane domain. A-domain retains the conserved TGEK motif, but it is unclear whether A-domain is functional, because due to absence of TM2 it is attached to the M-domain with only one linker instead of two in the full-length protein. The retention of essential components of the enzyme needed for ion transport and ATP hydrolysis suggests that PINA could have ATPase and copper-transport activity. Indeed, the rat PINA protein was shown to rescue the phenotype in yeast deficient in the endogenous Cu^{+}-ATPase (Borjigin *et al.*, 1999), although to a lesser extent than complete ATP7A used as a control.

Synchronous transcription of PINA and melatonin synthesis-related genes, such as NAT, may indicate that the PINA protein is important either for the functioning of the melatonin synthesis pathway, or that it is needed elsewhere for the circadian-regulated "cell maintenance" procedures.

Interestingly, a public mRNA database contains a corresponding entry for human ATP7B splice variant, ATP7B.K (Totoki *et al.*, 2005; "AceView", 2015; GenBank accession number: AB209461), which was encountered in brain tissue during human genome sequencing. This sequence is remarkably similar to rat PINA: it represents a truncation of human ATP7B at the Met residue (M796) homologous to that of rat ATP7B (M788). There is, however, a significant difference as well: the predicted protein lacks 18 amino acid residues at the border of TM3 (ATP7B nomenclature) and the nascent extracellular loop (Fig. 2.10 and Fig. 2.11).

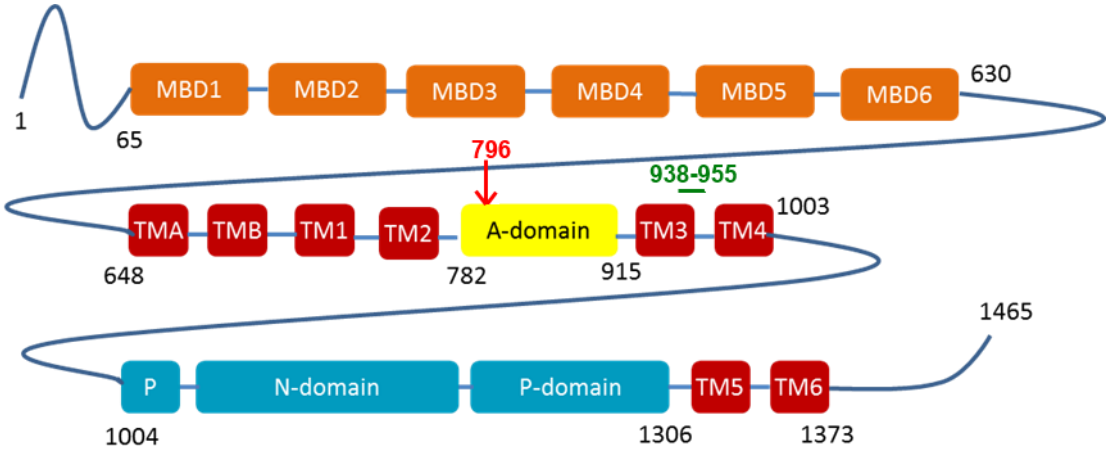

Figure 2.10: Schematic view of domain composition of ATP7B. Red arrow indicates the beginning of the putative PINA protein. Green line denotes the deletion of 18 a.a. in ATP7B.K

A glimpse on a possible structure of such an unusual protein can be made using a known crystal structure of the "parent" protein, ATP7B, described above. The model (Fig. 2.11) shows a construct truncated at M796, with the deletion region highlighted with green colour. Most features of the putative human PINA protein – such as retained essential components of the copper transduction pathway (CPC and YN/MS motifs) in the transmembrane segment, intact cytoplasmic domains and C-terminus – indicate a strong possibility that this protein can indeed be a functional copper transporting ATPase with novel regulation properties (A-domain attached only with one

linker, missing S-domain, missing MBDs, preserved C-terminal tail). The question is whether the features of the protein really make it a specially-regulated copper pump important in diurnal metabolism.

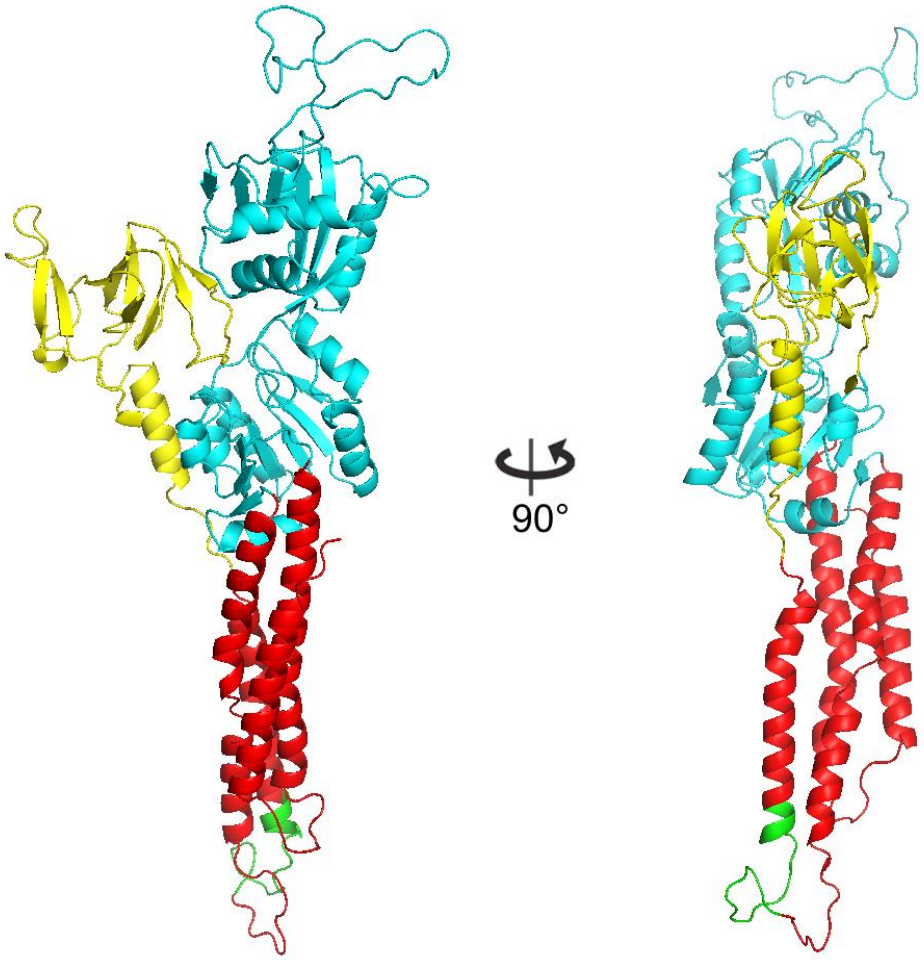

Figure 2.11: Model of putative PINA homologue from human, corresponding to $\Delta^{1\text{-}795}$ATP7B. Yellow – A-domain, cyan – ATP-binding domain (P- and N-domains), red – transmembrane domain, green – deletion in ATP7B.K (model is based on homology model from Schushan *et al.*, 2012).

Our hypothesis is that PINA – a novel splice variant of ATP7B – is present in pinealocytes and is involved in circadian regulation of copper metabolism in the brain.

3. Materials and Methods

3.1. Molecular Biology Methods and Strain Description

Plasmid preparation.

Single colonies were selected on LB-ampicillin plates, inoculated into 5 mL of liquid LB-ampicillin medium, and grown for 16 hours at 37°C with shaking at 220 r.p.m. Plasmids were isolated using Mini-Prep kits (Qiagen, Burlington, ON) and suspended in sterile double distilled water. Plasmids were stored at -20°C.

Restriction digestion.

All restriction enzymes were purchased from ThermoFisher Scientific (Waltham, MA). DNA restrictions were set up in 20 µL volumes with 0.5 – 2.0 µg of plasmid DNA, 0.5-1 µL of each restriction enzyme, 2 µL of appropriate 10x NEB reaction buffer. Restriction digestions were incubated at 37°C for 90 minutes.

Ligation Reactions

Ligation reactions were set up in 20 µL volumes. Each reaction contained vector DNA and the insert DNA at a ratio of 1:3, 2 µL of 10x T4 DNA ligase buffer, and 0.5 U of T4 DNA ligase (New England Biolabs, Ipswich, MA). Ligation mixtures were incubated for 16 hours at 16°C.

E. coli transformations.

Chemically competent *E. coli* cells were prepared using $CaCl_2$, essentially as described previously (Dagert and Ehlrich, 1979). Competent cells (50 µL) were incubated with 0.5 µg plasmid DNA on ice, for 45 minutes. The cells were then heat shocked for 45 seconds at 42°C, incubated on ice for 10 minutes, and then transferred into 1 ml of LB broth and incubated at 37°C for 1 hour with gentle shaking. After the 1 hour growth the cells were plated on LB-ampicillin agar plates and incubated for 16 hours at 37°C.

Description of strains used in cloning and expression

E. coli DH5α

The *Escherichia coli DH5α* strain is commercially available (Invitrogen, Burlington ON) and is ideal for cloning and storage of plasmids because of its ability to take up and retain plasmid DNA. *DH5a* cells have the genotype: F^- Φ80*lac*ZΔM15 Δ(*lac*ZYA-*arg*F) U169 *rec*A1 *end*A1 *hsd*R17 (rK^-, mK^+) *pho*A *sup*E44 λ^- *thi*-1 *gyr*A96 *rel*A1.

E. coli BL21(DE3)

BL21(DE3) strain is commercially available (New England Biolabs, Ipswich MA) and is ideal for overexpression of recombinat proteins because it contains DE3, a λ prophage carrying a gene of T7 polymerase. T7 polymerase expression is driven by *lac* promoter (IPTG is used as an inducer). Vector expression is driven by a strong T7 promoter, and is suppressed until induction by IPTG. The genotype is *fhuA2 [lon] ompT gal (λ DE3) [dcm] ΔhsdS; λ DE3 = λ sBamHIo ΔEcoRI-B int::(lacI::PlacUV5::T7gene1) i21 Δnin5*

K. lactis YCT-284

The *Kluyveromyces lactis YCT-284* yeast strain is commercially available (New England Biolabs, Ipswich MA) and is easy to use high productivity eukaryotic expression system. It has a number of advantages over other yeast and bacterial systems: it's a safe strain used in food industry and capable of quickly reaching high cell density and recombinant protein production, the expression is driven by a strong *LAC4* promoter with no background expression in *E. coli*, and antibiotic-free selection method that uses *amdS* gene in the transformation vector that allows cells to utilize acetamide as a sole source of carbon. The YCT-284 cells have genotype: haploid, mat*α*, Δ*cts*1.

3.2. Plasmid Construction and Description

The base plasmid used for cloning and expression of ATP7B and its variants was the pKLAC2 plasmid (New England Biolabs, Ipswich MA; Fig. 3.1), which is designed to have both yeast and bacterial origins of replication.

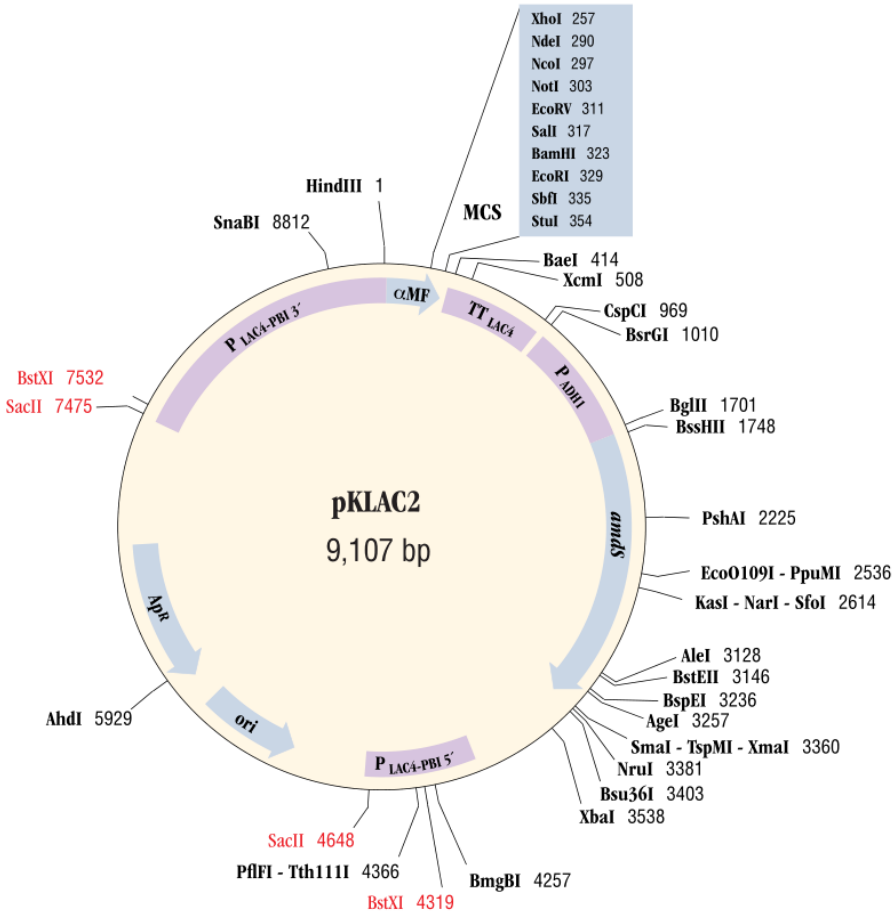

Figure 3.1: pKLAC2 (9107 bp) contains the 5′ and 3′ ends of the LAC4 promoter ($P_{LAC4\text{-}PBI}$) separated by DNA encoding β-lactamase (Ap^R) and the pMB1 origin (ori) to allow for its propagation in E. coli. The *K. lactis* α-mating factor secretion leader sequence (α-MF), multiple cloning site (MCS), and the LAC4 transcription terminator (TT) lie immediately downstream of 3′ $P_{LAC4\text{-}PBI}$. The yeast ADH1 promoter (P_{ADH1}) drives expression of an acetamidase selectable marker gene (amdS). The vector can be linearized by digestion with SacII or BstXI to create a linear DNA fragment capable of inserting into the native LAC4 promoter region of the *K. lactis* genome.

Plasmid pKLAC2-ATP7B (Fig. 3.2) was constructed previously by Dr. Nataliya Dolgova, Dmitriev lab. To produce truncated derivatives of ATP7B, the pcDNA3.1-$WNDP^{Gly875/HindIII}$-vector (containing ATP7B cDNA, prepared by Dr. Nataliya Dolgova, Dmitriev lab) was used as a template to produce DNA sequence encoding His-tagged protein $\Delta^{1\text{-}795}$ATP7B (Fig. 3.3). The sequence was produced using PCR with matching primers, with forward primers starting at Met^{796} having Met+6xHis addition and *Hind*III restriction site (DT-PINAaF), and the reverse primer having *Not*I restriction site (DT-7BR). This DNA sequence was cloned into pKLAC2 plasmid using

*Hind*III and *Not*I restriction sites. Cloning with these sites is necessary to remove α-mating secretion sequence from pKLAC2 plasmid, so the proteins of interest would integrate into the intracellular compartments and not secreted from yeast cells. Automated DNA sequencing was used to verify the construct.

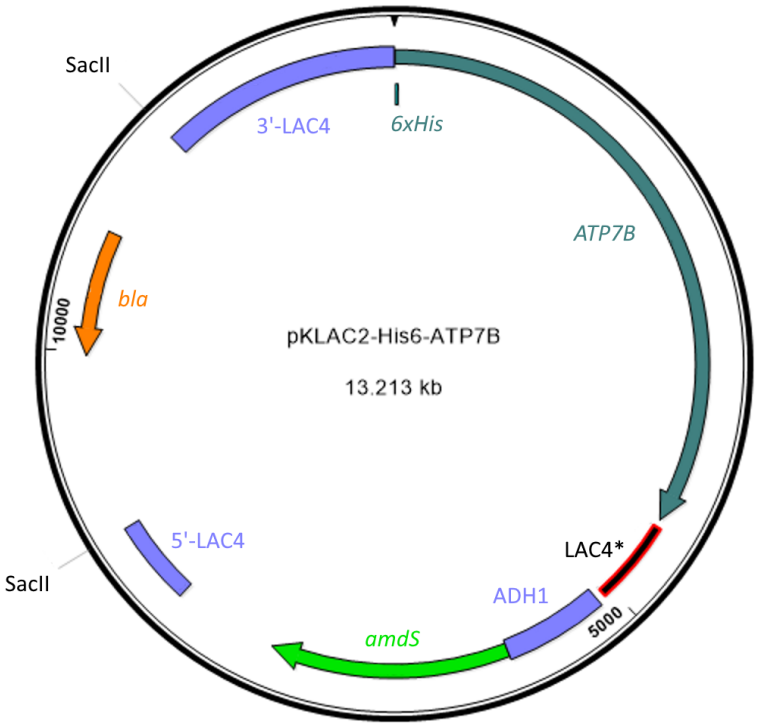

Figure 3.2: Map of pKLAC2-ATP7B vector. *ATP7B* gene is in turquoise, acetamidase in green, bacterial ampicillin resisitance is in orange. ADH1 yeast promoter and parts of LAC4 promoter are in purple, yeast transcription terminator is in red-black colours. *Sac*II restriction sites for linearization are indicated.

Construct for cloning and expression of ATP7B.K (Fig. 3.3) was produced by deleting a sequence of 54 bp encoding 18 amino acids that are not present in ATP7B.K versus the corresponding part of human ATP7B by around-the-plasmid PCR of pKLAC2-$\Delta^{1\text{-}795}$ATP7B and blunt-end self-ligation of the product. The resulting vector was checked using restriction analysis and automated DNA sequencing to verify correct deletion.

Cloning of all the vectors was done in *E. coli DH5α*, and plasmids were isolated from liquid cultures using a Miniprep DNA extraction kit (Qiagen).

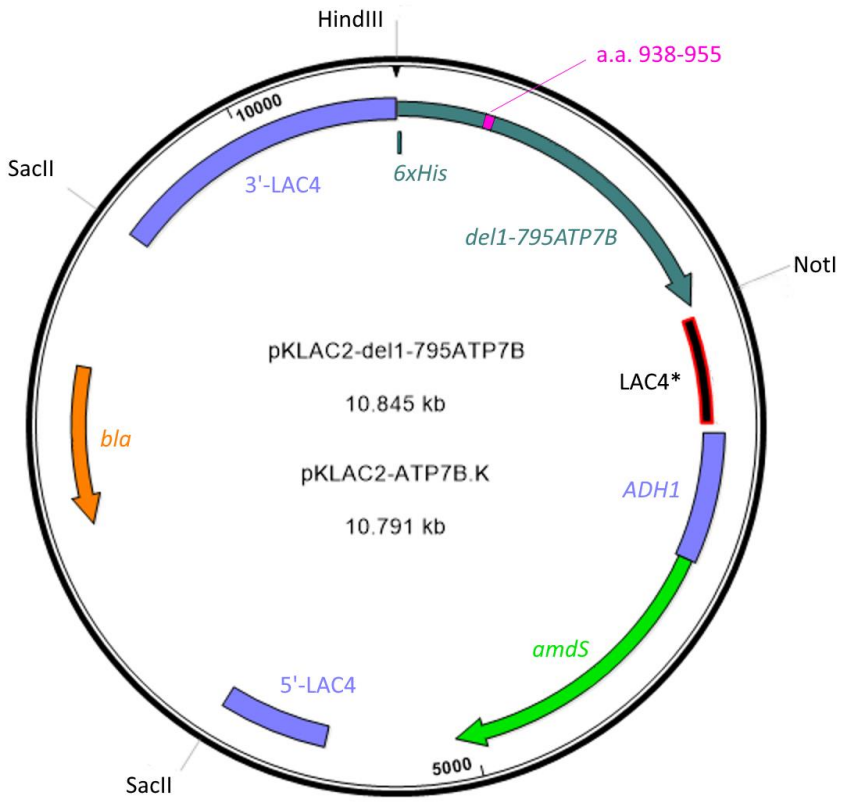

Figure 3.3: Map of pKLAC2-$\Delta^{1\text{-}795}$ATP7B and pKLAC2-ATP7B.K vectors. *$\Delta^{1\text{-}795}$ATP7B/ATP7B.K* gene is in turquoise, acetamidase in green, bacterial ampicillin resistance is in orange. ADH1 yeast promoter and parts of LAC4 promoter are in purple, yeast transcription terminator is in red-black colours. Magenta segment indicates fragment missing in pKLAC2-ATP7B.K *Sac*II restriction sites for linearization, *Hind*III and *Not*I cloning sites are indicated.

Table 3.1: Table of primers used in generation of plasmids

Primer name	Sequence
DT-PINAaF	5'-TTTAAGCTTATGCATCATCATCATCATCAT ATGTCTCTCCAAGCCACAGAAGCCACCGTT
DT-7BR	5'-ATCCGCGGCCGCTCAGATGTACTGCTCCT CAT
DT3to4-F	5'-AACCCCAACAAGCACATCTCC
DT3to4-R	5'-CACCAACGTCAAAGTTGACATG

3.3. Protein Expression and Purification

3.3.1. Transformation and Expression in *K. lactis*

The *K. lactis* cells were transformed using lithium acetate method (Gietz and Woods, 2001, with modifications): yeast cells were grown in YPD medium (10% yeast extract, 20% bacto-peptone, 2% glucose) to OD_{600} of 0.6 – 1.0 (10 mL per transformation), washed in 0.5 volumes of wash buffer (1 M sorbitol, 10 mM Bicine-NaOH pH 8.35, 3% ethylene glycol (v/v), 5% DMSO (v/v)), suspended in 0.02 volumes of the same solution, and aliquots of 200 µL were frozen at -80°C for storage. Later, cells were thawed on ice, spun down for 2 minutes at 3000 g with supernatant removal. A total of 360 µL of the transformation mixture (25% PEG-4000 (w/v), 100 mM lithium acetate, 2.5 mg of boiled and ice-chilled salmon sperm DNA, 25 – 40 µg of vector DNA digested with SacII to produce a recombination cassette) was added to the cells and mixed gently. The whole mixture was kept for 30 minutes at 42°C with shaking (700 r.p.m.). Then the cells were pelleted by centrifugation, resuspended in 0.35 ml of water and plated on an YCB-acetamide plate. Colonies were re-streaked on a fresh YCB-acetamide (yeast carbon base mix from New England Biolabs contains all required nutrients except a nitrogen source, 0.5 mM acetamide, 1.4% agar) plate and tested for expression.

Transformed yeasts were transferred from the acetamide plate into YPGal medium (10% yeast extract, 20% bacto-peptone, 2% galactose), where galactose would induce expression by inducing LAC4 promoter. Initially, small-scale cultures of several clones of each strain were expressed to find the best timeline and the best clones.

3.3.2. *K. lactis* Culture Growth and Protein Expression

Strains of *K. lactis* expressing proteins of interest were grown in liquid YPGal medium (1% yeast extract, 2% peptone, 2% galactose) at 30°C with 220 rpm shaking for 72 hours (final OD_{600} recorded was 60-80). Then, the cells were pelleted at 3500 g for 10 minutes and resuspended at 4°C in deionized water (water volume equal to the initial culture volume), and pelleted by centrifugation at 3500 g. Whole cell samples were disrupted with glass beads for 5 minutes in GBD-buffer (20 mM Tris-HCl pH 7.9, 10 mM $MgCl_2$, 1 mM EDTA, 5% glycerol, 1 mM DTT, 0.3 mM

$(NH_4)_2SO_4$; protease inhibitors cocktail), and analyzed by SDS-PAGE and Western blot to determine the level of protein expression.

3.3.3. Isolation of Membrane Fractions from *K. Lactis* Cells

The TG-200 buffer (10% glycerol, 50 mM Tris-HCl, pH 7.5, 200 mM NaCl, 5 mM $MgCl_2$) was used for all subsequent purification steps, which were performed at +4°C. The cell pellets were suspended in TG-200 buffer with 1 mM DTT and Roche ULTRA protease inhibitors (as recommended by manufacturer) at 0.2-0.25 g wet weight per mL, and homogenized using Potter glass-Teflon homogenizer with subsequent disruption in cell disruptor at 39,000 p.s.i. (pounds per square inch). The resulting homogenate was fractionated by successive centrifugation steps at 1000 g for 10 min and 120,000 g for 60 min. Supernatants and pellets were analyzed using western blot to determine fractions containing proteins of interest.

The crude membrane fraction (120,000 g pellet) was suspended in a small amount of the TG-200, frozen in liquid nitrogen and stored at -80°C. For ATP7B purification, sucrose gradient fractionation of the membranes was used to achieve better purity.

Crude membranes were separated on a stepwise sucrose gradient (65%, 50%, 35%, 18% w/v in 20 mM HEPES pH 7.5, 1 mM DTT) at 200000 g for 2 hours. Membrane fraction enriched in ATP7B, was collected from the 35%-50% interface, pelleted again at 200,000 g for 1 hour in 20 mM HEPES pH 7.5, 1 mM DTT, suspended in a small amount (2–3 ml) of TG-200, frozen in liquid nitrogen and stored at -80°C.

3.3.4. Affinity Purification of ATP7B and its Variants on Ni-NTA Agarose

Purification of His-tagged ATP7B and its variants requires extraction of the protein from lipids by means of solubilisation in detergent. To solubilize ATP7B, the 35-50% membrane fraction was resuspended in TG-200 with 1 mM DTT, protease inhibitors cocktail and 1% LMPG (final protein concentration 2 mg/ml) for 30 minutes on ice, insoluble components were removed by centrifugation at 120,000 g for 1 hour, ATP7B.K was extracted from the crude membranes, instead of 35%-50% fraction, using the same protocol.

Ni-NTA agarose resin (Qiagen, Missisauga, ON) was washed with 5 column volumes (CV) of double distilled water and by 10 CV of the TG-200 buffer before the protein-detergent mixture was applied. The protein-detergent mixture was incubated with the Ni-NTA agarose (0.083 mL of Ni-NTA agarose beads per mg of total protein) with gentle agitation at 4°C for 30-40 minutes and then loaded into a chromatographic column. The column was eluted at the gravity flow.

The column was washed with 20 column volumes of the TG-500 buffer (10% glycerol, 50 mM Tris-HCl, pH 7.5, 500 mM NaCl, 5 mM $MgCl_2$) supplemented with 1 mM DTT, protease inhibitors cocktail, 0.1% LMPG and 20 mM imidazole. The protein was eluted with 5 column volumes of the TG-500 buffer, pH 8.5, supplemented with 1 mM DTT, protease inhibitors cocktail, 0.1% LMPG, and 150 mM imidazole for ATP7B, or 1 mM DTT, protease inhibitors cocktail, 0.2% LMPG, and 80 mM imidazole for ATP7B.K and $\Delta^{1\text{-}795}$ATP7B. Fractions were analyzed using SDS-PAGE with subsequent Coomassie staining. Fractions containing the purified protein were pooled, concentrated by centrifugation in VivaSpin concentrator (Satorius, Göttingen, Germany) with molecular weight cut-off of 50 kDa (ATP7B) or 30 kDa (ATP7B.K and $\Delta^{1\text{-}795}$ATP7B) and stored in liquid nitrogen.

3.3.5. Size Exclusion Chromatography

Size exclusion chromatography was performed using ÄKTA FPLC system (GE Healthcare, Mississauga, ON). Superose 6 10/300 GL column (GE Healthcare, Mississauga, ON) was equilibrated with 1 column volume of TG-500 buffer supplemented with 0.1% (for ATP7B) or 0.2% (for ATP7B.K and $\Delta^{1\text{-}795}$ATP7B) LMPG, protease inhibitors cocktail and 1 mM DTT. The protein sample was eluted with 1 column volume of the same buffer, 1 ml per fraction.

Fractions were analyzed using SDS-PAGE with subsequent Coomassie staining. Fractions containing the purified protein were pooled, concentrated by centrifugation in VivaSpin concentrator (Satorius, Göttingen, Germany) with molecular weight cut-off of 50 kDa (ATP7B) or 30 kDa (ATP7B.K and $\Delta^{1\text{-}795}$ATP7B) and stored in liquid nitrogen.

A small aliquot of purified protein (20 µl) was analyzed for protein concentration and purity by SDS-PAGE in 3.5%-20% polyacrylamide gels (Laemmli, 1970) and subsequent SYPRO Ruby

staining (see below). Purity of the proteins was calculated in SYPRO Ruby stained gels by densitometry using ImageJ software (NIH), version 1.49v.

3.4. Proteoliposomes Preparation

To make pre-formed asolectin liposomes, 50 mg of dry asolectin (Sigma Technologies) was dissolved in 5 ml of chloroform. The chloroform was then evaporated under a stream of argon and the lipid was dried overnight in a desiccator under vacuum. Asolectin was then dissolved at 25 mg/ml in HEPES buffer (10 mM HEPES pH 7.5, 150 mM NaCl, 1 mM DTT, 1.5% octylglycoside) with stirring. The asolectin suspension was then dialysed against 500 mL the same buffer without octylglucoside twice at +4°C for 4 hours and then overnight using a 12,000-14,000 Da molecular weight cut-off SpectraPor dialysis tubing (Spectrum Laboratories Inc., Rancho Domingeuz, California). The pre-formed liposomes were stored in liquid nitrogen until used.

For protein reconstitution, the pre-formed liposomes were thawed on ice, extruded using Avanti Mini-Extruder (Avanti, Alabaster, AL) with Whatman polycarbonate membrane (Ge Healthcare, Piscataway, NJ) with 400 nm pore size to ensure uniform size distribution. LMPG was added to the extruded liposomes at a final concentration of 0.02%. After 1 hour incubation on ice, purified protein was added to the liposomes at the protein to lipid ratio of 1:100 w/w, and the liposomes were incubated for 15 min on ice. The mixture was then treated with Bio-Beads (Bio-Rad, Hercules, CA) to remove the detergent. The Bio-Beads were changed three times, each incubation was done for 18 minutes. Then, the proteoliosomes were pelleted down at 150,000 g for 1 hour at 4°C, suspended in MES-AT buffer (50 mM MES, pH 6.0, 10% glycerol, 150 mM NaCl, 3 mM $MgCl_2$, 1 mM ascorbic acid, 0.1 mM TCEP) for activity assays (see below) and stored in liquid nitrogen for up to 3 days. Before use, thawed proteoliposomes were again extruded as described above.

3.5. Activity Assays

Malachite Green Inorganic Phosphate Detection Assay

To measure ATPase activity of ATP7B and its variants we chose a method of detection of liberated inorganic phosphate, a malachite green assay. It is the most sensitive colourimetric

method available (Lanzetta *et al.*, 1979). We used an improved malachite green mixture formulation employing polyvinyl alcohol that has been described previously (Singh and Shukla, 2003).

The following base buffer (MES buffer) was used: 50 mM MES, pH 6.0, 10% glycerol, 150 mM NaCl, 3 mM $MgCl_2$. To remove heavy metal ions and Cu^{2+}, the buffer was treated with Chelex 100 resin (BioRad, Hercules, CA) prior to addition of $MgCl_2$ as recommended by the manufacturer.

The reaction mixture was composed of MES buffer with 1 mM ascorbate, 0.1 mM TCEP, 5 μM CuCl, 5 μM ATOX1 and varying amounts of ATP7B or ATP7B.K either in detergent or reconstituted into asolectin proteoliposomes. Prior to addition of (proteo)liposomes and ATP to the mixture, buffer containing copper, ATOX1-copper or ATOX1 was pre-incubated for 30 min at room temperature to reduce all oxidized copper and ATOX1, and to allow complete binding of copper to ATOX1. Two types of measurements with malachite green were done: single time point and a time course.

When conducting single time point experiment, the whole reaction mix was dispensed in equal amounts (total of 40 μL) into wells of 96-well plate, and the plate was incubated for 20 or 30 minutes at 37°C with shaking. In the end of reaction, four reaction mix volumes (160 μL) of malachite green mix was added to the plate, and OD_{630} was read out on Spectra Max M2 spectrophotometer (Molecular Devices, Sunnyvale, CA).

For the time course, the whole reaction mix was incubated in an Eppendorf tube at 37°C with shaking, and equal amounts of it were taken out every 3, 10 or 20 minutes and mixed with 1 M EDTA solution (final EDTA concentration 125 mM) to stop the reaction by chelating Mg^{2+} ions. In the end of reaction, four reaction mix volumes (160 μL) of malachite green mix was added to the plate, and OD_{630} was read out.

Statistical analysis of the results has been carried out with GraphPad Prism v.5 using Student t-test.

Copper Transport Measurements Using Fluorescent Probe

Copper transport activity was measured using a highly selective synthetic fluorescent sensor CS-1. Uncharged copper-free CS-1 can freely diffuse across the lipid bilayer into the proteoliposomes. Prior to the start of reaction, all copper in the solution is bound to ATOX1, and is not detected by CS-1. Upon addition of ATP, copper ATPase accepts copper from ATOX1 and transports it across the liposome membrane. Inside, copper ions bind to CS-1, producing a fluorescent complex, which is detected with fluorescence spectrometer. The complex of CS-1-with copper is charged and cannot cross the membrane. Therefore as copper is transported inside the proteoliposome lumen, CS-1-Cu concentration inside increases, resulting in the increased fluorescence.

The reaction was carried out in 1 mL quartz glass cuvette. Reaction medium contained MES buffer (pH 6.0, 50 mM MES, 150 mM NaCl, 5% glycerol, 3 mM $MgCl_2$) with 1 mM ascorbate, 0.1 mM TCEP, 5 μM CuCl, 5-7.5 μM ATOX1 and 0.2-1 μM CS-1. A total of 230 μg of liposomes or proteoliposomes by lipid content was added. Prior to addition of (proteo)liposomes and ATP to the mixture, buffer containing copper, ATOX1-copper or ATOX1 was pre-incubated for 30 min at room temperature to reduce all oxidized copper and ATOX1, and to allow complete binding of copper to ATOX1. Copper transport reaction was started by addition of 1 mM ATP (final concentration). The measurements were performed using a Perkin-Elmer LS55 fluorescent spectrophotometer with emission at 556 nm and excitation at 540 nm.

3.6. Immunofluorescence and Microscopy

The 18x18 mm microscopic slides (VWR, Radnor, PA) were incubated in poly-L-lysine for 1 hour at room temperature, rinsed with PBS and double distilled water, and left to dry. Yeast cells expressing ATP7B and ATP7B.K grown in YPGal medium with or without added 1 mM $CuCl_2$ were collected by centrifugation at 3500 g, resuspended in double distilled water and centrifuged again. The collected cells were fixed in paraformaldehyde (final concentration 0.9%) for 15 minutes with shaking at 4ºC. After that, the cells were washed with 1 M sorbitol, 50 mM HEPES, pH 7.5, twice. A 20 μL aliquot of yeast pellet was dissolved in 100 μl of the same buffer with 2 mg/ml Lyticase (Sigma-Aldrich, Oakville, ON) added, and incubated for 1 hour at 30ºC. Then the cells were collected by centrifugation at 2000 g, washed with 0.5 ml of 50 mM HEPES,

1 M sorbitol, pH 7.5, centrifuged again, resuspended in the same buffer with 0.1% Triton added, and incubated for 10 minutes on ice. Then 20 μL of the cell suspension was applied to the dry poly-L-lysine coated slides and dried under a gentle stream of air.

These dried samples were rinsed with PBS and blocked with 5% BSA in PBS, and stained with antibodies against either the His-tag or N-terminus of ATP7B.

Mouse Anti-His antibody (AM1010a from Abgent, San Diego, CA) in 1:200 dilution in 2% BSA in PBS was applied for 1 hour at room temperature. After that the slide was washed in PBS, and the secondary antibodies anti-rabbit-Texas Red conjugate (Santa Cruz Biotechnology, Dallas, TX) in dilution 1:250, were applied for 1 hour at room temperature in the dark, and left to dry.

Rat anti-ATP7B (a gift from Svetlana Lutsenko, John Hopkins University, Baltimore, MD) in 1:500 dilution in 2% BSA in PBS were applied for 1 hour at room temperature. Secondary antibodies rabbit anti-rat-GFP conjugate IgG (Rockland Immunochemicals, Limerick, PA) in dilution 1:500, for the anti-ATP7B were applied for 1 hour at room temperature in the dark, and left to dry.

Dried slides were mounted onto microscope slides using Fluoroshield liquid mounting medium with DAPI (Sigma-Aldrich, Oakville, ON), and left to dry again for 48 hours in the dark.

The samples were imaged on a Leica SPS5 confocal microscope using 488 nm excitation for GFP, 595 nm for Texas Red, and 360 nm for DAPI.

3.7. Rat Tissue Processing

Healthy, untreated Sprague-Dawley rats were used to investigate temporal expression pattern of PINA. Adult rats were housed in UCACS facility at 12:12 light cycle. Animals were given 7 days to adapt to the new light cycle conditions.

This series of experiments involved keeping animals at 7 PM – 7 AM night cycle, and sampling was performed at 10 AM, 4 PM, 10 PM and 4 AM, two samples per time point.

Pineal gland tissue (~4 mg) was homogenized in tissue lysis buffer (0.25 M sucrose, 20 mM Tris-HCl pH 7.5, 0.1 M NaCl, 1 mM DTT, Roche ULTRA inhibitors as recommended by manufacturer), 50 µL of buffer for each sample, with a plastic pestle. Liver tissue (~2 g) was homogenized in the tissue lysis buffer (10 mL) in a glass-Teflon Potter homogenizer. Total protein concentration was determined by bicinchoninic acid assay. To obtain the membrane fraction, the homogenate was centrifuged for 10 min at 2000 g, supernatant was collected and centrifuged at 120000 g for 60 minutes. The resulting pellet was resuspended in 50 or 100 µL of buffer. Total protein concentration was determined by bicinchoninic acid (BCA) assay. Tissue homogenate and membrane samples were analysed by SDS-PAGE and Western blot.

3.8. Miscellaneous Methods

SDS-PAGE

SDS-PAGE was carried out essentially as described previously (Laemmli, 1970). The stacking gel layer contained 3.5% acrylamide, and the separating gel contained a linear gradient of 3.5% to 20% acrylamide.

Western Blot Analysis

Western blot analysis was carried out as previously described (Towbin *et al.*, 1979). Protein was transferred to PVDF or nitrocellulose membrane by electroblotting at 350 mA for 60 minutes. To detect His-tagged proteins, Western blots were probed using the Qiagen monoclonal anti-pentahistidine horse radish peroxidase (HRP) conjugate antibody (1:10,000 dilution) (Qiagen, Mississauga, ON) according to manufacturer's instructions. Western blots were done with either a primary polyclonal rabbit anti-ATP7B antibody H-94 (Santa Cruz Biotechnology, Dallas, TX) or primary polyclonal rabbit anti-ATP7B antibody PA2262 (Bosterbio, Pleasanton, CA). The secondary antibody used was goat anti-rabbit HRP conjugate antibody (TermoFisher Scientific, 1:10,000 dilution in PBS with 0.1 % Tween-20).

Both anti-ATP7B antibodies were raised against the unique epitope in the C-terminal tail in ATP7B. The epitope used for production of the H-94 antibody: Q1372-I1465. The epitope used for production of the PA2262 antibody: D1450-I1465.

Expression and Purification of ATOX1

ATOX1 expression and purification was done according to a protocol previously established in our lab (Dolgova *et al.*, 2013). In brief, *E. coli BL21(DE3)* transformed with the pTYB12 vector (New England Biolabs, Ipswich, MA) encoding human *ATOX1* gene (a gift from Svetlana Lutsenko, John Hopkins University, Baltimore, MD) was grown in LB medium for 16 hours, and transferred to M63 minimal medium. Expression was induced by isopropyl β-D-thiogalactoside (final concentration 0.5 mM), the cells were grown for 16 hours, and collected by centrifugation. The cells were disrupted in the cell disruptor, cell debris and membranes were removed by centrifugation, and the purification was done on chitin resin, followed by size-exclusion chromatography. The protein concentration was quantified using Lowry assay.

Protein Quantification

Total protein quantification in whole cell extracts, tissue extracts, and membrane preparations was done using Pierce BCA Protein Assay Kit (ThermoFisher Scientific, Waltham, MA) per manufacturer's manual. BSA standard curves ranging from 1.2 μg to 12 μg per sample were used with each assay. The reaction mixture was supplemented with 2% SDS (final) to release proteins from the membranes and improve accuracy.

Purified proteins were quantified by in-gel staining with SYPRO Ruby fluorescent dye (ThermoFisher Scientific, Waltham, MA). SDS gels were stained according to manufacturer's protocol. BSA standards ranging from 0.02 μg to 1 μg of protein per sample were included with each assay. Two or three sample dilutions were used to insure assay linearity. Gel images were analyzed using ImageJ (National Institute of Health, Bethesda, MD) and LibreOffice Calc software.

ATOX1 concentration determination was carried out as previously described (Lowry *et al.*, 1951). BSA standard curves ranging from 3 μg – 60 μg per sample were conducted with each assay.

4. Results

4.1. Expression of ATP7B and its variants in yeast *Kluyveromyces lactis*

In order to obtain recombinant human ATP7B and its variants – ATP7B.K (putative PINA homologue from human genome) and $\Delta^{1\text{-}795}$ATP7B (ATP7B with its N-terminus truncated at M796) for activity studies, they had to be expressed in a eukaryotic organism. There are multiple reasons for that. First of all, ATP7B and, presumably, its shorter variants, normally reside in compartments of the endomembrane system, which is absent in prokaryotic cells. Protein synthesis machinery in prokaryotes may lack necessary components for production of eukaryotic proteins, such as glycosylation, methylation and other modifying enzymes, specific chaperones, trafficking proteins. *Kluyveromyces lactis* expression system from New England Biolabs is used in industrial production of recombinant proteins, and has a number of advantages in comparison to the other systems. Mammalian expression systems are expensive, and the yield of protein is quite low; the same cost issues also apply to insect cells. Yeast expression systems allow protein production in large culture volumes at high yield at comparatively low cost. In comparison to the other yeast species, like *Pichia* or *Saccharomyces*, *Kluyveromyces lactis* YCT284 offers an easy induction approach which involves galactose as both carbon source and inducer.

Expression vectors encoding proteins of interest (His_6-ATP7B, His_6-$\Delta^{1\text{-}795}$ATP7B and His_6-ATP7B.K) were generated and cloned in *E. coli* DH5α, then transformed and expressed in *K. lactis*. Yeast cells were transformed with a linear integration cassette carrying the recombinant gene and *amdS* gene, which encodes acetamidase. Acetamidase enables the transformed cells to utilise acetamide as a sole source of nitrogen when they are grown on a minimal medium for selection. Expression of the cloned gene is driven by a strong *K. lactis* LAC4 promoter, induced by growth on galactose-containing medium.

Expression of ATP7B and its two truncated variants was detected in crude cell extracts with antibodies against C-terminus of ATP7B (Fig. 4.1). The observed slight discrepancy in the expected and actual molecular weight can be attributed to the fact that the electrophoretic mobility of membrane proteins can vary due to such factors as detergent binding (Rath *et al.*, 2008).

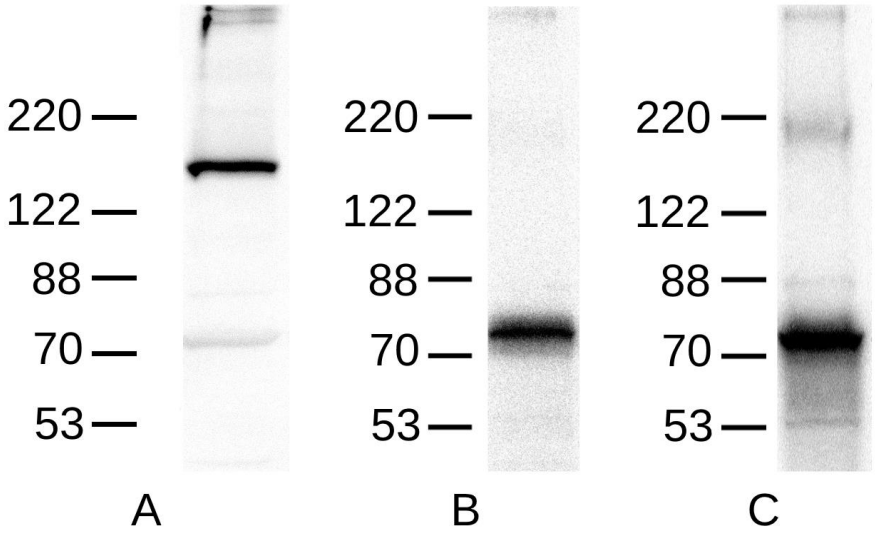

Figure 4.1: Expression of the ATP7B variants in *K. lactis* detected by Western blotting. Expressed recombinant proteins were detected in crude cell extracts by Western blot analysis with the polyclonal Anti-ATP7B antibody against C-terminus (H-94, Santa Cruz Biotechnology). All cell samples were disrupted with glass beads, and 10 µg of total protein were loaded on SDS-PAGE gels for subsequent analysis.
A – ATP7B (calculated MW 157 kDa); *B* – $\Delta^{1\text{-}795}$ATP7B (calculated MW 71 kDa); *C* – ATP7B.K (calculated MW 69 kDa)

Even though mammalian membrane proteins are generally expressed and folded well in the yeast expression systems, we needed to check if this is also true for the ATP7B variants. Heterologously overexpressed membrane proteins can be misfolded, and then degraded or accumulated in inclusion bodies. Folded and inserted enzymes still can be non-functional. An easy way to establish whether ATP7B protein is folded properly is to check its trafficking behaviour. This protein is known to be trafficked between various membrane compartments in mammalian hepatocytes in response to changes in copper concentration. By subjecting yeast to high and low copper concentrations, it should be possible to induce protein relocalization in the cells, which would indicate proper folding of the enzyme. It has been shown previously that $\Delta^{MBD1\text{-}5}$ATP7B does indeed relocalize in yeast after their treatment with copper (II) chloride, and the solubility of the protein in detergent changes as well (Portmann and Solioz, 2005). Change in solubility means that there is different lipid environment, which is an indication of a different membrane compartment, and also can be used to assess relocalization.

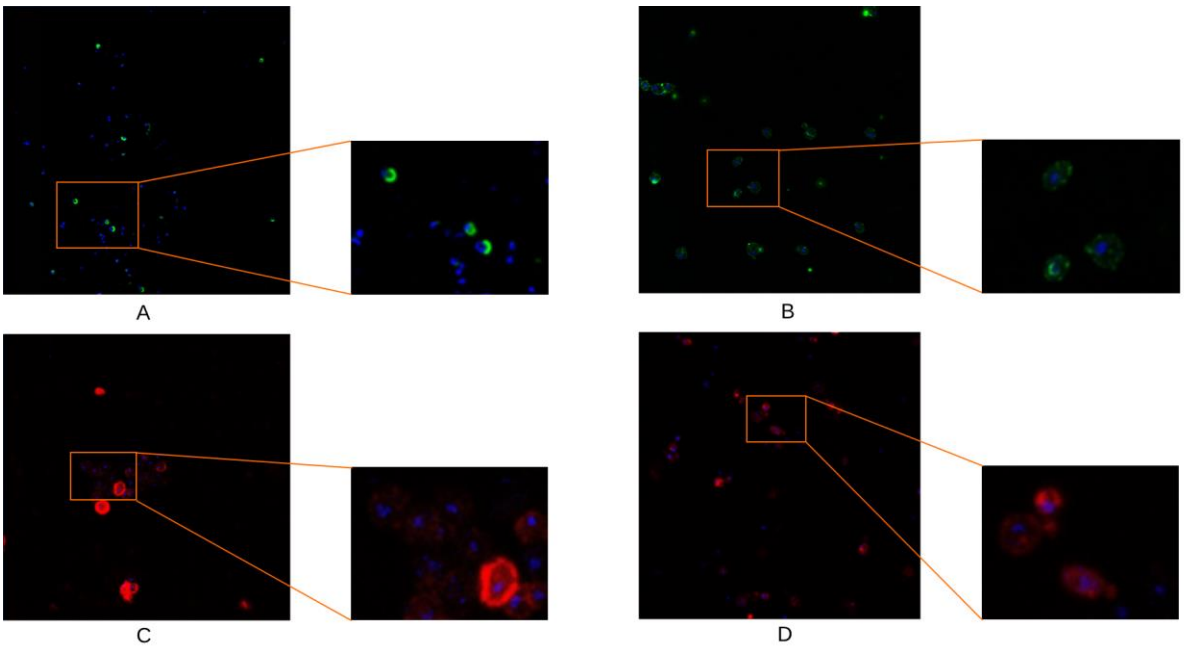

Figure 4.2: Recombinant ATP7B and ATP7B.K visualization in fixed *K. lactis* yeast cell by immunostaining (in false colours). Blue – nucleus (DAPI), green – ATP7B (anti-ATP7B, Santa Cruz), red – ATP7B.K (anti-ATP7B, Santa Cruz). A – ATP7B expressing yeast grown without added copper; B – ATP7B expressing yeast grown in 1 mM $CuCl_2$; C - ATP7B.K expressing yeast grown without added copper; D - ATP7B.K expressing yeast grown in 1 mM $CuCl_2$

To test if ATP7B and ATP7B.K expressed in yeast change their intracellular localization in response to high copper concentration, the cells expressing ATP7B and ATP7B.K have been grown in YPGal medium with or without added $CuCl_2$, fixed on a microscopic slide and immunostained with antibodies against the C-terminus of ATP7B. The results indicate that the protein responds to elevated copper by relocalization between different cell compartments (Fig. 4.2).

ATP7B showed a distinctively different localization in cells grown in low and high copper concentrations. Without added copper, the expressed protein is localized in compact fashion in close proximity to nucleus – a typical pattern for TGN localization. When cells are grown at elevated copper, the protein localizes mainly to the cytoplasmic membrane.

ATP7B.K staining in yeast grown without additional copper shows a granular pattern, mainly in cytoplasm (Fig. 4.2, C). In the presence of high copper amounts it also tends to relocalize to the plasma membrane (Fig. 4.2, D).

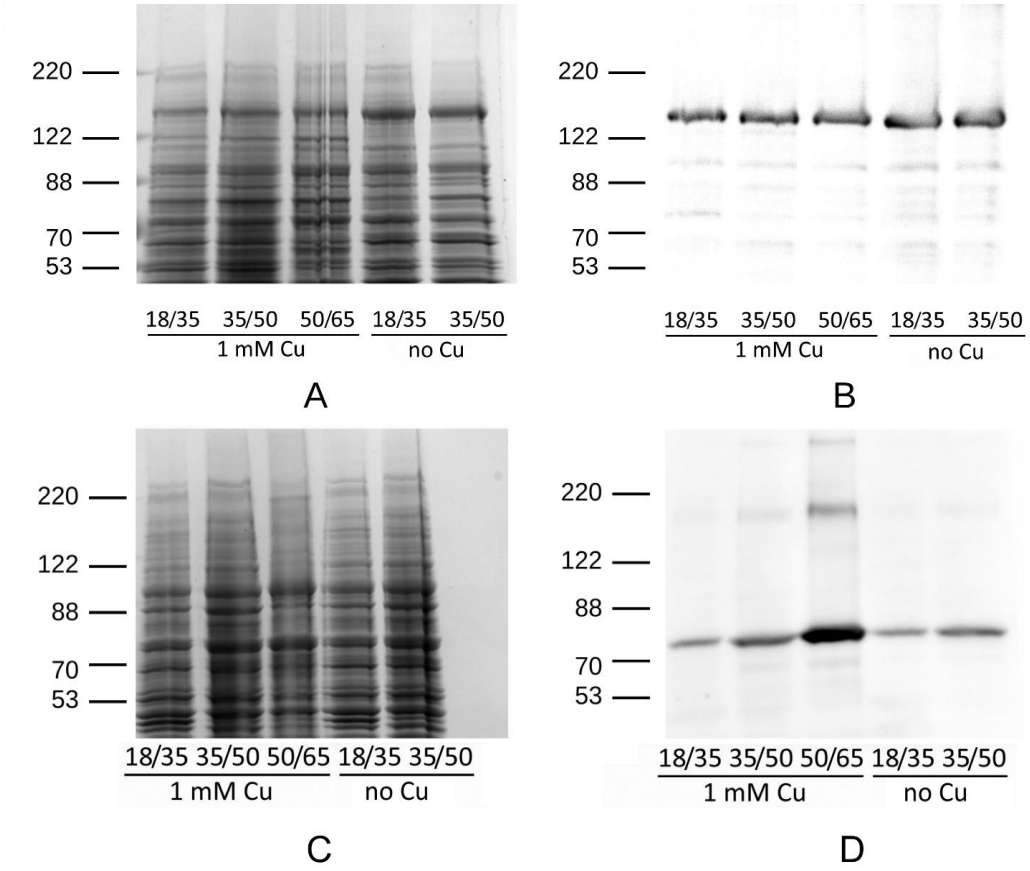

Figure 4.3: Distribution of the recombinant ATP7B and ATP7B.K proteins between various membrane fractions of *K. lactis* cells grown in presence or absence of 1 mM $CuCl_2$. Crude membrane fractions were separated on sucrose gradients, and 10 µg of total protein was loaded on SDS-PAGE gels for subsequent analysis. 50-65% fraction from cells grown in low copper concentration was not analyzed because there was no visible membrane material at the interface of 50% and 65% solutions.
A – ATP7B, Coomassie stain; *B* – ATP7B, Western blot with anti-PentaHis antibody; *C* – ATP7B.K, Coomassie stain; *D* – ATP7B.K, Western blot with anti-PentaHis antibody.

Movement of a protein between membrane compartments can be traced by separating the crude membrane fraction of a cell into sub-fractions using density gradients (Liu and Fagotto, 2011). To see how ATP7B and ATP7B.K is distributed among various membrane fractions in cells grown with or without added copper, crude membranes of the cells expressing ATP7B and ATP7B.K grown without added copper or in presence of 1 mM $CuCl_2$ were fractionated using sucrose gradient separation.

When subjected to sucrose gradient fractionation, the crude membrane fraction of ATP7B-expressing *K. lactis* grown without added copper separated into two distinct fractions: at the interface of 35% and 50% sucrose solutions (major fraction), and at the interface of 18% and 35% solutions (minor fraction), with no visible membrane material at the interface of 50% and 65% solutions (Fig. 4.3, A-B).

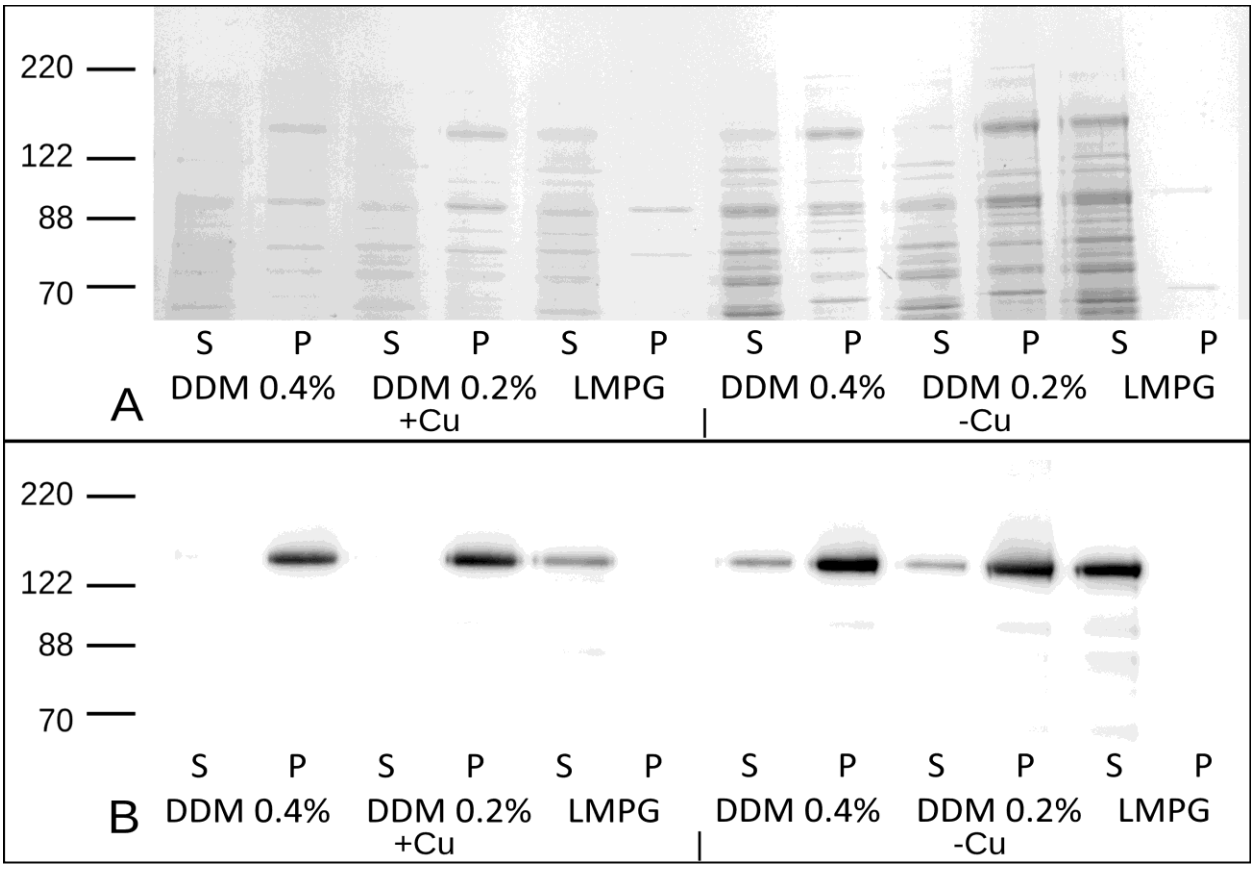

Figure 4.4: Solubilisation of the recombinant ATP7B protein from crude membrane fraction of *K. lactis* cells grown in presence or absence of 1 mM $CuCl_2$. Crude membrane fractions (total protein 2 mg/ml) were solubilised in various concentrations of DDM and LMPG.
A - Coomassie stain; *B* - Western blot with anti-PentaHis antibody
S – soluble fraction, P – insoluble fraction; DDM concentrations are indicated; LMPG was taken at 1% concentration

The crude membrane fraction of cells grown in the presence of 1 mM copper (II) chloride separated into three fractions: the aforementioned 18-35% and 35-50%, and also a heavier 50-65% minor fraction. This fraction most likely represents protein-loaded transport vesicles which are

involved in protein trafficking to the plasma membrane. This agrees with the immunofluorescence data (Fig. 4.2) that copper in the growth medium induces trafficking of the protein.

Previously (Portmann and Solioz, 2005) it was shown that elevated copper concentration in the growth medium makes Δ^{MBD1-5}ATP7B expressed in *S. cerevisiae* soluble in dodecyl maltoside (DDM) at a total membrane protein to detergent ratio 1:1 (*w/w*). We have conducted solubilisation trial to see whether the same applies for the full-length ATP7B expressed in *K. lactis* (Fig. 4.4). The experiment has shown that elevated copper concentration does not significantly change solubility of the full-length ATP7B from *K. lactis* crude membranes in either 1:1 protein-detergent ratio (*w/w*; 0.2% of DDM) or 1:2 ratio (*w/w*; 0.4% of DDM).

ATP7B.K expressing yeast cells showed somewhat different protein compartmentalization. Membrane fraction pattern for cells grown with and without copper were similar to the cells expressing full-length ATP7B (two fractions without copper and three fractions with 1 mM $CuCl_2$); however protein distribution between the fractions was different, with higher relative amount of ATP7B.K in 50-65% fraction (Fig. 4.3, C-D).

Response to copper from the expressing host may serve as another indication of the recombinant ATP7B and variants function. To test this response, we have grown the transformed yeast on YPGal-agar plates supplemented with copper ranging from 0 to 5 mM.

Background strain of *K. lactis* and cells expressing ATP7B.K or Δ^{1-795}ATP7B all showed good growth at elevated copper levels. Because the gene of the endogenous *K. lactis* Cu-transporting ATPase, CCC2, is present in all transformants, the similar response to copper concentration may be due to CCC2 activity. However, the cells expressing ATP7B showed lower viability when copper content in the medium exceeded 2 mM and higher (Fig. 4.5). This may be caused by ATP7B suppressing the expression of the yeast CCC2 and not being able to function as effectively in yeast cells, for example, it might be unable to load cuproenzymes such as SOD properly. The recombinant ATP7B can also interfere with the endogenous copper transport pathway by not being able to transfer copper to yeast copper acceptors efficiently and competing for them with CCC2, undermining its function. Yeast cells may also lack some yet unknown effectors that would enable proper copper export by ATP7B from a cell, leading to excessive copper accumulation and toxicity. The

truncated constructs ATP7B.K or $\Delta^{1\text{-}795}$ATP7B expressed in *K. lactis* cells did not have the effect of the full-length enzyme on the yeast growth on high copper containing medium, which suggests that they do not interfere with the yeast metabolism in the same was as ATP7B does. The findings mentioned above suggest that the recombinant proteins, namely ATP7B, $\Delta^{1\text{-}795}$ATP7B and ATP7B.K, are not degraded and folded properly.

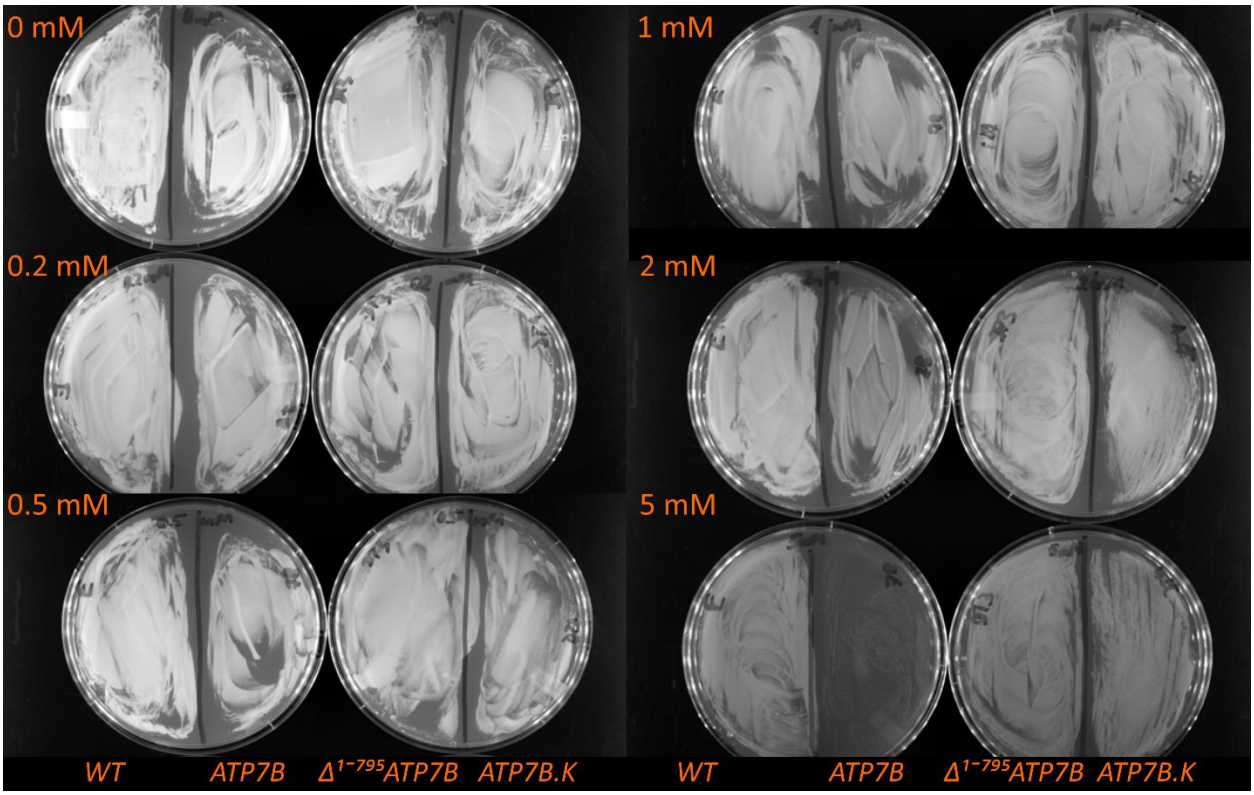

Figure 4.5: *K. lactis* yeast cells grown on YPGal-agar medium at various copper concentrations. Copper concentration is indicated to the left of each pair of plates; the expressed protein is indicated below each series of plates. WT – background strain (non-transformed).

Because the purification procedure – detergent treatment in particular – might have an adverse effect on enzymes, we also conducted ATPase activity measurements in 35-50% microsomes from the transformed yeast to see how the proteins behave in membrane environment, and how they compare with the activity of subsequently purified proteins. Because the host *K. lactis* cells have their own intrinsic copper ATPase, all measurements should be compared to the background strain.

The yeast expressing ATP7B showed significantly ($p < 0.05$) higher ATPase activity in their 35-50% membrane fraction than the background strain of yeast (Fig. 4.6 and Fig. 4.9). The activity in the membranes of ATP7B.K expressing yeast was comparable to that of ATP7B-expressing strain, also significantly ($p < 0.05$) higher than the background strain. This serves as an indication of activity of both of these constructs *in vivo* when expressed heterologously. The activity in the membranes of $\Delta^{1\text{-}795}$ATP7B expressing yeast was not different from that of the background strain of yeast (Fig. 4.8 and 4.9), but additional copper activated the enzyme (Fig. 4.9).

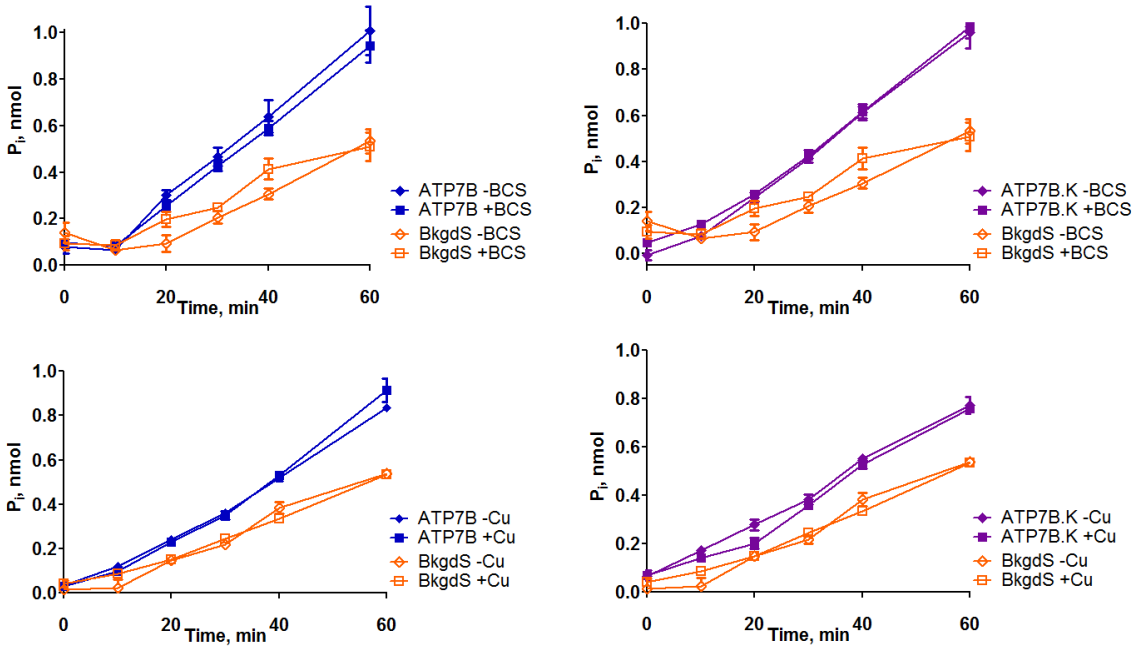

Figure 4.6: Time course of P_i production by 35-50% membrane fraction of background strain of *K. lactis* cells (BkgdS), ATP7B and ATP7B.K transformants: response to copper stimulation or BCS. The assay contained 14.3 ng of total membrane protein per reaction. Measurements were done in triplicates. Concentrations used are: copper 3 μM, BCS 100 μM

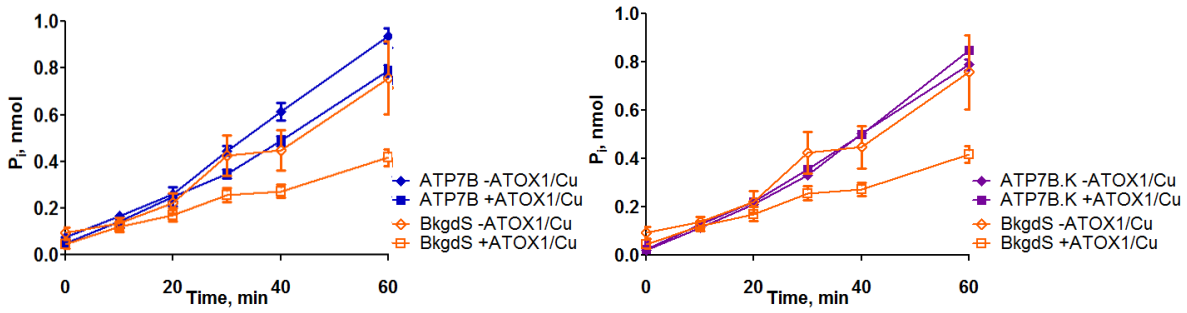

Figure 4.7: Time course of P_i production by 35-50% membrane fraction of background strain of *K. lactis* cells (BkgdS), ATP7B and ATP7B.K transformants: response to copper-ATOX1 stimulation. The assay contained 14.3 ng of total membrane protein per reaction. Measurements were done in triplicates. Concentrations used are: copper 3 μM, ATOX1 5 μM

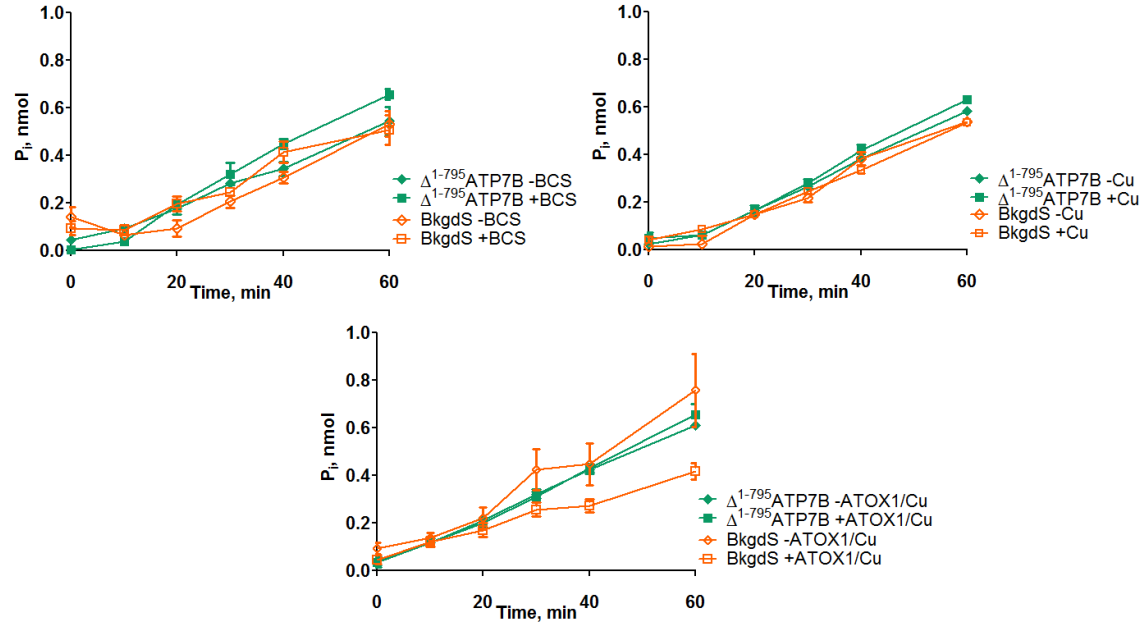

Figure 4.8: Time course of P_i production by 35-50% membrane fraction of background strain of *K. lactis* cells (BkgdS) and $\Delta^{1\text{-}795}$ATP7B transformants: response to copper, ATOX1-Cu stimulation or BCS. The assay contained 14.3 ng of total membrane protein per reaction. Measurements were done in triplicates. Concentrations used are: copper 3 μM, ATOX1 5 μM, BCS 100 μM

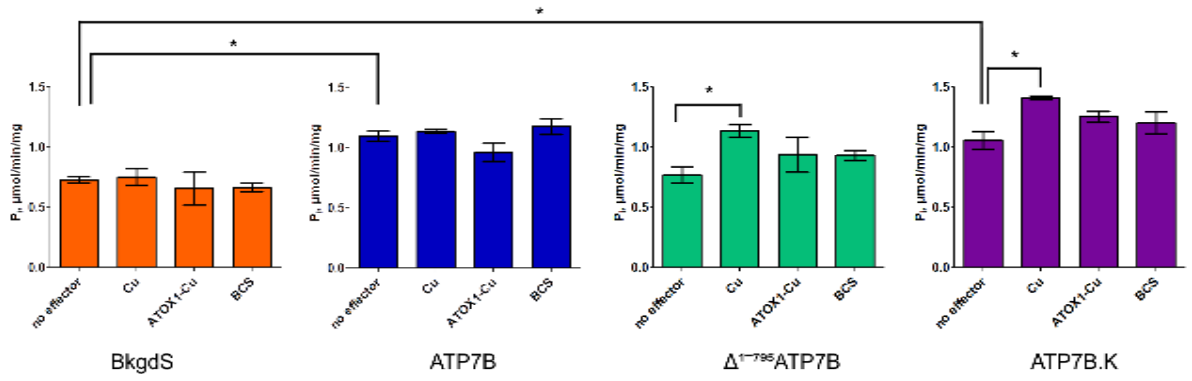

Figure 4.9: Comparison of specific ATPase activity in membranes of non-transformed yeast and yeast transformed with ATP7B, $\Delta^{1\text{-}795}$ATP7B and ATP7B.K. Specific activity is based on total microsomal protein amount. BkgdS – background strain.
Statistics include 6 (all "no effector" series), 2 ($\Delta^{1\text{-}795}$ATP7B/Cu and ATP7B.K/Cu series) or 3 (the rest) biological replicates, each biological replicate contains 3 technical replicates. Standard error of the mean is indicated by error bars.

In some experiments, ATOX1-Cu showed inhibiting effect on activity in the membranes of the background strain (Fig. 4.7), but increasing sampling size eliminated this difference (Fig. 4.9). The calculated specific activities with respect to total microsomal protein (Fig. 4.9) show similar rates for both ATP7B and ATP7B.K. However, because the amount of ATP7B in the membranes is usually around two times greater than the truncated constructs, the actual rate of ATPase activity of ATP7B.K in the membranes is probably higher than that of the full-length ATP7B.

It is worth noting that additional copper did not further activate the full-length ATP7B, and 100 µM BCS failed to inhibit activity in any of the membrane preparations (Fig. 4.6, fig 4.8 and Fig. 4.9). Other groups (Pilankatta *et al.*, 2009) also reported that much higher concentrations of BCS are needed for inhibition of copper-dependent ATPase activity in the microsomes. The K_d of BCS for copper is 10^{-20} M (Rae *et al.*, 1999), while for ATOX1 it is $10^{-17.4}$ M (Xiao and Wedd, 2010). The affinity of the enzyme to copper should be much higher than these, because even 1 µM residual copper in the reaction medium has been shown to stimulate the ATPase activity (Tsvikovskii *et al.*, 2002), and is the most probable reason for the lack of additional copper stimulation of the enzymes in our experiments.

4.2. Protein Purification of ATP7B and its Variants

Obtaining a protein of sufficient purity is essential for activity studies. Purification of membrane proteins usually presents a greater challenge than that of soluble proteins, because it requires solubilisation of a protein of interest with an empirically chosen detergent. Some detergents can have detrimental effect on the enzymatic activity due to excessive delipidation and conformational alterations of the enzyme. It is generally more difficult to achieve high purity with membrane proteins than with soluble ones.

Previous attempts to solubilize ATP7B in membranes obtained from *K. lactis* cell in various detergents (Dolgova, unpublished data) showed that only lysomyristoyl phosphatidyl glycerol (LMPG) and chemically similar detergents (lysopalmitoyl phosphatidyl glycerol, LPPG) were capable of complete or near-complete solubilisation of the protein. Treatment of the yeast cells with copper did not change the solubility properties of ATP7B from different membrane fractions (Dolgova, unpublished data). Immunoblots (figs. 4.3 and 4.5) demonstrated that there is no effect of elevated copper on ATP7B synthesis, and only slight increase in ATP7B.K synthesis. The ATP7B.K amount in 50-65% membrane fraction of copper-treated yeast (Fig. 4.3, panel D, lane 50/65) per microgram of total protein fraction is greater than in other fractions, but the relative volume of 50-65% fraction is small in comparison with other fractions. Therefore, we concluded that copper treatment is not a required step for protein purification, and should not be used.

Typically, purification of membrane proteins involves several steps, including isolation of a membrane fraction from the host cells, treatment of these membranes with a detergent to solubilise the protein of interest, subsequent purification on affinity medium, and often a secondary purification step (size-exclusion chromatography or additional affinity step). Initial purification protocol for His_6-ATP7B was developed in our lab (Dolgova and Dmitriev, unpublished data) and employed sorbitol-based buffer, 1% LMPG as a solubilising agent, and Ni-NTA affinity purification.

The purification process for ATP7B and its variants consists of several steps. First, the grown yeast cells are collected by pelleting at low speed. Then the cell mass is suspended in a buffer with protease inhibitors and disrupted in cell disruptor, and the crude membrane fraction is

extracted by a series of centrifugation steps. The resulting membrane fraction can be either separated further using sucrose gradients (ATP7B) or taken as is for detergent treatment to solubilise the proteins of interest. The protein-detergent mixture is then subjected to Ni-NTA affinity chromatography, where a partially pure protein is obtained. In order to increase the purity, the protein is concentrated and subjected to size-exclusion chromatography. The fractions that contain larger amounts of the protein of interest and smaller amounts of contaminants are collected, pooled together and concentrated.

In order to get ATP7B and its variants at sufficient purity, we have undertaken a series of optimization steps, which have enabled us to enhance the purity of ATP7B. This included using a glycerol-based buffer instead of sorbitol-based, reducing detergent treatment time, and increasing salt concentration and shifting elution pH to 8.5 at the stage of affinity chromatography. Both Ni-NTA affinity chromatography and size exclusion chromatography are necessary to get protein of reproducible purity. Affinity purification on Ni-NTA produces the protein of 20%-30% purity (Fig. 4.10), while the additional size-exclusion step increases the purity up to 70%-80% (Fig. 4.11). In addition, the size exclusion chromatography serves as imidazole removal step, eliminating need for buffer exchange or dialysis, which is a lengthier process.

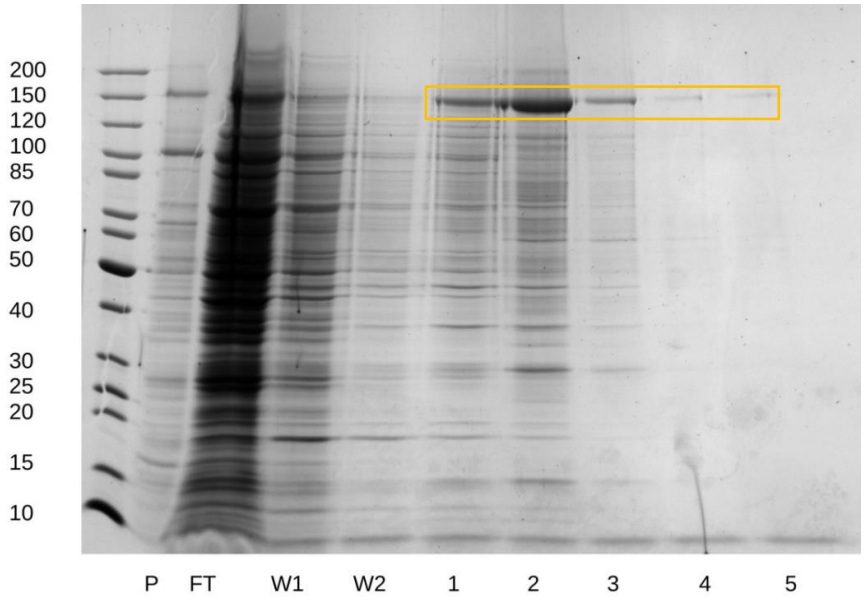

Figure 4.10: Purification of ATP7B by Ni-NTA affinity chromatography of crude membrane extract. P – insoluble fraction; FT – column flow-through, W1-W2 – column wash fractions; 1-5 – column elution fractions. Orange box indicates the ATP7B protein in the elution fractions. The samples were analyzed by SDS-PAGE followed by Coomassie staining.

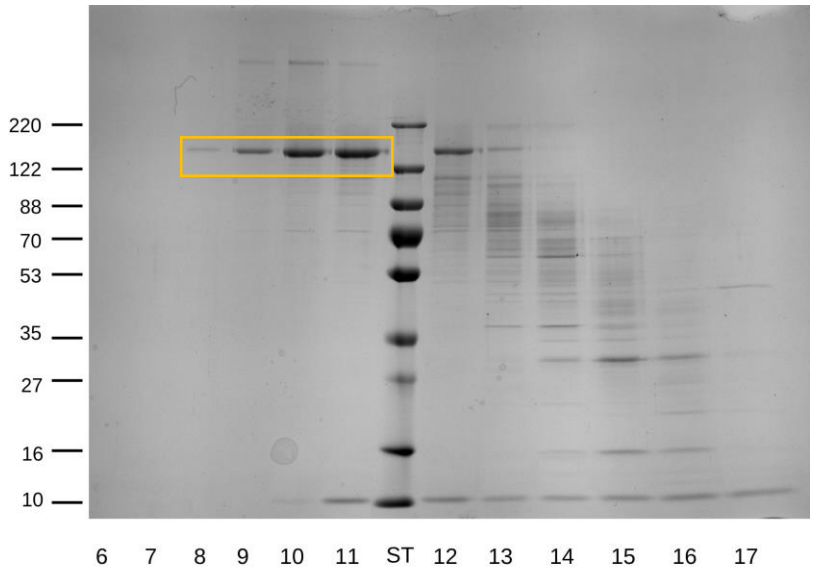

Figure 4.11: Purification of Ni-NTA-purified ATP7B by size-exclusion chromatography. ST – molecular weight standard; 6-17 – elution fractions. Orange box indicates the ATP7B protein in the elution fractions which were pooled for concentrating. The samples were analyzed by SDS-PAGE followed by Coomassie staining.

ATP7B.K has a very different structure, so we have tested its properties with respect to solubilisation in various detergents to establish the most suitable candidate. Because none of the alternative detergents were as effective as LMPG (Fig. 4.12), this detergent was selected for further purification of ATP7B.K and the very similar Δ^{1-795}ATP7B.

Because ATP7B.K and Δ^{1-795}ATP7B have different domain composition compared to the full-length ATP7B, they behave differently during purification process. First, as can be seen below (Fig. 4.12), ATP7B.K is somewhat less soluble in comparison to ATP7B (Fig. 4.4) even with 1% of LMPG. The same is valid for Δ^{1-795}ATP7B, which, in our experience, behaves very similarly to ATP7B.K during expression and purification.

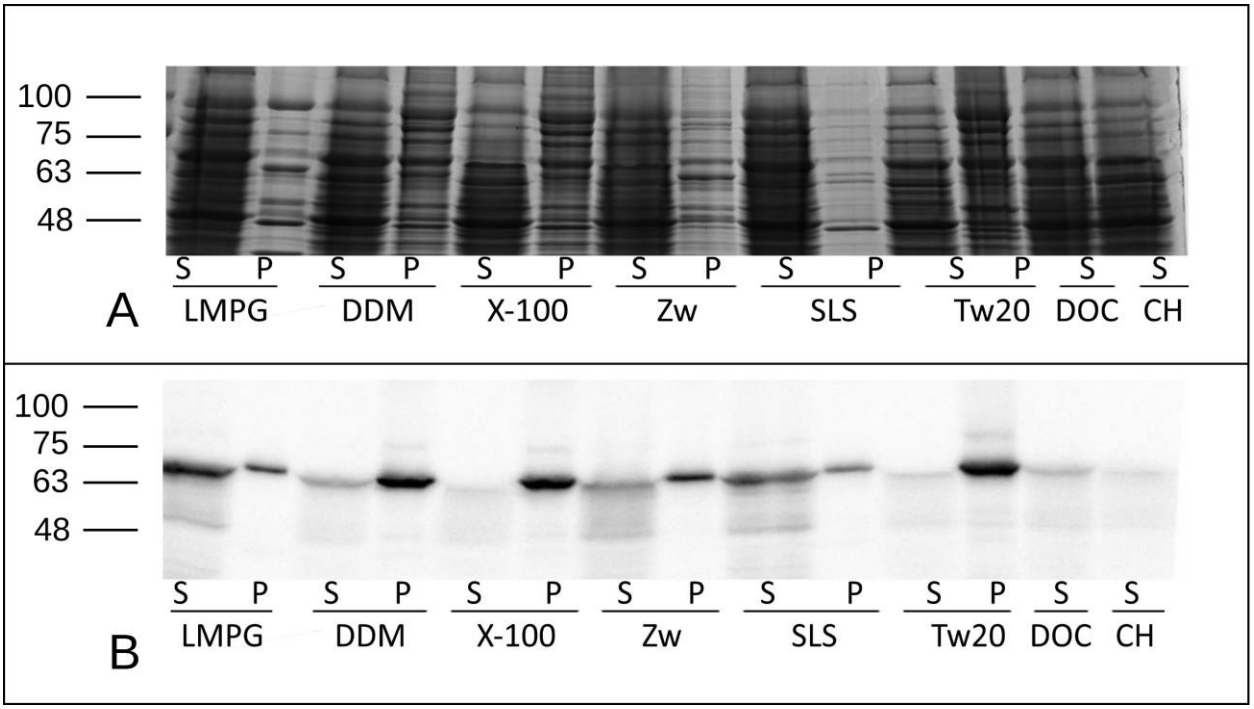

Figure 4.12: Solubilisation of the recombinant ATP7B.K protein from crude membrane fraction of *K. lactis* cells. Crude membrane fractions were solubilised in various concentrations of DDM and LMPG.
A – Coomassie stain; *B* – Western blot with anti-PentaHis antibody
S – soluble fraction, P – insoluble fraction; X-100 – Triton X100; Zw – Zwittergent 3:18; SLS – sodium lauroyl sarkosinate; Tw20 – Tween 20; DOC – deoxycholate sodium salt; CH – CHAPS. Insoluble fractions resulter from treatment with deoxycholate and CHAPS are not shown

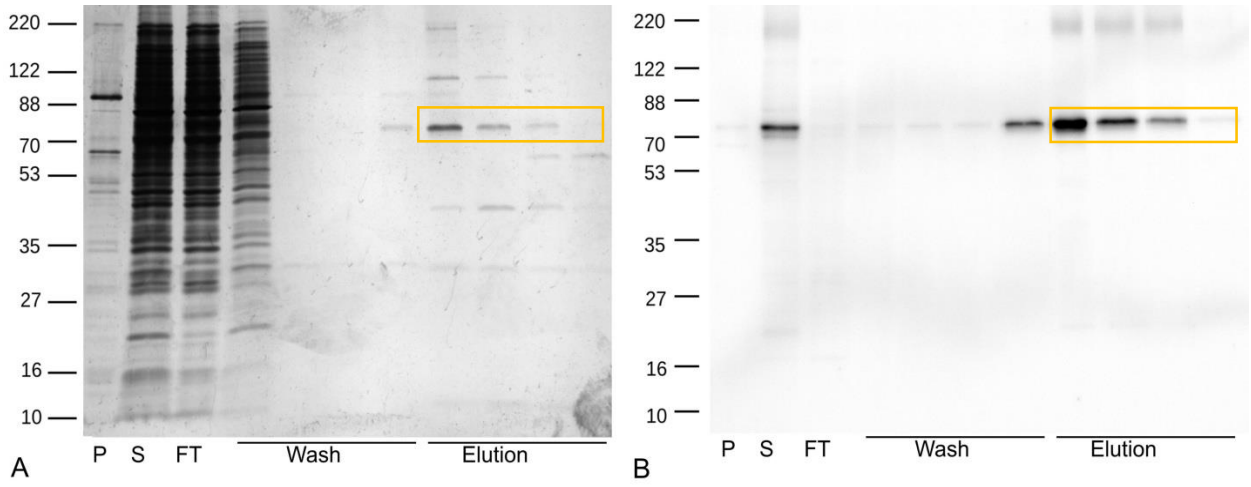

Figure 4.13: Purification of $\Delta^{1\text{-}795}$ATP7B by Ni-NTA affinity chromatography of crude membrane extract. P – insoluble fraction; S – soluble fraction; FT – column flow-through. Orange box indicates the $\Delta^{1\text{-}795}$ATP7B protein in the elution fractions. The samples were analyzed by SDS-PAGE followed by silver staining (panel A) and Western blot with anti-PentaHis HRP-conjugated antibody (Qiagen) (Panel B).

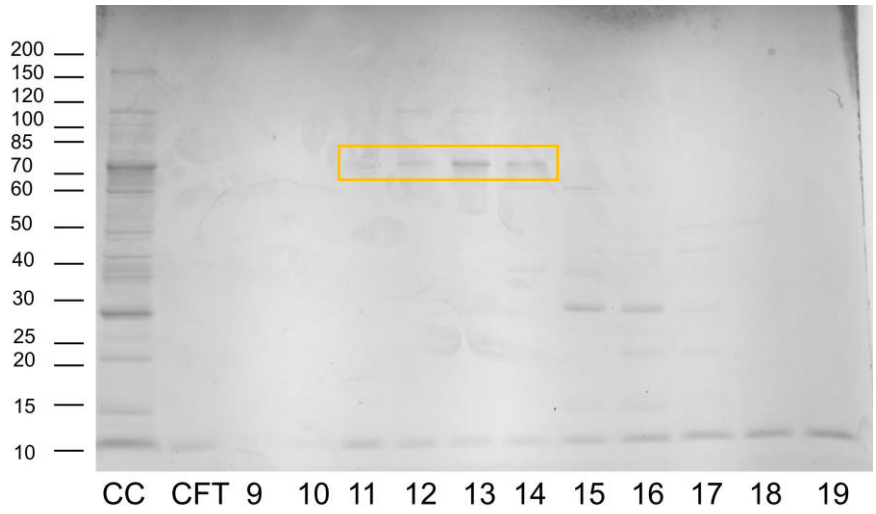

Figure 4.14: Purification of Ni-NTA purified $\Delta^{1\text{-}795}$ATP7B by size-exclusion chromatography.
CC – $\Delta^{1\text{-}795}$ATP7B concentrated after the Ni-NTA purification; CFT – concentrator flow-through; 9-19 – elution fractions. Orange box indicates the $\Delta^{1\text{-}795}$ATP7B protein in the elution fractions which are collected for concentration. The samples were analyzed by SDS-PAGE followed by Coomassie staining.

Ni-NTA purification of $\Delta^{1\text{-}795}$ATP7B (Fig. 4.13, panel A) usually yields protein of less than 15% purity (Fig. 4.14, lane CC), while the size exclusion chromatography helps to increase the

purity up to 30%-40% (Fig. 4.14, lanes 11-14). Δ^{1-795}ATP7B binds less tightly to the Ni-NTA agarose, and therefore lower concentration of imidazole (80 mM) is needed for efficient elution. As a side effect this leads to lower purity of the eluted protein in comparison to ATP7B.

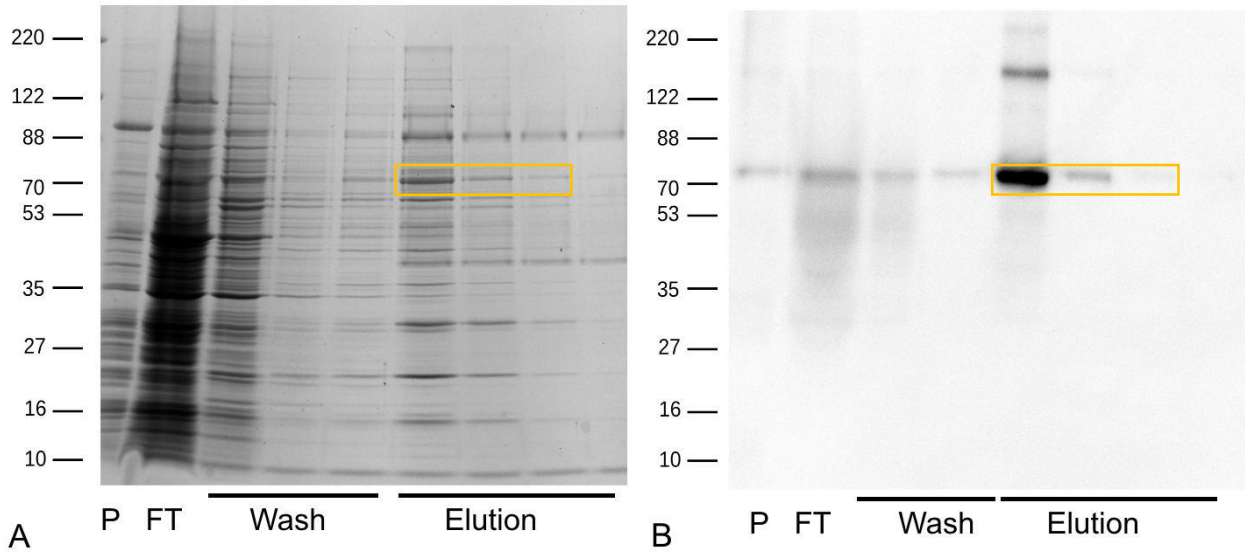

Figure 4.15: Purification of ATP7B.K by Ni-NTA affinity chromatography of crude membrane extract.
P – insoluble fraction; FT – column flow-through; W1-2 – column wash fraction; 1-6 – column elution fractions. Orange box indicates the ATP7B.K protein in the elution fractions. The samples were analyzed by SDS-PAGE followed by followed by Coomassie staining (pane A) and Western blot with anti-ATP7B H-94 antibody (Santa Cruz Biotechnology) + anti-rabbit IgG (ThermoFisher Scientific) (Pane B).

A very similar observation can be made concerning the purification of ATP7B.K. The Ni-NTA purification produces a protein with a very low degree of purity, as low as 6% (Fig. 4.15, panel A). The size-exclusion step helps to achieve purity similar to that of Δ^{1-795}ATP7B, in the range of 30%-40% (Fig. 4.16).

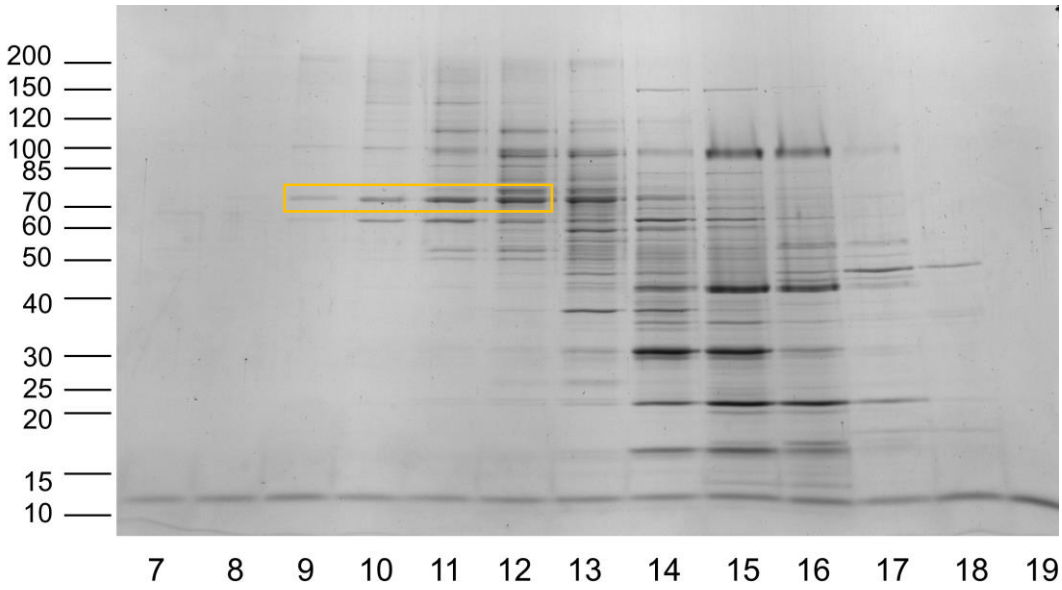

Figure 4.16: Purification of Ni-NTA purified ATP7B.K by size-exclusion chromatography.
7-19 – elution fractions. Orange box indicates the ATP7B.K protein in the elution fractions which are collected for concentration. The samples were analyzed by SDS-PAGE followed by Coomassie staining.

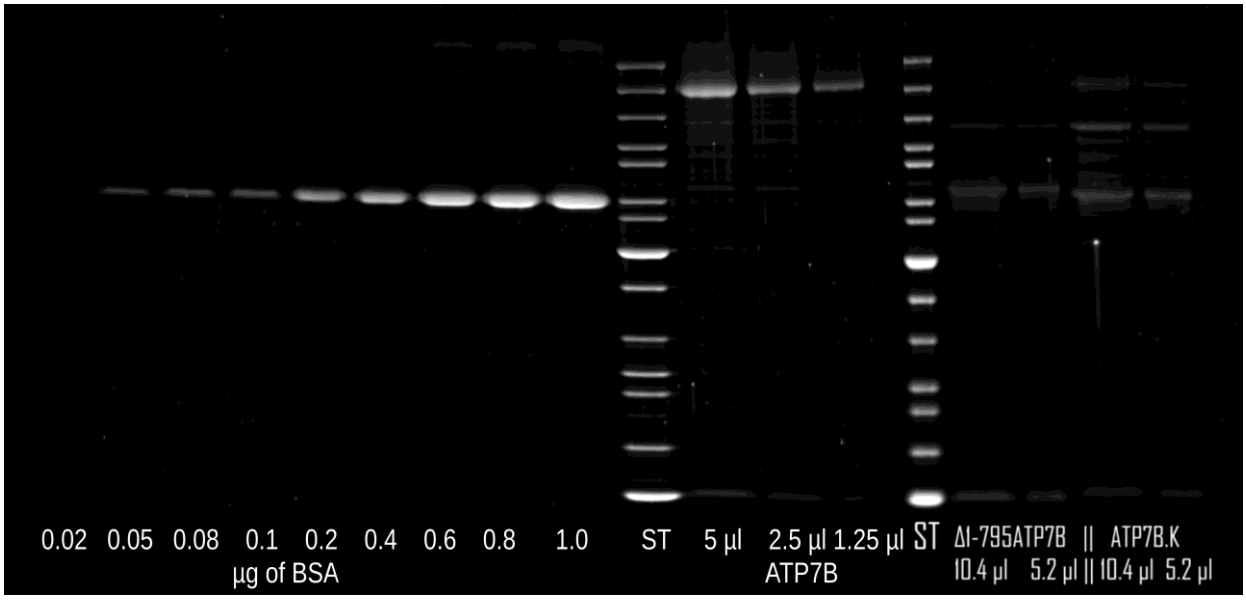

Figure 4.17: SYPRO Ruby stained SDS polyacrylamide gel of purified ATP7B and its variants. ST – molecular weight standard, quantities of BSA in micrograms and microliters of purified ATP7B are indicated below the corresponding lanes. Quantity standards used for ATP7B.K and $\Delta^{1\text{-}795}$ATP7B are not shown.

In order to correctly assess specific activity of an enzyme, one has to know the exact protein concentration. Hence, reliability of protein quantification is of utmost importance. Our method of

choice for quantification of ATP7B and its variants was in-gel staining using SYPRO Ruby fluorescent dye. SYPRO Ruby is a sensitive dye with linear quantification range of over three orders of magnitude (Invitrogen, 2007), which shows consistent results for different protein types. By running a set of protein standards along with the sample, it is possible to determine the quantity of the protein of interest with good precision, even in the presence of contaminating proteins.

Due to generally lower expression levels of the truncated proteins, as well as weaker biding to the Ni-NTA agarose, the overall yield and purity are lower than those of the full-length ATP7B.

According to the in-gel quantification, protein yield was 0.10 – 0.15 mg of protein per 1 L of cell culture for ATP7B and 0.05 – 0.08 mg of protein per 1 L of cell culture for the truncated variants (ATP7B.K and $\Delta^{1\text{-}795}$ATP7B). Low yield is not unusual for membrane proteins, which are known to be produced in lower quantities than soluble proteins. The densitometry-based purity of the samples is as follows: ATP7B – 75%, $\Delta^{1\text{-}795}$ATP7B – 51%, and ATP7B.K – 41% (Fig. 4.17).

4.3. ATPase Activity of the Purified ATP7B and its Truncated Variants

ATPase activity of the three purified enzymes was assayed using the malachite green phosphate detection assay. It is the most sensitive colourimetric assay that can be used for the purpose of characterization of ATPase activity of an enzyme. The method (Baykov *et al.*, 1987; Singh and Shukla, 2003) is suitable for detection of inorganic phosphate in amounts as low as 10 nmol of P_i per millilitre. Previous reports on the activity of purified and reconstituted $\Delta^{MBD1\text{-}5}$ATP7B (Portmann and Solioz, 2005) showed P_i production of 50-240 nmol of phosphate per mg of protein. Hence, this assay sensitivity was likely to be sufficient for our purposes.

MES buffer, pH 6.0, with 3 mM $MgCl_2$ was selected as a reaction medium, because pH 6.0 was reported previously as more favourable for the P_{IB}-ATPases phosphorylation by ATP (Solioz and Odermatt, 1995; Tsvikovskii *et al.*, 2002). Our initial setting contained TCEP as a reducing agent for disulphide bonds, and ascorbic acid as a reducer of copper to ensure all copper stays in +1 oxidation state. To compare kinetic properties of the ATP7B and its variants, a time course measurement is needed. From P_i accumulation curve it is possible to establish initial rate of reaction, which enables characterization of enzyme activity. But since no favourable conditions were known for our purified proteins, these had to be probed first with a single time point experiment.

The purified proteins were reconstituted into asolectin liposomes, to provide more natural environment for the enzymes.

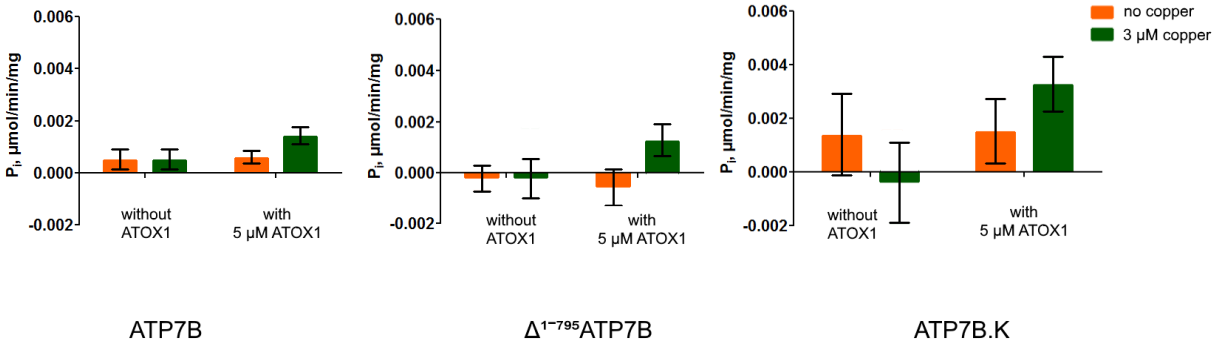

Figure 4.18: Specific activity of ATP7B and its variants reconstituted into asolectin liposomes estimated from single point measurements in MES buffer with 1 mM ascorbic acid and 100 µM TCEP. All measurements were done in triplicates; reaction time was 20 minutes. Specific activity is based on total protein amount in the purified samples.
Statistics include 3 technical replicates. Standard error of the mean is indicated by error bars.

First, we tested ATPase activity of proteins, reconstituted into asolectin liposomes, in MES buffer supplemented with 1 mM ascorbic acid, which would reduce all oxidized copper to Cu(I), and 0.1 mM TCEP, which is needed in order to reduce disulphide bonds involved in copper binding in the proteins. Cu(I) is a transport substrate of the enzymes, and is needed to activate ATP hydrolysis coupled to copper transport. ATOX1 is known to supply ATP7B with copper, presumably activating it. However, specific activity in the presence of ascorbic acid and TCEP (MES-AT) was very low for all three proteins and was in the nanomol/min/mg range (Fig. 4.18), and was lower than what has been found in literature regarding the activity of $\Delta^{MBD1\text{-}5}$ATP7B (Portmann and Solioz, 2005) and ATP7B in microsomes (Pilankatta *et al.*, 2009). ATOX1-copper seemed to have certain stimulating effect on the enzymes, ATP7B and $\Delta^{1\text{-}795}$ATP7B in particular. Due to the very low activity, which was on the lower edge of detection of the system, there was low signal-to-noise ratio, and as a consequence big scatter in data point values between repeats. As a result, no statistically significant ($p < 0.05$) differences can be observed.

Ascorbic acid in the presence of transition metals can have detrimental effect on lipids and proteins by free radical damage (Buettner and Jurkiewicz, 1996). In MES buffer without ascorbic

acid (MES-T), we observed approximately tenfold higher specific activity than with ascorbic acid (Fig. 4.19). There was no stimulatory effect of ATOX1-copper on ATP7B and ATP7B.K. Higher signal provided less scatter, and the quality of data was better.

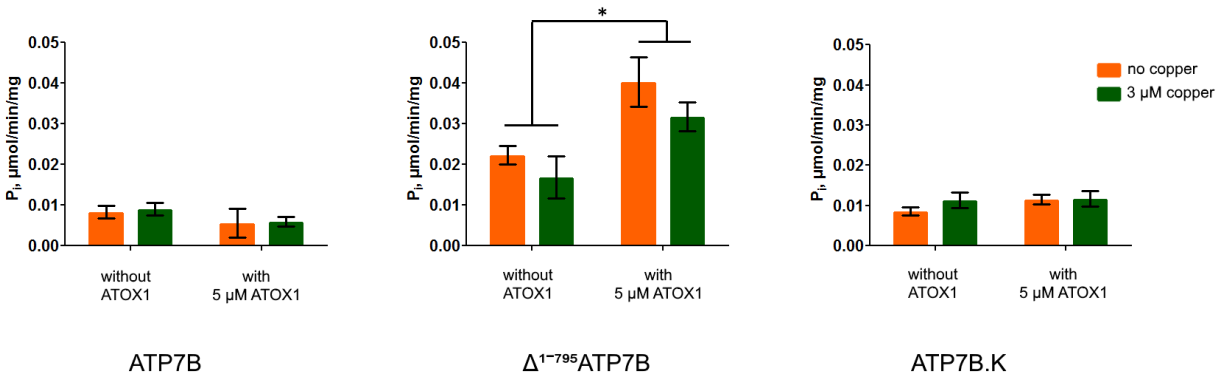

Figure 4.19: Specific activity of ATP7B and its variants reconstituted into asolectin liposomes estimated from single point measurements in MES buffer with 100 µM TCEP. All measurements were done in triplicates; reaction time was 30 minutes. Specific activity is based on total protein amount in the purified samples. Statistics include 3 technical replicates. Standard error of the mean is indicated by error bars.

However, statistically significant ($p < 0.05$) difference is observed only for the effect of ATOX1 on $\Delta^{1\text{-}795}$ATP7B: the copper chaperone shows stimulating effect, however, it still does not depend on copper. This effect may be because contaminating copper amounts are sufficient to activate $\Delta^{1\text{-}795}$ATP7B, and additional copper does not contribute to the reaction rate. The assay buffer without ascorbate appeared to be more favourable for ATP7B and its variants, so it was chosen for the time course measurements.

The time course experiments compared the activity of the purified enzymes in two conditions: 1) in the MES-T buffer, and 2) in the MES-T buffer with copper-loaded ATOX1. The proteins activity was measured in detergent, because reconstitution into liposomes made it difficult to achieve protein quantity in the reaction mixture sufficient for a reproducible good signal to noise ratio. The observed difference in P_i accumulation curves is very small, which supports the idea that residual copper in the buffer is sufficient to activate the enzymes (Fig. 4.20). ATOX1-Cu showed a slight inhibition trend on ATP7B and ATP7B.K. There's a discrepancy with the single time point measurement in case of the $\Delta^{1\text{-}795}$ATP7B: ATOX1 did not activate the enzyme. This may be because additional copper exhibited an inhibitory effect on enzyme. Similar behaviour was

reported for human Δ^{MBD1-5}ATP7B purified from *S. cerevisiae* (Portmann and Solioz, 2005), albeit in higher copper concentration.

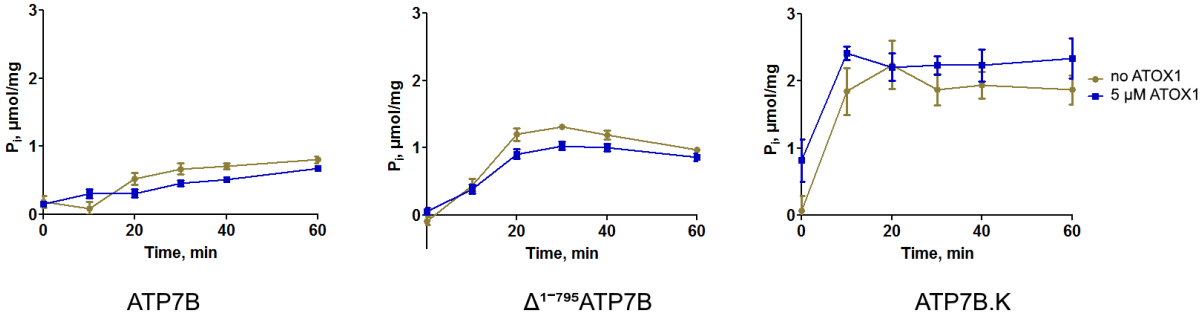

Figure 4.20: Time course of P_i production by ATP7B and its two variants in MES buffer with 100 µM TCEP. Measurements were done in triplicates. Specific activity is based on amount of total protein in purified sample.

An assay with higher sampling frequency was needed to see the P_i accumulation details within the 10 minutes period (Fig. 4.21), because this enzyme shows much faster rates than ATP7B or Δ^{1-795}ATP7B. The non-linear character of kinetic curves is traditionally explained by transported substrate depletion, ATP exhaustion or inhibition by the product of reaction. Substrate or ATP depletion is unlikely in our experimental system, but inhibition by ADP or Cu^{2+} is possible.

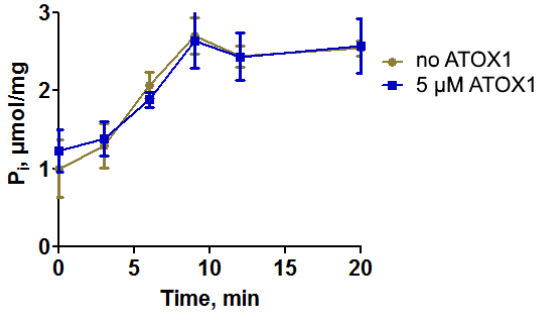

Figure 4.21: Time course of P_i production by ATP7B.K in MES buffer with 100 µM TCEP, smaller time step. Measurements were done in triplicates. Specific activity is based on amount of total protein in purified sample.

The calculated initial rates for the purified enzymes measured in detergent are: 0.010-0.015 µmol/min/mg for the full-length ATP7B, 0.090-0.130 µmol/min/mg for Δ^{1-795}ATP7B, and 0.400-0.500 µmol/min/mg for ATP7B.K. These rates are based on quantities of the corresponding proteins as assessed by SYPRO Ruby in-gel quantification. The numbers for activity of the full-length protein are similar to the measurements conducted by previous groups (Portmann and Solioz, 2005).

First of all, it should be noted that the activity of ATP7B after purification is considerably lower than the activity that can be estimated from the microsomal measurements. It means that the enzyme is either severely inhibited by the purification process or detergent, or that it misses important yet unknown additional factors, which are absent in our *in vitro* system. The same holds true for ATP7B.K. Purified $\Delta 1^{-795}$ATP7B shows activity rates comparable to those of the other two constructs even without added copper.

4.4. Development of Copper Transport Assay for ATP7B Using CS-1 Fluorescent Sensor

The substrate transport activity of a membrane-embedded transporter molecule can be measured either in membrane vesicles (microsomes), or in liposomes. Measurements in the vesicles require the transporter molecule to be unique in the organism used for expression, or the transporter to have an efficient specific inhibitor so that a clear control experiment can be made. The advantage of this approach is that one does not have to purify the protein from the membrane. Liposomes, on the other hand, have an advantage of a strictly controlled environment. Because *K. lactis* has the intrinsic CCC2 copper transporter, we used the liposomes method. The most widely used approach for measurements of copper transport involves radioactive copper isotope ^{64}Cu (Dancis *et al.*, 1994; Solioz and Odermatt, 1995; Voskoboinik *et al.*, 1998). However, this method is complicated by the fact that ^{64}Cu half-life is only 12.7 hours, making such measurements logistically difficult.

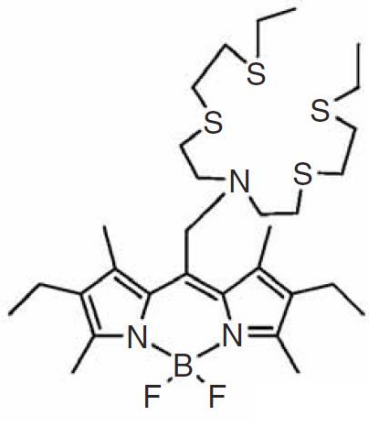

Figure 4.22: Chemical structure of CS-1 (Li *et al.*, 2005)

Thus, in order to study the copper transport properties of the ATP7B and its variants, we had to develop a novel method, which would rely on stable compounds and would be sensitive enough to detect slight changes in copper concentrations.

CS-1 (Fig. 4.22) is a synthetic organic dye developed previously (Zeng *et al.*, 2006). It was designed specifically for studies of copper in living tissues. It is water soluble and highly selective

towards Cu^+. It was found to be able to penetrate cell membrane and bind intracellular copper; CS1:Cu^+ complex can be detected by fluorescence emission at 560 nm (excitation wavelength – 540 nm). The complex of the dye with copper is charged and cannot cross the membrane.

Preliminary studies conducted in our lab (O'Grady and Dmitriev, unpublished data) found that reducing agents, DTT in particular, quench the fluorescence of CS-1. We tested the CS-1 assay for compatibility with the MES buffer with ascorbate and TCEP that was used to measure ATPase activity of the ATP7B and its variants at the time of assay development.

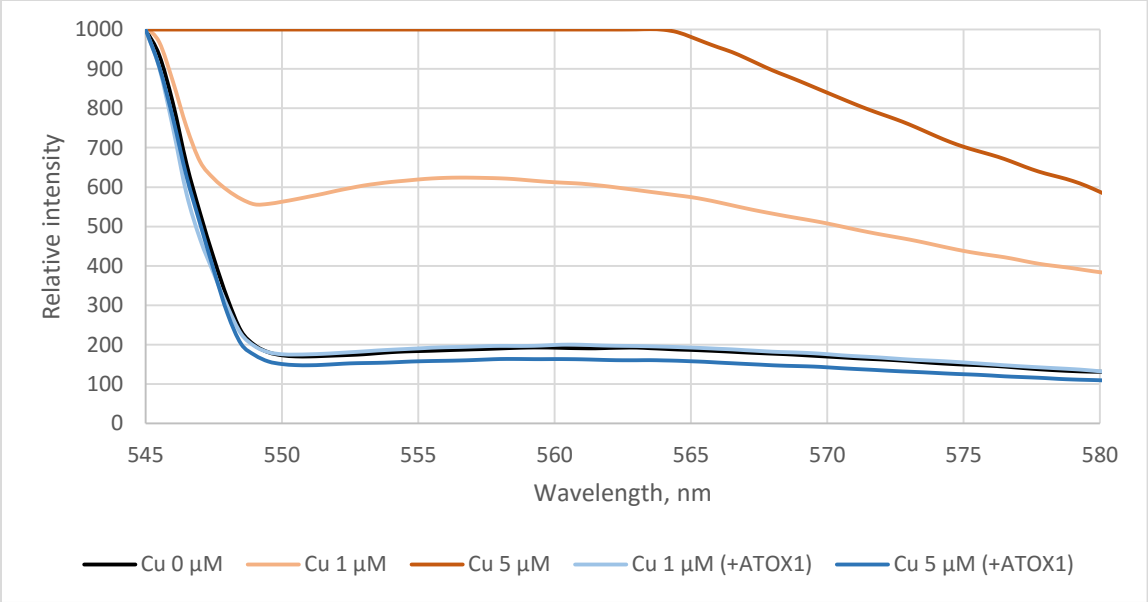

Figure 4.23: Dependence of CS-1 fluorescence in response to various copper and copper-ATOX1 concentrations in MES-AT buffer. Copper concentrations are colour-coded with corresponding values displayed. CS-1 was used in 0.2 µM concentration.

In MES buffer with 1 mM ascorbic acid and 0.1 mM TCEP (MES-AT) CS-1 showed a response to 1 µM and higher [Cu^+] with maximum fluorescence at 556 nm (Fig. 4.23). In order to test whether CS-1 could also sense copper bound to ATOX1, we have tested the sensor in the same conditions with ATOX1 preloaded with copper. Fluorescence measurements of CS-1 with ATOX1-Cu showed no significant fluorescent response from the sensor to copper bound to ATOX1 (Fig. 4.24). This means that the binding affinity of ATOX1 for copper is much higher than that of CS-1, so the sensor cannot detect copper bound to ATOX1.

Even though the sensor should bind copper in a 1:1 ratio, we still can observe a response even when the concentration of copper exceeds the concentration of CS-1. This may be because CS-1 appears to form colloid particles in solution (Dolgova and Dmitriev, unpublished data), thus lowering the effective concentration of the sensor.

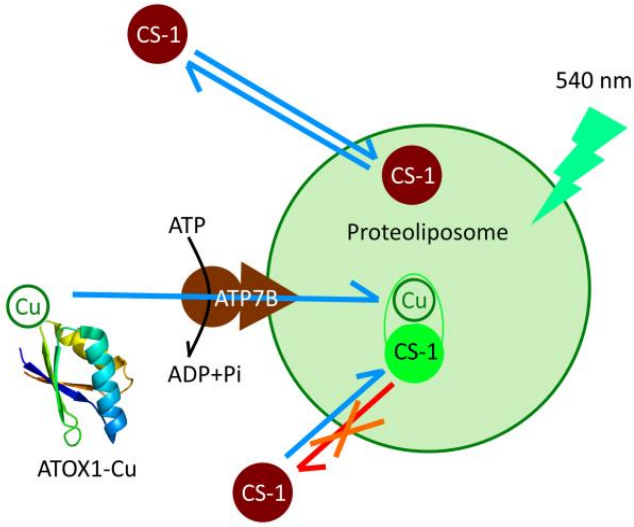

Figure 4.24: Principle scheme of CS-1 fluorescence copper transport assay. Before the start of the reaction copper is bound to ATOX1. After the reaction is initiated by the addition of ATP, copper is pumped by ATP7B across the membrane into the proteoliposome. Uncharged free CS-1 can go across the lipid bilayer of a proteoliposome in both directions, while CS-1 that binds the intraliposomal copper stays inside and can produce fluorescent response to irradiation with green (540 nm) light.

These findings led us to the idea that CS-1 might be a suitable *in vitro* copper probe for the studies of copper transport activity of ATP7B and its variants in proteoliposomes. In our system, copper is supplied to the ATP7B integrated into proteoliposomes by ATOX1. Outside proteoliposomes, all the copper is bound to ATOX1 and will not be detected by CS-1. ATP7B will accept copper from ATOX1 and transport it inside the proteoliposomes. Copper ions would not be able to cross the lipid bilayer back into the solution. Metal free CS-1 on the other hand is amphiphilic and will diffuse across the lipid bilayer into the proteoliposome lumen, where it will bind copper. The CS-1 complex with copper is charged and cannot cross the lipid membrane. Thus, CS-1-Cu will be trapped inside the proteoliposomes and detected by fluorescence readout. (Fig. 4.24).

Amphiphilic nature of CS-1 makes it necessary to take into account CS-1-lipid interactions. To investigate how CS-1 responds to copper in the presence of lipids, we tested CS-1 mixed with liposomes made of asolectin from soybean or polar lipid from rat liver.

The behaviour of the sensor in the presence of liposomes was much more complex than without lipid. In the system with asolectin liposomes CS-1 showed a considerably lagged response to free copper (Fig. 4.25), while in the system with liver lipid there was a significant fluorescence of the sensor in the sample with ATOX1-bound copper (Fig. 4.26).

The latter can be explained by the fact that ATOX1 may interact with liver lipids, so interactions with lipid can change affinities of ATOX1 and CS-1 for copper, resulting in copper transfer from ATOX1 to CS-1 which was not observed in aqueous phase. The association of ATOX1 with lipids has been shown before (Flores and Unger, 2013).

These results indicate that asolectin lipids are preferable to liver lipid for our transport assay because the latter stripped copper from ATOX1 increasing background fluorescence, which could further complicate the interpretation of data and would require more controls to be done. Also, it became apparent that the system needed about 10 min equilibration time before initiating the reaction, so that CS-1 would partition completely between aqueous and lipid phases and fluorescence would stabilize.

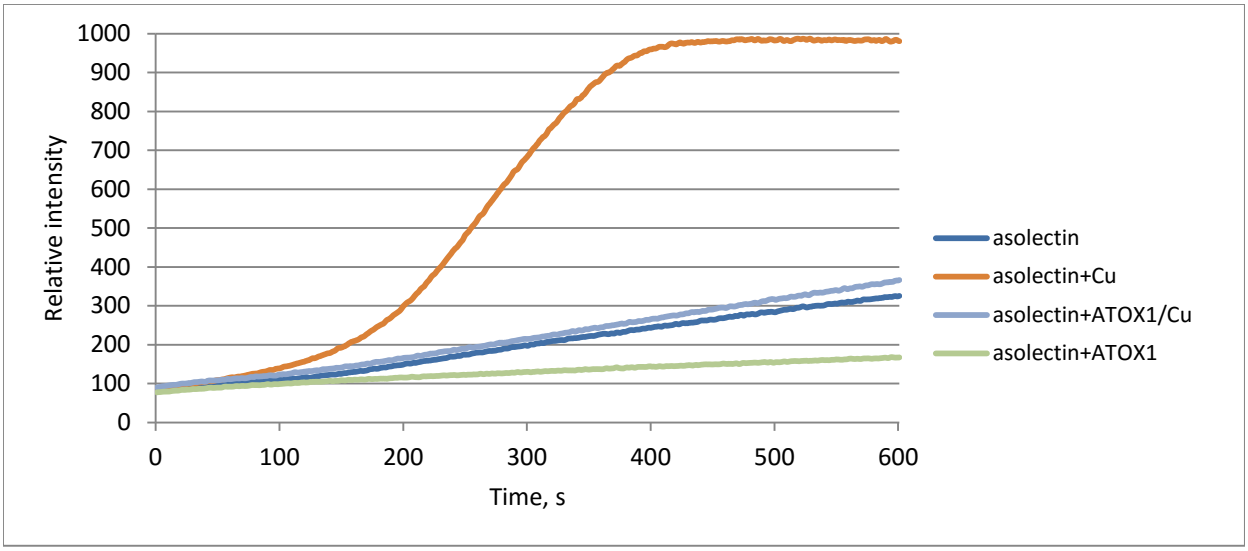

Figure 4.25: Time course of CS-1 response to different combinations of asolectin, 5 µM ATOX1 and 3 µM Cu^{+} in MES buffer with 1 mM ascorbate and 0.1 mM TCEP. CS-1 was 0.3 µM. Each reaction contained 625 µg of lipid in 1 mL volume. Fluorescence emission at 556 nm was measured at 1 second interval.

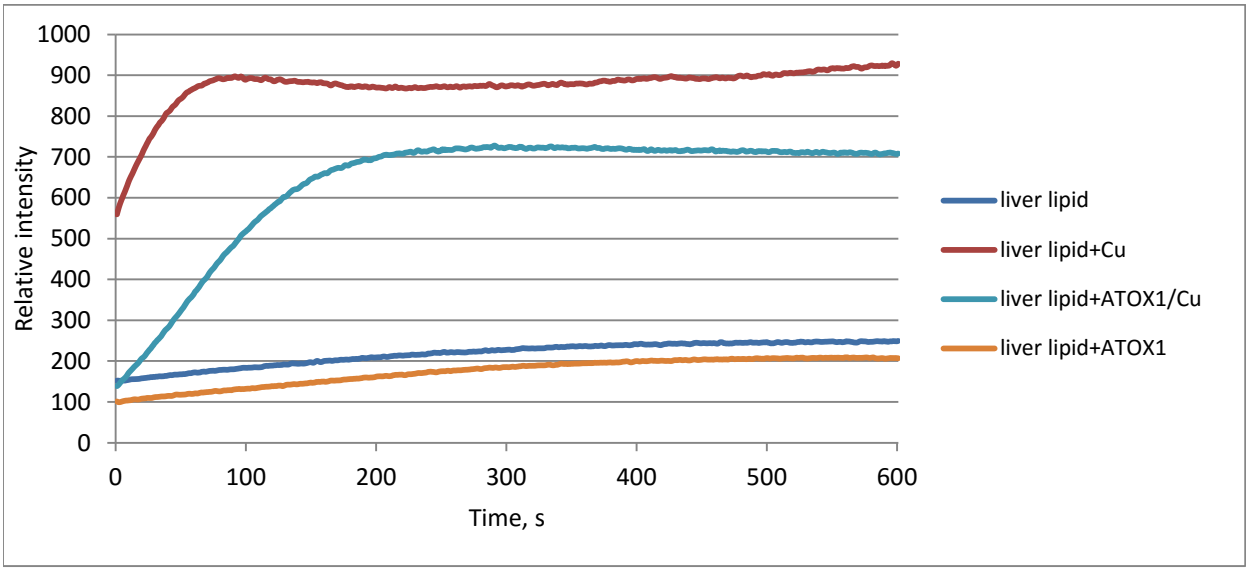

Figure 4.26: Time course of CS-1 response to different combinations of liver lipid, 5 µM ATOX1 and 3 µM Cu^{+} in MES buffer with 1 mM ascorbate and 0.1 mM TCEP. CS-1 was 0.3 µM. Each reaction contained 625 µg of lipid in 1 mL volume. Fluorescence emission at 556 nm was measured at 1 second interval.

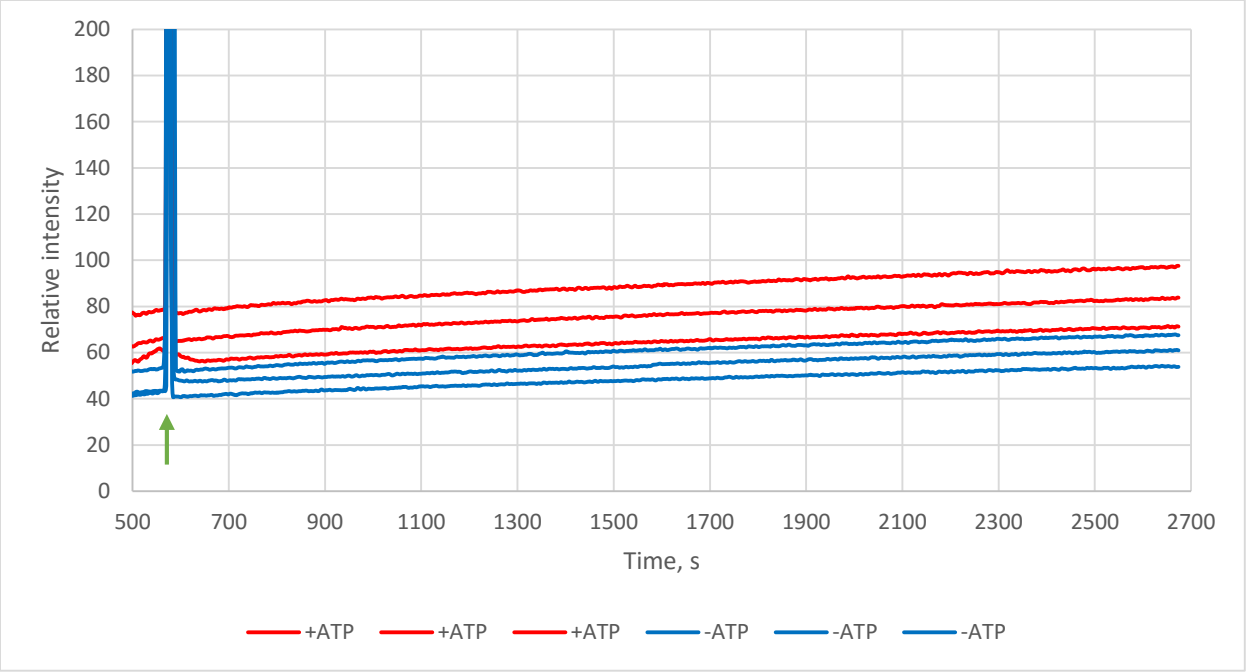

Figure 4.27: Time course of CS-1 response to transport activity of ATP7B reconstituted into asolectin liposomes in MES-AT buffer. ATOX1 was 5 μM, Cu^{+} was 3 μM, CS-1 was 0.3 μM. Each reaction contained 128 μg of lipid and 1.28 μg of incorporated ATP7B in 0.6 mL volume. Measurements with and without ATP were done in triplicates (displayed). Arrow indicates moment of ATP or buffer addition, with a spike produced due to mixing with a pipette. Fluorescence emission at 556 nm was measured at 2 seconds interval.

Even with the equilibration stage, the change in fluorescence response between samples supplemented with ATP and control samples was negligible (Fig. 4.27), and it was not possible to detect ATP-dependent copper transport activity. One possible reason is that the CS-1 sensitivity is insufficient to detect small change that was produced by ATP7B. An additional serious complication is the complex interactions of the CS-1 and the lipids, which could mask or alter the fluorescent response of the sensor. Quite a low amount of protein that was available for several repeated measurements and relatively big reaction volume (minimum 0.5 mL) may be the other reasons for undetectable change in fluorescence.

4.5. Detection of the Putative Copper Transporter PINA in Rat Pineal Gland

PINA is a putative truncated version of ATP7B. Its mRNA was detected in extracts of pineal gland of *R. norvegicus*. Its domain composition predicted from the mRNA sequence is rather

unusual: the whole N-terminal segment containing metal-binding domains and first four transmembrane helices is missing. To establish whether this mRNA is translated into a protein *in vivo*, we tried to detect PINA in the pineal gland tissue by Western blotting. First we tested if the commercially available antibodies against C-terminus of ATP7B have sufficiently high sensitivity and specificity to detect the ATP7B protein expressed at a basal level in tissue extracts. The rat liver tissue is a good benchmark for ATP7B detection, because this enzyme is expressed there at high level compared to other tissues. Also, rat liver is much larger than pineal gland and therefore provides more material for antibody testing.

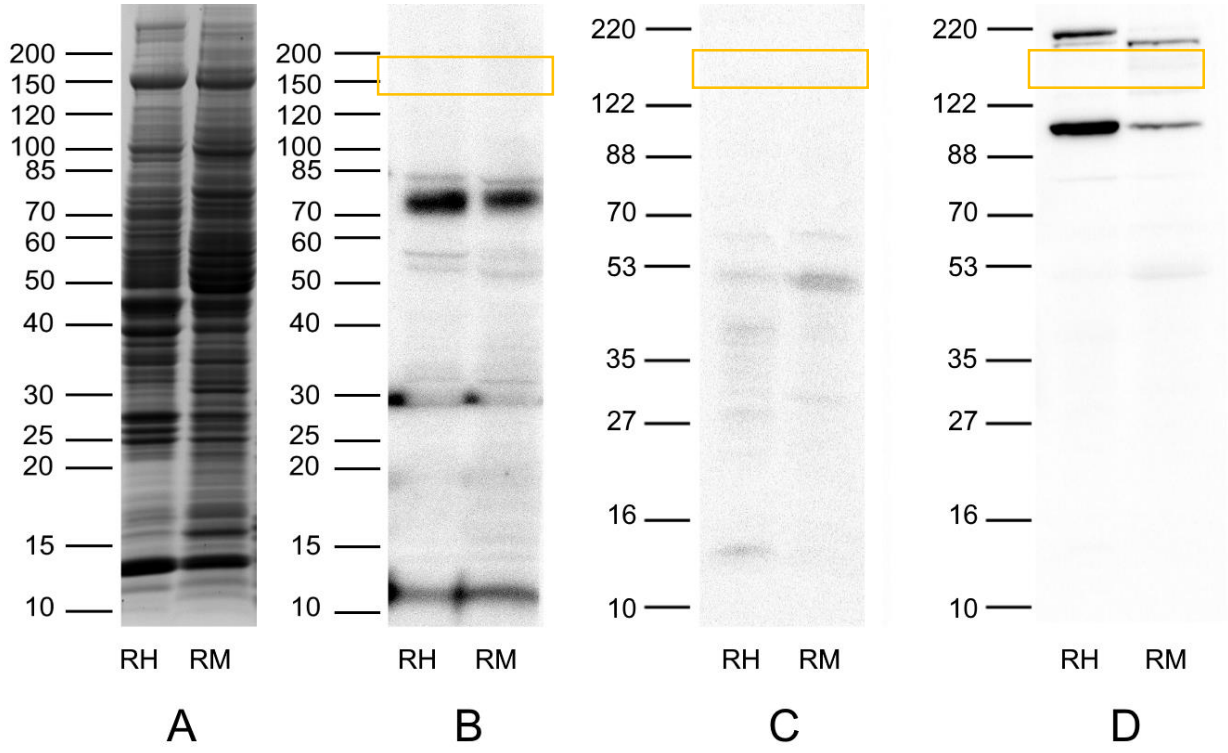

Figure 4.28: Testing antibodies for ATP7B detection in rat liver tissue. Rat liver homogenate and membranes were loaded on SDS polyacrylamide gel (10 µg of total protein per lane).
RH – rat liver crude homogenate; RM – rat liver crude membrane fraction.
A – Coomassie staining; B – anti-ATP7B (Santa Cruz H-94 polyclonal) + anti-rabbit IgG (ThermoFisher Scientific); C – anti-rabbit IgG only; D – anti-ATP7B (Boster Bio PA2262 polyclonal) + anti-rabbit IgG. Orange boxes indicate the region where a band corresponding to ATP7B is expected

Several commercial antibodies against rat ATP7B are available. These are mostly polyclonal antibodies against the characteristic C-terminal tail of the enzyme, and should detect both for

the full-length ATP7B and PINA. We have tested polyclonal antibodies manufactured by Santa Cruz Biotechnology (California, USA) designated “H-94”, and Boster Bio (California, USA) designated “PA2262” (Fig. 4.28). Only a faint signal from the area of interest has been detected in rat liver crude membrane fraction by antibody obtained from Boster Bio, while the antibodies from Santa Cruz were unable to detect the protein in the liver tissue at all. However, both antibodies successfully detect the overexpressed ATP7B.K recombinant protein from humans (Fig. 4.29), and the manufacturer specifications indicate that the antibodies are suitable for rat ATP7B as well. The identity of epitope sequences for the H-94 antibody is 84% (epitope length 94 amino acids, 17 amino acids difference) and 81% for the PA2262 antibody (epitope length 16 amino acids, 3 amino acids difference). Thus, it was decided to check the pineal gland tissue.

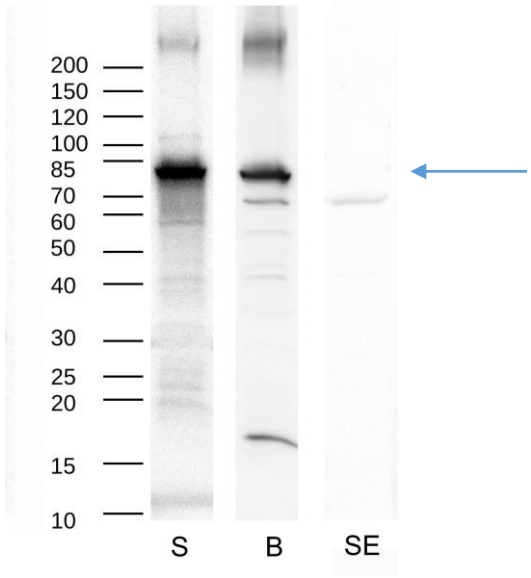

Figure 4.29: Western blot of ATP7B.K in whole cell extracts of *K. lactis* cells. S – anti-ATP7B H-94 from Santa Cruz Biotechnology + anti-rabbit IgG (ThermoFisher Scientific); B – anti-ATP7B pa2262 from Boster Bio + anti-rabbit IgG (ThermoFisher Scientific); SE – non-transformed yeast whole cell extract stained with H-94 antibody + anti-rabbit IgG. The arrow indicates the ATP7B.K band.

Pineal gland tissues were obtained from Sprague-Dawley rats, kept at a controlled 12:12 h day-night cycle, at various time points during the light and dark periods. When collecting dark period samples, special care was taken to protect animals from accidental exposure to light: cages were transported to a procedure room under a non-transparent cover, and the procedures were

carried out under red light, which has no effect on photodetection system that regulates the circadian processes (Okano and Fukada, 2001).

The Santa Cruz antibody produced a signal at the expected molecular weight of approximately 70 kDa (Fig. 4.30), which consisted of three closely spaced bands, where the upper and the lower band did not show any variation, while the middle band did show a slight intensity increase in the dark period samples (11 pm – 4 am).

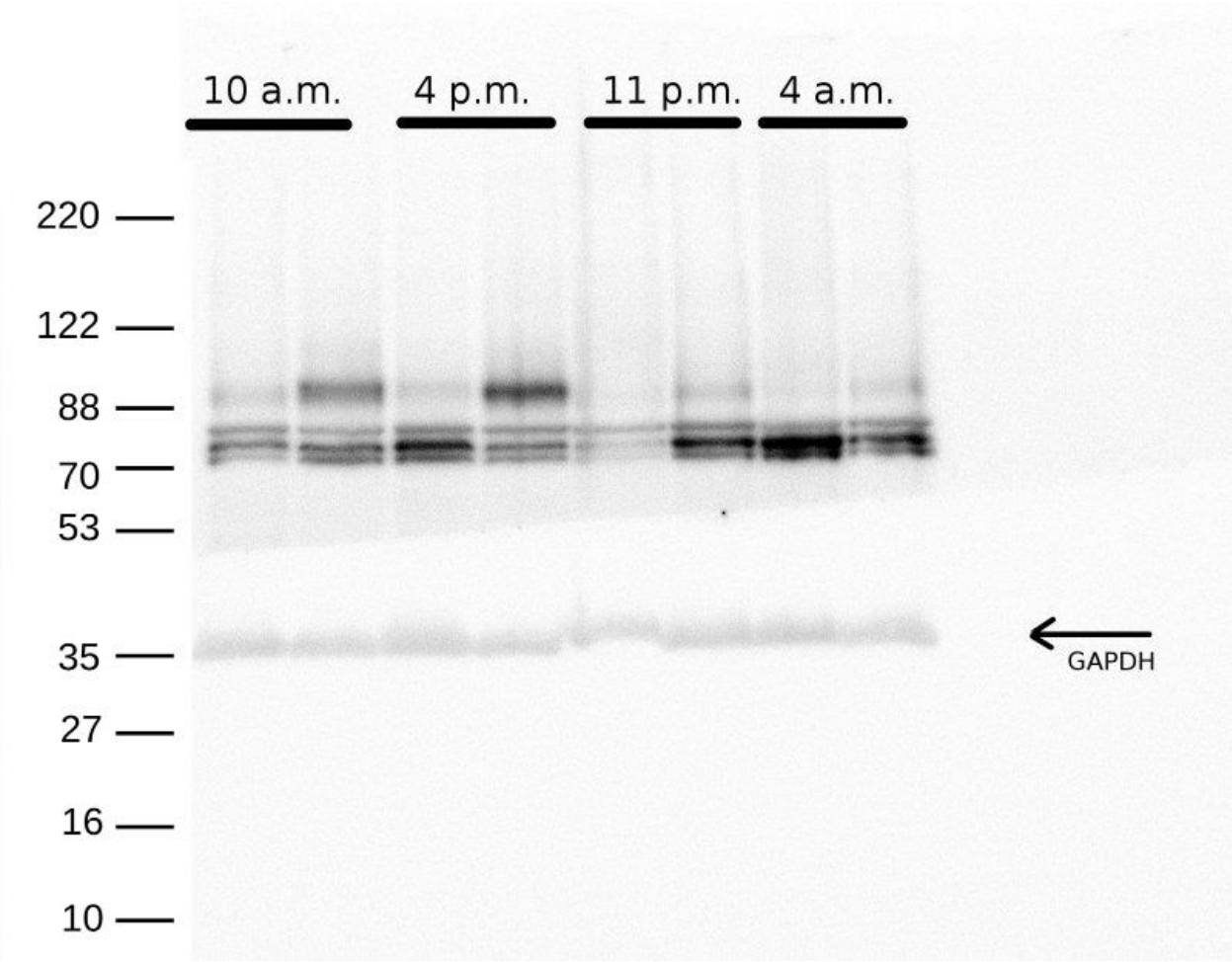

Figure 4.30: Western blot of rat pineal gland tissue extract, anti-ATP7B (Santa Cruz Biotechnology). The harvesting time of the samples is indicated above the lanes; lanes represent samples from different animals. Anti-GAPDH antibody was applied to the lower part of the membrane as a loading control.

To confirm that the PINA is represented by one of the bands, the region of a gel that contained the triple band was cut out and bands were sent for identification by in-gel tryptic digest

fingerprint. The results indicated presence of the following proteins: heat shock protein HSP72, transketolase, rat serum albumin precursor, V-type proton ATPase, periplakin, PHD finger protein 21B, dynamin and several automatically predicted proteins. No peptide fragments of copper-transporting P-type ATPases were detected.

In the next experiment, the H-94 and PA2662 antibodies were used to detect PINA in pineal gland membrane fraction. Isolating membrane fraction was intended to enrich for membrane-located putative PINA protein, and as a result get a clear expression pattern on the Western blot. Unfortunately, there was no signal from the PA2262 (Fig. 4.31, panel A), and very weak residual signal from the H-94 (Fig. 4.31, panel B) that resembled that of the tissue extracts.

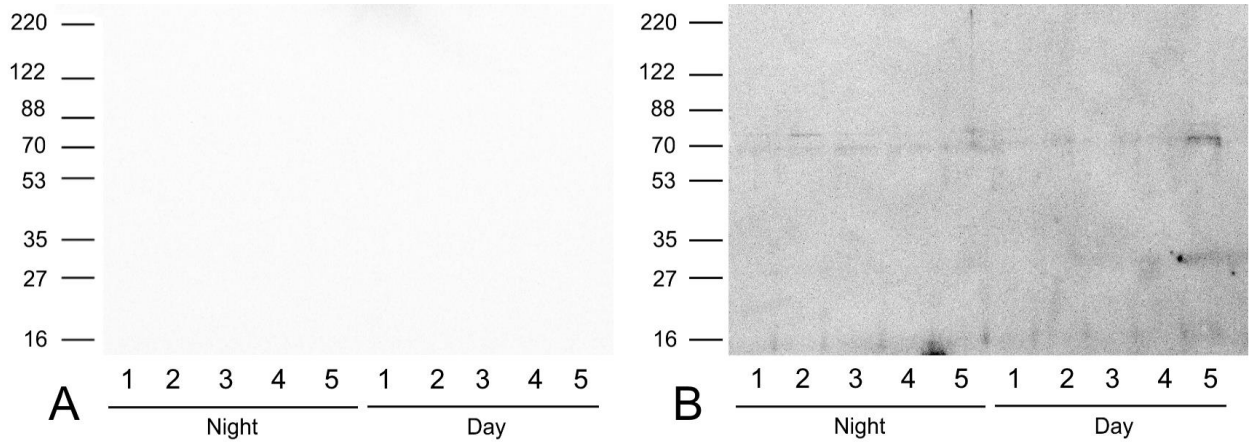

Figure 4.31: Western blot of rat pineal gland membrane fraction. 1-5 – samples from different animals. Panel *A*: Western blot with PA2262 anti-ATP7B antibody (BosterBio) + anti-rabbit IgG-HRP conjugate (ThermoFisher Scientific). Panel *B*: Western blot with H-94 anti-ATP7B antibody (Santa Cruz Biotechnology) + anti-rabbit IgG-HRP conjugate (ThermoFisher Scientific).

Inability to reliably detect the PINA protein in the pineal gland extracts and membrane fraction can be explained by the small amount of material that can be obtained from a rat pineal gland, which is usually not larger than 1 mm in diameter and 3 mg in weight. If PINA is a low-abundance protein, like ATP7B, there is a high chance it would not be detected with antibodies without additional enrichment methods, such as immunoprecipitation. However, getting sufficient amount of material for the immunoprecipitation from rat pineal glands poses difficulties due to the size of the organ, and hence a large number of experimental animals needed.

5. Discussion

The putative pineal night-specific ATPase PINA is a peculiar splice variant of ATP7B, which lacks 795 amino acids of N-terminus. The goals of this project were: 1) to find out whether the putative PINA protein is translated from its mRNA in the rat pineal gland, 2) to find out whether the protein levels follow diurnal cycle observed for PINA mRNA, 3) to find out whether this protein is a functional copper-transporting ATPase, and 4) if it is a functional enzyme, to establish whether its enzymatic activity compares to that of the full-length ATP7B.

We were unable to conclusively establish the existence of PINA protein *in vivo*, however our data show that such a protein can exist, because it was expressed and incorporated into membrane in *K. lactis* host, and showed enzymatic activity. This encouraged us for further studies of properties of truncated proteins. To compare the enzymatic activity of recombinant PINA with the full-length protein, the full-length ATP7B was purified. Although several functional studies on ATP7B have been conducted to date (Hung *et al.*, 1997; Forbes *et al.*, 1999; Tsvikovskii *et al.*, 2001; Lutsenko *et al.*, 2003; Portmann and Solioz, 2005; Pilankatta *et al.*, 2009), no successful purification of the full-length human ATP7B has been reported to date. In this study, we were able to design and fine-tune purification procedure of this protein expressed in *K. lactis* cells so we could purify the full-length human ATP7B and study its activity for the first time. The ATP7B gene was modified to produce two truncated constructs: ATP7B.K (putative human PINA mRNA found in the GenBank) with a characteristic 18 a.a. deletion, and $\Delta^{1\text{-}795}$ATP7B, a protein essentially homologous to the rat PINA, without the deletion predicted in ATP7B.K. The purified proteins were active, and we were able to characterize their ATPase activity.

5.1. Expression of ATP7B and its Variants

Full-length human ATP7B has been expressed previously in several eukaryotic expression systems, such as mammalian cells (Lockhart and Mercer, 2001; Voskoboinik *et al.*, 2001; Pilankatta *et al.*, 2009), insect cells (Tsvikovskii *et al.*, 2002; Barnes *et al.*, 2005) and yeast (Hung *et al.*, 1997; Iida *et al..*, 1998; Forbes *et al..*, 1999; Portmann and Solioz, 2005). Characterization of functional properties of endogenously expressed ATP7B in human cells appeared to be difficult due to very low expression levels (Beck *et al.*, 2011), while insect cells expression system could

produce much larger quantities of functional protein (Tsvikovskii *et al.*, 2002). A full-length human ATP7A enzyme was purified from insect cells (Hung *et al.*, 2007). Only the yeast system was used to produce truncated human ATP7B protein for further purification (Portmann and Solioz, 2005). Yeast expression systems have big advantages in terms of costs accompanying production of sufficient quantities of a protein for purification. It should be noted, however, that only a protein lacking MBD1-5 was expressed and purified from *S. cerevisiae*, while only CCC2 complementation assays were performed on the full-length protein.

Upon expression in *K. lactis* cells recombinant full-length ATP7B, as well as ATP7B.K and $\Delta^{1\text{-}795}$ATP7B, were successfully incorporated into the membrane, as confirmed by Western-blot analysis of membrane fractions of transformed yeast. Proper expression and folding of ATP7B and ATP7B.K were assessed *in vivo* by inducing intracellular trafficking by treating yeast cells with 1 mM $CuCl_2$ and subsequent immunofluorescent labelling with fluorescent antibodies. The experiments showed that ATP7B prominently relocalizes from Golgi to the plasma membrane in the yeast cells in response to elevated copper, which suggests proper folding and regulation of the protein in the cell. The localization of ATP7B.K in response to $CuCl_2$ changes too, however, the change is more subtle. In response to high copper, the truncated protein also tends to go to the plasma membrane, although to a smaller extent than the full-length ATP7B. The pattern of protein distribution seen in the cytoplasm changes too (Fig. 4.2).

The conclusion on cellular compartment localization of the protein can be drawn with the help of membrane fractionation experiment (Fig. 4.3). A heavier membrane fraction, which was not detectable in the untreated cells, appeared at the 50-65% interface on the sucrose gradient in the cells treated with copper. A typical response of a cell to toxic copper levels is to activate export of the metal ions from the intracellular space. In mammalian cells, ATP7B normally drives copper transport into the exocytic vesicles, which then fuse with the plasma membrane excreting copper outside the cell (Cater *et al.*, 2006). Hence, it is possible that the 50-65% fraction that appears in copper-treated cells is a heavy protein-loaded vesicular fraction. Relatively higher amount of ATP7B.K in this fraction indicates that this protein when expressed in yeast tends to localize into these exocytic vesicles to a greater extent than ATP7B.

The copper toxicity study showed that the yeast expressing ATP7B were in fact more susceptible to copper than those that expressed the truncated constructs or only the intrinsic copper ATPase CCC2. The possible reason for that is that overexpression of ATP7B suppresses the intrinsic CCC2, but ATP7B cannot properly integrate into yeast copper metabolism. An example of downregulation of the host protein expression by a homologous recombinant proteins has been reported previously (Napoli *et al.*, 1990). If CCC2 is downregulated, it is possible that ATP7B is incapable of efficient loading of CCC2 targets, such as yeast SOD, which can lead to higher sensitivity towards free radical damage caused by high copper concentration. Also, inability to properly integrate into the yeast copper metabolism can be due to structural differences between CCC2 and ATP7B, in particular in the N-terminal region. ATP7B has six metal-binding domains versus only two in CCC2, so yeast cells may lack proper regulation mechanisms for such an enzyme.

Trafficking of the proteins inside the cells in response to high copper concentration signifies proper folding and insertion of the full-length ATP7B and its variants into membranes, which opens way to functional studies of these enzymes.

5.2. Purification of ATP7B and its Variants

Purification of membrane proteins is generally more challenging than purification of soluble proteins. First, a membrane protein has to be extracted from the membrane. This is done using detergents, which are chosen empirically for each protein. Cost and application suitability (i.e. crystallographic studies, activity studies, NMR studies, etc.) are important factors in choosing detergents for screening. Previous reports (Portmann and Solioz, 2005) indicated that Δ^{MBD1-5}ATP7B could be solubilised from *S. cerevisiae* membranes by DDM, but only after copper treatment of the yeast cells. We were unable to solubilise either full-length ATP7B or truncated proteins in DDM, either with or without copper treatment. There are two possible explanations for this fact. First, in *K. lactis* the proteins may have a different lipid environment. Second is that our protein constructs are different. Even similar proteins may require different detergents. Among several tested detergents, LMPG was the most effective for solubilisation of ATP7B, ATP7B.K and Δ^{1-}

^{795}ATP7B. Moreover, structurally it is much more similar to membrane phospholipids than other widely used detergents as DDM or Triton X-100.

All proteins were successfully purified by affinity chromatography on Ni-NTA agarose and subsequent size exclusion chromatography. Truncated constructs were obtained using slightly modified protocol of ATP7B purification.

Because truncated constructs were expressed at a lower level than ATP7B, they were purified from the crude membranes to increase protein yield. Sucrose gradient separation was beneficial for the full-length ATP7B purification, helping to achieve better purity. Although membrane fractionation on sucrose gradient helps to improve protein purity, it leads to increased losses of the protein of interest. We found that 0.2% of LMPG in the buffer used in affinity and size exclusion chromatography is preferred for the truncated constructs, while 0.1% is sufficient for ATP7B. This can be explained by higher hydrophobicity of the truncated constructs, because they lack a very big soluble component on the N-terminus. The affinity purification on Ni-NTA agarose alone produced proteins of very low purity (as low as 6% purity for the truncated versions), so additional size exclusion step was necessary. It helped to increase purity of ATP7B to 80%, and truncated constructs – to 50%. Additional benefit from the size exclusion step was that imidazole was simultaneously removed from the protein, so no separate buffer exchange or dialysis step was needed.

The final purity obtained after the size exclusion chromatography is lower for the truncated constructs than for the full-length ATP7B due to the lower expression level of the truncated constructs in comparison to the full-length protein. Another reason is the location of the His-tag in the truncated constructs: it is attached directly to the A-domain, versus attachment to the flexible N-terminus of the full-length protein. This leads to weaker binding of the truncated constructs to the Ni-NTA agarose in comparison with the full-length ATP7B, which leads to elution of the truncated constructs with more contaminants. The purification method we developed yields up to 0.15 mg of ATP7B, and up to 0.08 mg of ATP7B.K or $\Delta^{1\text{-}795}$ATP7B per 1 L of yeast culture.

5.3. Enzymatic activity of ATP7B variants.

The enzymatic activity of copper-transporting P-type ATPases has been mostly studied *in vivo,* or in membrane vesicles, although reconstitution into proteoliposomes has also been done

for ATP7B lacking several metal-binding domains (Portmann and Solioz, 2005). There are no published studies of the enzymatic activity of purified full-length ATP7B or constructs similar to PINA/ATP7B.K. All previous measurements of the full-length ATP7B activity have been done in membrane vesicles from insect cells (Tsvikovskii *et al.*, 2002; Barnes *et al.*, 2005) and mammalian cells (Voskoboinik *et al.*, 2001; Lockhart and Mercer, 2001; Pilankatta *et al.*, 2009). Comparative analysis of phosphorylation/dephosphorylation rates of human copper ATPases in membrane vesicles from insect cells (Barnes *et al.*, 2005) suggested 6 times lower turnover rates of ATP7B in comparison with ATP7A. Pilankatta and coworkers (Pilankatta *et al.*, 2009) were able to evaluate specific activity of the recombinant human full-length enzyme in microsomal fraction of COS (simian) cells. Their measurements showed activity of 0.030 μmol/mg of total microsomal protein/min. To date, one study of enzymatic activity of purified truncated Δ^{MBD1-5}ATP7B has been done (Portmann and Solioz, 2005). In that study, the purified protein ATPase activity was studied using the malachite green assay. Copper transport activity was studied for murine ATP7B using radioactive copper isotope, ^{64}Cu, detection in microsomes from CHO cells (Voskoboinik et al., 2001), and was shown to be 0.0001 μmol Cu/mg of total microsomal protein/min.

Although the assay employing ^{32}P labelling with subsequent molybdate-benzene extraction and analysis by scintillation counter is the most sensitive phosphatase assay available, we, as well as other groups who aimed to establish specific activity of the enzyme, chose colourimetric approach, because it is easier and quicker to conduct and does not involve radioactive materials.

ATPase activity measurements in microsomes indicated that the full-length ATP7B is active in the yeast membranes, and the putative human PINA homologues, Δ^{1-795}ATP7B and ATP7B.K, are active ATPases. The turnover rate of ATP7B.K and copper-activated Δ^{1-795}ATP7B in microsomes is most likely higher than that of the full-length ATP7B because the amount of the overexpressed truncated protein in membranes is approximately two times smaller than of the full-length protein.

Our measurements of purified ATP7B ATPase activity (0.010-0.015 μmol/mg/min) produced results similar to those reported before (0.004-0.008 μmol/mg/min in purified reconstituted Δ^{MBD1-5}ATP7B by Portmann and Solioz, 2005). That experiment was done in similar conditions

(pH 6.0, 37°C, added copper in micromolar range). Specific ATPase activity of ATP7B in our and previous experiments lies in the same order of magnitude. The difference in these measurements can arise from various factors such as protein medium (liposomes, detergent, buffer composition), and purification procedure. The turnover number – 1.6-2.4 min^{-1} – of ATP7B is small in comparison with such fast ATPases as SERCA1 – 2700 min^{-1} (Lytton *et al.*, 1992) or Na/K-ATPase – 1900 min^{-1} (Sweadner, 1985). This is explained by different physiological roles of these ATPases: SERCA and Na/K-ATPase need fast reaction rates to regulate fast processes, such as muscle contraction and neural signal transduction. Copper levels, on the other hand, do not change dramatically fast, and copper concentration in the cell is very low.

The purified putative human PINA homologue ATP7B.K has the highest activity of 0.400-0.500 μmol/min/mg (turnover number – 27.7-34.6 min^{-1}), nearly 15 times higher than the purified full-length protein. Δ^{1-795}ATP7B, unlike in microsomes, is active even in the absence of added copper and has somewhat lower specific activity of 0.090-0.130 μmol/min/mg (turnover number – 6.4-9.3 min^{-1}), approximately 4 times faster than the full-length enzyme. Apparently, in the microsomal environment Δ^{1-795}ATP7B is downregulated when the concentration of copper is very low, either by lipid environment or proteins which can associate with it. These inhibiting factors may be removed during purification.

The truncated constructs have significantly higher activity than the full-length ATP7B. This may be explained by structural differences between ATP7B and truncated variants. For example, MBDs of N-terminus has been shown to interact with the N-domain of ATP7B (Tsvikovskii *et al.*, 2001). It has further been shown that MBD1-4 can have an inhibitory effect on ATP7B, while deletion of these domains led to acceleration of the catalytic cycle (Huster and Lutsenko, 2003). The cytoplasmic entrance for copper ions as well as the exit are formed by helices that are missing in the truncated constructs. When these helices are missing, the main copper-binding site(s) become much more accessible, which could increase the rate of ion translocation across the membrane. Normally, the rate of ion translocation is tightly coupled to the rate of ATP hydrolysis, so in case of increased ion translocation rate the rate of ATP hydrolysis would increase as well. Alternatively, deletion of several helices could result in uncoupling of ion transport and ATPase activity – it is known that structural alterations in P-type ATPases can lead to such phenomenon (Andersen

and Vilsen, 1995; Lutsenko and Kaplan, 1995; Bramkamp and Altendorf, 2005). Fast rates of ATP7B.K may be additionally explained by the 18 a.a. deletion present in its M-domain, mainly involving the extracellular loop (Fig. 2.11). This deletion probably further activates the enzyme, and is important for regulation of its activity in the microsomes, as compared to $\Delta^{1\text{-}795}$ATP7B without the deletion, which requires higher copper concentration for activation.

Another peculiarity is that the reaction product accumulation curves are nonlinear. According to our observations, the faster the enzyme, the faster the reaction ceases. Typically, time-dependent activity decrease is observed either because of transported substrate depletion, depletion of ATP or inhibition by ADP, but in our assay conditions both these scenarios seem unlikely. Less than 0.1% of added ATP, was hydrolyzed by the time the reaction reached a plateau. Copper supply cannot be a limiting factor either, because the reaction is carried out in detergent, not in the liposomes, so even low amounts of copper would be "recycled" many times instead of being sequestered in the liposomes. We have calculated the maximum number of enzyme cycles of ATP7B.K and $\Delta^{1\text{-}795}$ATP7B to be around 200, after which the enzymes halt. We are unsure about the reasons behind such behaviour. Because decrease in the reaction rate is determined by the number of enzyme turnovers, rather than time, a logical conclusion could be that the proteins are inhibited by either some product of reaction (such as oxidized copper (II)), or by changes in the redox potential.

We did not observe activation by added copper for any of the three constructs when they were purified and tested in detergent, which is most likely accounted for by the effect of the residual copper in reaction buffer. ATP7B as well as bacterial copper transporter CopB have been previously shown to display basal activity even in absence of any added copper (Wyler-Duda and Solioz, 1996; Bissig *et al.*, 2001; Tsvikovskii *et al.*, 2001; Portmann and Solioz, 2005).

The measurements of the ATPase activity in the membranes of transformed yeast, however inaccurate in terms of specific activity with regard to expressed proteins amount, suggest that purification process and/or detergent has severely adverse effect at the full-length ATP7B and its variants, because prior to purification their activity seem to be very much higher. Detergents are known to inhibit enzymes during and after purification (Carpenter *et al.*, 1990; Kurkela *et al.*, 2002).

The rate of transport of copper ions across a lipid bilayer is another important property of a copper-transporting ATPase. The traditional method of measuring copper transport employs radioactive ^{64}Cu isotope. It was not our first method of choice due to the short isotope half-life time, logistical difficulties, and labour-intensive nature of such analysis.

Instead, we set out to design a method based on nonradioactive compounds, which would be sensitive enough to study copper-transporting activity of ATP7B and its variants. CS-1 fluorescent sensor gave promise as a sensitive, non-toxic and very specific to copper (I).

Unfortunately, we were unable to detect copper transport in liposomes with incorporated ATP7B using the developed method. One of major complications that we encountered was complex interactions of the amphiphilic sensor with lipids. These interactions result in prolonged (10 minutes or even longer) nonlinear fluorescence dynamics that can easily obscure slight changes in dye fluorescence caused by copper binding. As ATP7B is a relatively slow ATPase, the change in free copper concentration is probably very small, and the sensitivity of the sensor in the presence of lipids and TCEP is insufficient to provide a detectable signal. Considering the prolonged period of system equilibration (10 minutes) before adding ATP, the protein might partially lose its activity. Large reaction volume (minimum 0.5 mL) together with modest quantities of available protein complicate the measurements even further.

Thus, the method of detection of ATP-dependent copper transport by CS-1 need extensive further development in order to be suitable for measurements of copper transport activity in reconstituted proteoliposomes. For example, a different equipment could be used, where the reaction volume can be small, so the proteoliposomes would be less diluted. Different lipid composition of liposomes may also positively contribute to the assay behaviour. Buffer composition may also play a role: various reducing agent may have different effects on the fluorescent sensor. Once the method is optimized sufficiently, it may become a useful tool to study copper transport in real-time.

5.4. Putative PINA ATPase Detection in Rat Pineal Gland

Although PINA mRNA was found, there's no direct evidence for the existence of corresponding protein. In order to find out whether the PINA mRNA is translated into protein in rat

pineal gland, and whether its translation follows the pattern of mRNA expression – abundant at night and undetectable at day – reported by Borjigin and coworkers (Borjigin *et al.*, 1999), analysis of pineal gland tissue taken from experimental animals by Western blot analysis was performed. Because PINA is identical to the C-terminal half of the full-length ATP7B, antibodies against the C-terminus of ATP7B should also detect PINA. As PINA is presumably expressed at night, we expected to detect antibody signal in the samples of pineal glands taken during the dark period.

A limiting factor in protein detection by Western blot is sensitivity and specificity of the primary antibodies. A band at the apparent molecular weight of PINA was detected in pineal gland tissue extracts with H-94 antibodies (Santa Cruz Biotechnology, Dallas, TX), and did show some diurnal variation. Non-specific reaction was also observed in the same molecular weight and range. No protein was detected with either H-94 or PA2262 antibodies (Boster Bio, Pleasanton, CA) in the isolated membrane fraction from pineal gland, so the protein detected in tissue extracts appears to be cytoplasmic rather than membrane bound. Mass spectrometry analysis failed to detect any PINA derived peptides.

Because both antibodies we used successfully detect the protein overexpressed in yeast, the most likely reason for the failure to detect PINA is low sensitivity of both antibodies. H-94 antibodies were unable to detect ATP7B in liver extracts and membranes, PA2262 antibody also was insufficiently sensitive. The detection is further complicated by the very small size of a rat pineal gland, and as a result, very small amount of material for analysis. The most straightforward way to fix this problem would be to use more animals to obtain more material, but such an approach is questionable both from financial and ethical points of view. One of the possible solutions to overcome detection limitations would be to either use a pineal gland from a larger animal (i.e. pig). This, however, would require prior search for PINA mRNA in that tissue, because this splice variant is not necessarily common for all animals. Another way to study PINA expression pattern could be culturing rat pinealocytes: it would be possible to grow more material in a controlled environment. Also, production or ordering of custom antibodies specially for the purpose of detecting PINA/ATP7B in tissue extracts is an option. Raising antibodies against a different epitope and selecting for the most sensitive ones might produce better results.

Even though we could not show the expression of PINA in the tissue, a recent finding (Dolgova and Dmitriev, unpublished data) shows that copper content in night pineal glands is noticeably higher than in day pineal glands. Since copper concentration in the pineal gland appears to fluctuate according to the circadian rhythms, pineal gland should contain a diurnally regulated copper transporter. This suggests that a putative PINA protein indeed has a possible physiological role. To understand the role of this protein, as well as the role of copper in pineal gland, further studies are needed, because current knowledge is scarce. Little is known about the function and role of splice variants of ATP7B. At least one case of alternative splicing, which removes exon 12 from the protein, has been shown to serve a "reparative" function in patients with 2810delT mutation, which makes the protein defective. Patients with this mutation were found to have an increased level of alternative splicing at the exon 12 (linker region between A-domain and TM3), omitting it completely, and thus partially rescuing the phenotype: ATP7B without exon 12 was shown to retain 80% of its activity, possibly accounting for mild symptoms of the Wilson's disease in such a case (Wan *et al.*, 2010). Another truncated 140 kDa version of ATP7B has been detected in mitochondria of cultured human hepatic cells, and it was suggested to take role in maintaining mitochondrial copper homoeostasis (Lutsenko and Cooper, 1998). It has been reported before that TMA and TMB are frequently absent in brain-specific splice variants of ATP7B, and that the brain has the biggest number of shorter splice variants than other tissues (Petrukhin *et al.*, 1994). The greater variation in splice variants of ATP7B in brain can be required for tighter control of copper levels, as the brain has low levels of antioxidants and antioxidant enzymes, but high levels of metals (Telianidis *et al.*, 2013).

Copper involvement in circadian rhythms is not well-studied either. It has been shown, however, that mice knockouts of PrP^{C} protein, post-translational modification of which leads to prion diseases, had only 20% of normal copper content in membrane fractions from brain tissues (Brown *et al.*, 1997), and that such mice had alterations in their circadian behaviour (Tobler *et al.*, 1996). There's evidence of diurnally varying copper levels in serum in human, with concentrations of the metal above mean at daytime and below mean at nighttime (Lifschitz and Henkin, 1971). Existence of copper-dependent diurnal oscillator is speculated in plants (Peñarrubia *et al.*, 2010).

Thus, pineal gland indeed may possess a copper-related diurnal cycle involving the putative PINA protein. Further studies are needed to establish its existence and role.

6. Conclusions

For the first time, full-length human ATP7B was successfully over-expressed in yeast host, extracted from membrane and purified. Truncated constructs – ATP7B.K (a putative human PINA homologue with a predicted peculiar 18 a.a. deletion) and $\Delta^{1\text{-}795}$ATP7B (a putative human PINA homologue without the deletion) – were successfully created, over-expressed, extracted and purified. The enzymes were shown to fold and traffic inside cells in response to elevated copper concentrations. All three proteins, – the full-length ATP7B, $\Delta^{1\text{-}795}$ATP7B and ATP7B.K, were active in the host microsomes. The purified proteins display ATPase activity and the truncated constructs have much faster rates in detergent than the full-length protein. Successful expression and purification of active ATP7B.K proves the possibility of existence of a structurally distinct and physiologically significant variant of ATP7B.

The copper transport activity measurements using CS-1 fluorescent sensor did not succeed, likely because of previously unknown complex behaviour of the sensor in presence of lipids (liposomes and proteoliposomes) and relatively slow turnover rate of ATP7B. The protocol needs further optimizations; alternative methods also should be considered (for example, use of ^{64}Cu isotope in *K. lactis* knockout on CCC2).

We were unable to detect PINA protein in the pineal gland, possibly due to the limited amount of material and insufficient antibody sensitivity. This may be overcome by developing very specific and sensitive antibodies tailored to this task. Alternative option is to switch to a different source of material (for example, pig pineal gland or cultured rat pinealocytes).

7. Future Directions

Copper transport activity assay using CS-1 should be optimized, or a more sensitive assay for copper transport activity of purified ATP7B and its truncated versions should be conducted in order to fully characterize the properties of the enzymes.

A separate confirmation of PINA mRNA in rat pineal gland and retina would be useful, as it was reported only once. Alternative strategy for establishing whether PINA is translated in pineal could be considered. One of such alternatives could be a pinealocyte culture – with it, it is possible to grow as many cells as needed without need for large quantities of animals. Because pinealocytes receive light information via norepinephrine signalling, it can be used in the culture medium to simulate the diurnal cycle.

Further optimization of activity assay conditions is possible. Certain lipid environments, and buffers can be more beneficial for the enzymes to work.

Crystallographic studies of ATP7B, $\Delta^{1\text{-}795}$ATP7B and ATP7B.K could be further considered after the optimization of expression and purification procedure, because only highly pure proteins are suitable for crystallography.

8. References

Abe, K., Tani, K., Nishizawa, T., and Fujiyoshi, Y. (2009). Inter-subunit interaction of gastric H^+,K^+-ATPase prevents reverse reaction of the transport cycle. EMBO J. *28(11)*, 1637–1643.

AceView Database, National Institute of Health, Bethesda, MD. ATP7B gene, *Homo sapiens*: http://www.ncbi.nlm.nih.gov/IEB/Research/Acembly/av.cgi?db=human&c=Gene&l=ATP7B

Andersen, J.P., and Vilsen, B. (1995). Structure-function relationships of cation translocation by Ca^{2+}- and Na^+,K^+-ATPases studied by site-directed mutagenesis. FEBS Let. *359*, 101–106

Aravind, L., Galperin, M.Y., and Koonin, E.V. (1998). The catalytic domain of the P-type ATPase has the haloacid dehalogenase fold. Trends Biochem. Sci. *23*, 127–29

Arnesano, F., Banci, L., Bertini, I., Ciofi-Baffoni, S., Molteni, E., Huffman, D.L., and O'Halloran, T.V. (2002). Metallochaperones and metal-transporting ATPases: a comparative analysis of sequences and structures. Genome Res. *12(2)*, 255–271.

Argüello, J.M., Eren, E., and Gonzáles-Guerrero, M. (2007). The structure and function of heavy metal transport P_{1B}-ATPases. BioMetals *20(3)*, 233–248

Asahi, M., Sugita, Y., Kurzydlowski, K., De Leon, S., Tada, M., et al. (2003). Sarcolipin regulates sarco(endo)plasmic reticulum Ca^{2+}-ATPase (SERCA) by binding to transmembrane helices alone or in association with phospholamban. Proc. Natl. Acad. Sci. *100*, 5040–5045

Axelrod, J. and Wurtman, R. J. (1968). Photic and neural control of indoleamine metabolism in the rat pineal gland. Adv. Pharmacol. *6*, 157–166.

Axelsen, K.B., and Palmgren, M.G. (1998). Evolution of substrate specificities in the P-type ATPase superfamily. J. Mol. Evol. *46*, 84–101

Baekgaard, L., Mikkelsen, M.D., Sørensen, D.M., Hegelund, J.N., Persson, D.P., et al. (2010). A combined Zn/Cd sensor and Zn/Cd export regulator in a heavy metal pump. J. Biol. Chem. *285*, 31243–31252

Banci, L., Bertini, I., Cantini, F., and Ciofi-Baffoni, S. (2010). Cellular copper distribution: a mechanistic systems biology approach Cell. Mol. Life Sci. *67*, 2563–2589

Barnes, N., Tsivkovskii, R., Tsivkovskaia, N., and Lutsenko, S. (2005). The Copper-transporting ATPases, Menkes and Wilson Disease Proteins, Have Distinct Roles in Adult and Developing Cerebellum. J. Biol. Chem. *280*, 9640-9645

Bartnikas, T.B., and Gitlin, J.D. (2001). How to make a metalloprotein. Nat. Struct. Biol. *8*, 733 - 734

Beck, M., Schmidt, A., Malmstroem, J., Claassen, M., Ori, A., Szymborska, A., Herzog, F., Rinner, O., Ellenber, J., and Aebersold, R. (2011). The Quantitative Proteome of a Human Cell Line. Mol. Syst. Biol. *7*, 549

Benloucif, S., Guico, M.J., Reid, K.J., Wolfe, L.F., l'Hermite-Balériaux, M., and Zee, P.C. (2005). Stability of Melatonin and Temperature as Circadian Phase Markers and Their Relation to Sleep Times in Humans. J, Biol. Rhythms *20(2)*, 178–188.

Bertinato, J., and L'Abbe, M.R. (2003). Copper modulates the degradation of copper chaperone for Cu,Zn superoxide dismutase by the 26 S proteasome. J. Biol. Chem. *278*, 35071–35078

Bissig, K., Wunderli-Ye, H., Duda, P., and Solioz, M. (2001) Structure–function analysis of purified *Enterococcus hirae* CopB copper ATPase: effect of Menkes/Wilson disease mutation homologues. Biochem. J. *357*, 217–223

Borjigin, J., Payne, A.S., Deng, J., Li, X., Wang, M.M., Ovodenko, B., Gitlin, J.D., and Snyder, S.H. (1999). A novel pineal night-specific ATPase encoded by the Wilson disease gene. J. Neurosci. *19*, 1018–1026

Borlikova, G., and Endo, S. (2009). Inducible cAMP Early Repressor (ICER) and Brain Functions. Mol. Neurobiol. *40(1)*, 73–86

Bramkamp, M., and Altendorf, K. (2005). Single Amino Acid Substitution in the Putative Transmembrane Helix V in KdpB of the KdpFABC Complex of *Escherichia coli* Uncouples ATPase Activity and Ion Transport. Biochem. *44*, 8260 – 8266

Brini, M., and Carafoli, E. (2009). Calcium pumps in health and disease. Physiol. Rev. *89*, 1341–1378

Brown, D.R., Qin, K., Herms, J.W., Madlung, A., Manson, J., Strome, R., Fraser, P.E., Kruck, T., von Bohlen, A., Schulz-Schaeffer, W., Giese, A., Westaway, D., and Kretzschmar, H. (1997). The cellular prion protein binds copper in vivo. Nature *390*, 684-687

Bublitz, M., Poulsen, H., Morth, J. P., and Nissen, P. (2010) In and out of the cation pumps: P-type ATPase structure revisited. Curr. Opin. Struct. Biol. *20*, 431−439

Buettner, G., Jurkiewicz, B.A. (1996) Catalytic Metals, Ascorbate and Free Radicals: Combinations to Avoid. Rad. Res. *145*, 532-541

Bull, P.C., Thomas, G.R., Rommens, J.M., Forbes, J.R., and Cox, D.W. (1993) The Wilson disease gene is a putative copper transporting P-type ATPase similar to the Menkes gene. Nat. Genet. *5*, 327–337

Carpenter, C.L., Duckworth, B.C., Auger, K.R., Cohen, B., Schaffhausen, B.S., and Cantley, L.C. (1990). Purification and characterization of phosphoinositide 3-kinase from rat liver. J. Biol. Chem. *265*, 19704–19711

Cater, M.A., La Fontaine, S., Shield, K., Deal, Y., and Mercer, J.F.B. (2005). ATP7B Mediates Vesicular Sequestration of Copper: Insight Into Biliary Copper Excretion. Gastroent. *130(2)*, 493–506

Culotta, V.C., Yang, M., and O'Halloran, T.V. (2006). Activation of superoxide dismutases: putting the metal to the pedal. Biochim Biophys Acta *1763*, 747–758

Dancis, A., Haile, D., Yuan, D.S., and Klausner, R.D. (1994). The *Saccharomyces cerevisiae* copper transport protein (Ctr1p). Biochemical characterization, regulation by copper, and physiologic role in copper uptake. J. Biol. Chem. *269*, 25660–25667

Devés, R., and Brodie, A.F. (1981). Active transport of Ca^{2+} in bacteria: bioenergetics and function. Mol. Cell. Biochem. *36*, 65–84

Dmitriev, O., Tsivkovskii, R., Abildgaard, F. *et al.* (2006) Solution structure of the N-domain of Wilson disease protein: distinct nucleotide-binding environment and effects of disease mutations. Proc. Natl. Acad. Sci. *103*, 5302–5307

Dolgova, N.V, Nokhrin, S., Yu, C.H., George, G.N., and Dmitriev, O.Y. (2013) Copper chaperone Atox1 interacts with the metal-binding domain of Wilson's disease protein in cisplatin detoxification. Biochem. J. *454(1)*, 147–156

Drees, S.L., Beyer, D.F., Lenders-Lomscher, C., Lübben, M. (2015) Distinct functions of serial metal-binding domains in the *Escherichia coli* P1B-ATPase CopA. Mol. Microbiol. *97(3)*, 423–438

Entrez Gene Database, National Institute of Health, Bethesda, MD. ATP7B ATPase, Cu++ transporting, beta polypeptide (*Homo sapiens*): http://www.ncbi.nlm.nih.gov/gene/540

Fan, B., and Rosen, B.P. (2002) Biochemical characterization of CopA, the *Escherichia coli* Cu(I)-translocating P-type ATPase. J Biol Chem *277*, 46987–46992

Fatemi, N., and Sarkar, B. (2002). Molecular mechanism of copper transport in Wilson disease. Environ. Health Perspect. *110(Suppl 5)*, 695–698

Festa, R.A., and Thiele, D.J. (2011). Copper: An essential metal in biology. Curr Biol *21*, 21, pR877–R883

Forbes, J.R., Hsi, G., and Cox, D.W. (1999). Role of the copper-binding domain in the copper transport function of ATP7B, the P-type ATPase defective in Wilson disease. J Biol Chem. *274(18)*, 12408–12413

Forrest, L.R., Tang, C.L., and Honig, B. (2006). On the accuracy of homology modeling and sequence alignment methods applied to membrane proteins. Biophys. J. *91(2)*, 508–517

Foulkes, N.S., Borjigin, J., Snyder, S.H., and Sassone-Corsi, P. (1996). Transcriptional control of circadian hormone synthesis via the CREM feedback loop. Proc. Natl. Acad. Sci. *93*, 14140 – 14145.

Freedman, M. S., Lucas, R. J., Soni, B., et al. (1999) Regulation of mammalian circadian behavior by non-rod, non-cone, ocular photoreceptors. Science *284*, 502–504

Fu, Y., Tsui, H.-C.T., Bruce, K.E., Sham, L.-T., Higgins, K.A.; Lisher, J.P., Kazmierczak, K.M., Maroney, M.J., Dann, C.E,. Winkler, M.E., and Giedroc, D.P. (2013) A new structural paradigm in copper resistance in *Streptococcus pneumoniae*. Nat. Chem. Biol. *9(3)*, 177–183

Furukawa, T., Morrow, E.M., and Cepko, C.L. (1997) Crx, a novel otx-like homeobox gene, shows photoreceptor-specific expression and regulates photoreceptor differentiation. Cell *91*, 521–530

González-Guerrero, M., and Argüello, J.M. (2008). Mechanism of Cu^+-transporting ATPases: Soluble Cu^+ chaperones directly transfer Cu^+ to transmembrane transport sites. Proc. Natl. Acad. Sci. *105*, 5992–5997

González-Guerrero, M., Eren, E., Rawat, S., Stemmler, T.L., and Argüello, J.M. (2008) Structure of the two transmembrane Cu^+ transport sites of the Cu^+-ATPases, J. Biol. Chem., *283(44)*, 29753–29759

Gourdon, P., Liu, X. Y., Skjorringe, T., Morth, J. P., Møller, L. B., Pedersen, B. P., and Nissen, P. (2011) Crystal structure of a copper-transporting PIB-type ATPase. Nature *475*, 59−64

Guo, Y., Nyasae, L., Braiterman, L.T., and Hubbard, A.L. (2005) NH2-terminal signals in ATP7B Cu-ATPase mediate its Cu-dependent anterograde traffic in polarized hepatic cells. Am. J. Physiol. Gastrointest. Liver Physiol., *289*, G904-916

Gupta, A., and Lutsenko, S. (2012) Evolution of Copper Transporting ATPases in Eukaryotic Organisms. Curr. Gen. *13*, 124–133

Hakansson, K.O. (2009). The structure of Mg-ATPase nucleotide-binding domain at 1.6 Å resolution reveals a unique ATP-binding motif. Acta Crystallogr., Sect.D *65*, 1181–1186

Hardeland, R., Pandi-Perumal, S.R., and Cardinali, D.P. (2006). Melatonin. Intl. J. Biochem. Cell Biol. *38 (3)*, 313–316

Horng, Y.C., Cobine, P.A., Maxfield, A.B., Carr, H.S., and Winge, D.R. (2004). Specific copper transfer from the Cox17 metallochaperone to both Sco1 and Cox11 in the assembly of yeast cytochrome *c* oxidase. J. Biol. Chem. *279*, 35334 –35340

Huang, Y., Nokhrin, S., Hassanzadeh-Ghassabeh, G., Yu, C. H., Yang, H., Barry, A. N., Tonelli, M., Markley, J. L., Muyldermans, S., Dmitriev, O. Y., and Lutsenko, S. (2014). Interactions Between Metal-Binding Domains Modulate Intracellular Targeting of Cu(I)-ATPase ATP7B, as Revealed by Nanobody Binding. J. Biol. Chem. *289(47)*, 32682–32693

Hung, Y.H., Layton, M.J., Voskoboinik, I., Mercer, J.F.B., and Camakaris, J. (2007). Purification and membrane reconstitution of catalytically active Menkes copper-transporting P-type ATPase (MNK; ATP7A). Biochem. J. *401(2)*, 569–579

Huster, D., and Lutsenko, S. (2003) The distinct roles of the N-terminal copper-binding sites in regulation of catalytic activity of the Wilson's disease protein. J. Biol. Chem. *278*, 32212–32218

Iida, M., Terada, K., Sambongi, Y., Wakabayashi, T., Miura, N., Koyama, K., Futai, M., and Sugiyama, T. (1998). Analysis of functional domains of Wilson disease protein (ATP7B) in *Saccharomyces cerevisiae*. FEBS Lett. *428(3)*, 281–285.

Invitrogen. (2007). SYPRO® Ruby Protein Gel Stain. (Product information)

Itoh, S., Kim, H.W., Nakagawa, O., Ozumi, K., Lessner, S.M., Aoki, H., Akram, K., McKinney, R.D., Ushio-Fukai, M., and Fukai, T. (2008). Novel role of antioxidant-1 (Atox1) as a copper-dependent transcription factor involved in cell proliferation. J Biol Chem. *283(14)*, 9157-9167

Jardetsky, O. (1966). Simple Allosteric Model for Membrane Pumps. Nature *211*, 969−970

Kalsbeek, A., Cutrera, R.A., Van Heerikhuize, J.J., van der Vliet, J., Buijs, R.M. (1999). GABA release from suprachiasmatic nucleus terminals is necessary for the light-induced inhibition of nocturnal melatonin release in the rat. Neurosci. *91,* 453–461

Ko, C.H., and Takahashi, J.S. (2006). Molecular components of the mammalian circadian clock. Hum. Mol. Gen. *15(2),* R271–R277

Kobayashi, M., and Shimizu, S. (1999). Cobalt proteins. Eur. J. Biochem. *261(1),* 1–9

Kurkela, M., García-Horsman, J.A., Luukkanen, L., Mörsky, S., Taskinen, J., Baumann, M., Kostiainen, R., Hirvonen, J., and Finel, M. (2003). Expression and Characterization of Recombinant Human UDP-glucuronosyltransferases (UGTs). J. Biol. Chem. *278,* 3536–3544

Kühlbrandt, W. (2004). Biology, Structure and Mechanism of P-Type ATPases. Nat. Rev. Mol. Cell Biol. *5*, 282-295

Laemmli, U.K. (1970) Cleavage of Structural Proteins during the Assembly of the Head of Bacteriophage T4. Nature *227*, 680–685

Lane, T.W., Saito, M.A., George, G.N., Pickering, I.J., Prince, R.C., and Morel, F.M.M. (2005). A cadmium enzyme from a marine diatom. Nature *435(42),* 42

Lenoir, G., Picard, M., Gauron, C., Montigny, C., Le Maréchal, P., Falson, P., Le Maire, M., Møller, J.V., and Champeil, P (2004). Functional properties of sarcoplasmic reticulum Ca(2+)-ATPase after proteolytic cleavage at Leu119-Lys120, close to the A-domain. J. Biol. Chem. *279*, 9156-9166

Li, X., Chen, S., Wang, Q., Zack, D.J., Snyder, S.H., Borjigin, J. (1998). A pineal regulatory element (PIRE) mediates transactivation by the pineal/retina-specific transcription factor CRX. Proc. Natl. Acad. Sci. *95*, 1876–1881.

Lifschitz, M.D., Henkin, R.I. (1971). Circadian variation in copper and zinc in man. J. Appl. Physiol. *31(1),* 88–92

Linder, M.C. (2013) Biochemistry of Copper. (Springer Science & Business Media), ISBN 1475794320, 9781475794328

Liu, X., and Fagotto, F. (2011). A Method to Separate Nuclear, Cytosolic, and Membrane-Associated Signaling Molecules in Cultured Cells. Science Sign. *4(203)*, pl2

Liu, Y, Tsinoremas, T.F., Johnson, C.H., Lebedeva, N.V., Golden, S.S., Ishiura, M., and Kondo, T. (1995). Circadian orchestration of gene expression in cyanobacteria. Genes Dev. *9(12)*, 1469–1478.

Lockhart, J.P., and Mercer, J.F.B. (2001). Functional analysis of the sheep Wilson disease protein (sATP7B) in CHO cells. Eur. J. Cell Biol. *80(5)*, 349–357

Lowry, O.H., Rosenbrough, N.J., Farr, A.L., and Randall, R.J. (1951). Protein measurement with the Folin phenol reagent. J. Biol. Chem. *193*, 265–275.

Lucas, R. J., Freedman, M. S., Munoz, M., Garcia-Fernandez, J. M., and Foster, R. G. (1999). Regulation of the mammalian pineal by non-rod, non-cone, ocular photoreceptors. Science *284*, 505–507

Lutsenko, S., Barnes, N.L., Bartee, Y.M., and Dmitriev, O.Y. (2007) Function and Regulation of Human Copper-Transporting ATPases Physiol Rev *87*, 1011-1046.

Lutsenko, S., and Cooper, M. J. (1998) Localization of the Wilson's disease protein product to mitochondria. Proc. Natl. Acad. Sci. *95*, 6004-6009

Lutsenko, S., Gupta, A., Burkhead, J.L., and Zuzel, V. (2008). Cellular multitasking: the dual role of human Cu-ATPases in cofactor delivery and intracellular copper balance. Arch. Biochem. Biophys. *476(1)*, 22–32

Lutsenko, S., Efremov, R.G., Tsivkovskii, R., and Walker, J.M. (2002). Human Copper-Transporting ATPase ATP7B (The Wilson's Disease Protein): Biochemical Properties and Regulation. J. Bioener. Biomem. *34(5)*, 351–362

Lutsenko, S., and Kaplan, J.H. (1995). Organization of P-type ATPases: significance of structural diversity. Biochem. *34(48)*, 15607–15613

Lytton, J., Westlin, M., Burk, S.E., Shull, G.E., and MacLennan, D.H. (1992). Functional Comparisons between Isoforms of the Sarcoplasmic or Endoplasmic Reticulum Family of Calcium Pumps. J. Biol. Chem. *267(20)*, 14483–14489

Mandal, D., Rulli, S.J., and Rao, R. (2003). Packing interactions between transmembrane helices alter ion selectivity of the yeast Golgi Ca^{2+}/Mn^{2+}-ATPase PMR1. J. Biol. Chem. *278*, 35292–35298

Mano, H. and Fukada, Y. (2006) A median third eye: pineal gland retraces evolution of vertebrate photoreceptive organs. Photochem. Photobiol. *83(1)*, 11–18

Maronde, E., and Stehle, J.H. (2007). The mammalian pineal gland: known facts, unknown facets. Trends Endocr. Metab. *18(4)*, 142–149

Menkes, J.H., Alter, M., Steigleder, G.K., Weakley, D.R., and Sung, J.H. (1962). A sex-linked recessive disorder with retardation of growth, peculiar hair, and focal cerebral and cerebellar degeneration. Pediatrics *29*, 764–779

Mertz, W. (1993). Chromium in Human Nutrition: A Review. J. Nutr. *123(4)*, 626–633

Michael, T.P., and McClung, C.R. (2003) Enhancer trapping reveals widespread circadian clock transcriptional control in *Arabidopsis*. Plant Physiol. *132(2)*, 629–639

Møller, J.V., Lenoir, G., Marchand, C., Montigny, C., Le Maire, M., Toyoshima, C., Juul, B.S., and Champeil, P (2002). Calcium transport by sarcoplasmic reticulum Ca(2+)-ATPase. Role of the A domain and its C-terminal link with the transmembrane region. J. Biol. Chem. *277*, 38647-38659

Molloy, S.A., and Kaplan, J.H. (2009). Copper-dependent Recycling of hCTR1, the Human High Affinity Copper Transporter. J. Biol. Chem. *284*, 29704-29713

Morgan, P.J., Barrett, P., Howell, H.E., and Helliwell, R. (1994). Melatonin receptors: localization, molecular pharmacology and physiological significance. Neurochem. Int. *24(2)*, 101–46

Morin, Y., Tětu. A., and Mercier, G. (1969). Quebec beer-drinkers' cardiomyopathy: Clinical and hemodynamic aspects. Ann. N. Y. Acad. Sci. *156*, 566–576.

Mukhopadhyay, R., Rosen, B.P., Phung, L.T., and Silver, S. (2002). Microbial arsenic: From geocycles to genes and enzymes. FEMS Microbiol. Rev. *26(3)*, 311–325

Nakashima, A.S.; and Dyck, R.H. (2009). Zinc and cortical plasticity. Brain. Res. Rev. *59(2)*, 347–373

Napoli, C., Lemieux, C., and Jorgensen, R (1990). Introduction of a Chimeric Chalcone Synthase Gene into Petunia Results in Reversible Co-Suppression of Homologous Genes in trans. Plant Cell *2(4)*, 279–289

Nevitt. T., Öhrvik, H., and Thiele, D.J. (2012). Charting the travels of copper in eukaryotes from yeast to mammals. Biochim, Biophys. Acta *1823(9)*, 1580–1593.

"NHLBI Workshop: Circadian Clock at the Interface of Lung Health and Disease. April 28-29, 2014 Executive Summary". National Heart, Lung, and Blood Institute.

Nilsson, L., Aden, J., Niemiec, M. S., Nam, K., and Wittung-Stafshede, P. (2013). Small pH and salt variations radically alter the thermal stability of metal-binding domains in the copper transporter, Wilson disease protein. J. Phys. Chem. *B117(42)*, 13038–13050

Nucifora, G., Chu, L., Misra, T.K., and Silver, S. (1989). Cadmium resistance from Staphylococcus aureus plasmid pI258 cadA gene results from a cadmium-efflux ATPase. Proc. Natl. Acad. Sci. *86*, 3544–3548

Nugent, T., Jones, D.T. (2009). Transmembrane protein topology prediction using support vector machines. BMC Bioinf. *10*:159

Ogra, Y., Aoyama, M., and Suzuki, K.T. (2006). Protective role of metallothionein against copper depletion. Arch. Biochem. Biophys. *451*, 112–118

Ogra, Y, Miyayama, T., and Anan, Y. (2010). Effect of glutathione depletion on removal of copper from LEC rat livers by tetrathiomolybdate. J. Inorg. Biochem. *104*, 858–862

Okano, T. and Fukada, Y. (2001) Photoreception and circadian clock system of the chicken pineal gland. Microsc. Res. Tech. *53*, 72–80

Prohaska J.R., Broderius, M., Brokate, B. (2003). Metallochaperone for Cu,Zn-superoxide dismutase (CCS) protein but not mRNA is higher in organs from copper-deficient mice and rats. Arch. Biochem. Biophys. *417*, 227–234

Palmgren, M.G., and Nissen, P. (2011). P-type ATPases. Annu. Rev. Biophys. *40*, 243–266

Panda, S., Antoch, M.P., Miller, B.H., Su, A.I., Schook, A.B., Straume, M., Schultz, P.G., Kay, S.A., Takahashi, J.S. and Hogenesch, J.B. (2002) Coordinated transcription of key pathways in the mouse by the circadian clock. Cell, *109*, 307–320

Pedersen, B.P., Buch-Pedersen, M.J., Morth, J.P., Palmgren, M.G., and Nissen P. (2007) Crystal structure of the plasma membrane proton pump. Nature *450*, 1111–1114

Peirson, S. and Foster, R.G. (2006) Melanopsin: another way of signaling light. Neuron *49*, 331–339

Peñarrubia, L., Andrés-Colás, N., Moreno, J., and Puig, S. (2010). Regulation of copper transport in *Arabidopsis thaliana*: a biochemical oscillator? J. Biol. Inorg. Chem. *15*, 29–36

Petris, M.J., Camakaris, J., Greenough, M., La Fontaine, S. and Mercer, J.F.B. (1998). A C-terminal di-leucine is required for localisation of the Menkes protein in the trans-Golgi network. Hum. Mol. Genet. *7*, 2063-2071

Petrukhin, K., Lutsenko, S., Chernov, I., Ross, B.M., Kaplan, J.H., and Gilliam, T.C. (1994). Characterization of the Wilson disease gene encoding a P-type copper transporting ATPase: genomic organization, alternative splicing, structure/function predictions. Hum. Mol. Genet. *3*, 1647–1656

Pilankatta, R., Lewis, D., Adams, C.M., and Inesi, G. (2009). High Yield Heterologous Expression of Wild-type and Mutant Cu^{+}-ATPase (ATP7B, Wilson Disease Protein) for Functional Characterization of Catalytic Activity and Serine Residues Undergoing Copper-dependent Phosphorylation. J. Biol. Chem. *284(32)*, 21307-21316

Post, R. L., and Sen, A. K. (1965) An Enzymatic Mechanism of Active Sodium and Potassium Transport. J. Histochem. Cytochem. *13*, 105−112

Punter, F.A., and Glerum, D.M. (2003). Mutagenesis reveals a specific role for Cox17p in copper transport to cytochrome oxidase. J. Biol. Chem. *278*, 30875–30880.

Rae, T. D., Schmidt, P. J., Pufahl, R. A., Culotta, V. C., and O'Halloran,T. V. (1999). Undetectable Intracellular Free Copper: The Requirement of a Copper Chaperone for Superoxide Dismutase. Science *284(5415)*, 805–808

Ralph, M. R., Foster, R. G., Davis, F. C., and Menaker, M. (1990) Transplanted suprachiasmatic nucleus determines circadian period. Science *247*, 975–978

Reiter, R.J., Tan, D.X., Terron, M.P., Flores, L.J., and Czarnocki, Z. (2007). Melatonin and its metabolites: new findings regarding their production and their radical scavenging actions. Acta Biochim. Pol. *54(1)*, 1–9

Rensing, C., Ghosh, M., Rosen, BP. (1999). Families of soft-metal-ion-transporting ATPases. J. Bacteriol. *181*, 5891–5897

Scharff O, Foder B. (1978). Reversible shift between two states of Ca^{2+}-ATPase in human erythrocytes mediated by Ca^{2+} and a membrane-bound activator. Biochim. Biophys. Acta *509*, 67–77

Schuschan, M., Bhattacharjee, A., Ben-Tal, N., and Lutsenko, S. (2012). A structural model of the copper ATPase ATP7B to facilitate analysis of Wilson disease-causing mutations and studies of the transport mechanism. Metallomics *4*, 669–678

Sekaran, S., Foster, R. G., Lucas, R. J., and Hankins, M. W. (2003) Calcium imaging reveals a network of intrinsically light-sensitive inner-retinal neurons. Curr. Biol. *13*, 1290–1298.

Singh, K., and Shukla, A.K. (2003) Poly-vinyl alcohol (PVA) and malachite green: a new reagent system for the microdetermination of phosphate in water and wastewater. Indian J. Environ. Health. *45(3)*, 203-208

Sitsel, O., Grønberg, C., Autzen, H.E., Wang, K., Meloni, G., Nissen, P., and Gourdon, P. (2015). Structure and Function of Cu(I)- and Zn(II)-ATPases. Biochemistry *54*, 5673−5683

Solioz, M., and Odermatt, A. (1995). Copper and Silver Transport by CopB-ATPase in Membrane Vesicles of *Enterococcus hirae*. J. Biol. Chem. *270*, 9217–9221

Son, M., and Elliott, J.L. (2014). Mitochondrial defects in transgenic mice expressing Cu,Zn superoxide dismutase mutations: the role of copper chaperone for SOD1. J. Neur. Sci. *336(1-2)*, 1–7

Sørensen, D.M., Buch-Pedersen, M.J., and Palmgren, M.G. (2010). Structural divergence between the two subgroups of P5-ATPases. Biochim. Biophys. Acta *1797*, 846–855

Sørensen, T.L.M, Møller, J.V., and Nissen, P. (2004). Phosphoryl Transfer and Calcium Ion Occlusion in the Calcium Pump. Science *304*, 1672–1675

Srivastava, S, and Goyal, P. (2010). Novel Biomaterials: Decontamination of Toxic Metals from Wastewater. (Springer-Verlag) ISBN 978-3-642-11329-1

Steveson, T.C., Ciccotosto, G.D., Ma, X.M., Müller, G.P., Mains, R.E., and Eipper, B.A. (2003). Menkes protein contributes to the function of peptidylglycine alpha-amidating monooxygenase. Endocrin. *144*, 188 –200.

Stipanuk, M.H. (2006). Biochemical, Physiological & Molecular Aspects of Human Nutrition. (W. B. Saunders Company), pp. 1043–1067. ISBN 978-0-7216-4452-3

Storch, K.F., Lipan, O., Leykin, I., Viswanathan, N., Davis, F.C., Wong, W.H. and Weitz, C.J. (2002) Extensive and divergent circadian gene expression in liver and heart. Nature, *417*, 78–83

Sweadner, K.J. (1985). Enzymatic Properties of Separated Isozymes of the Na,K-ATPase. J. Biol. Chem. *260(21)*, 11508–11513

Tanzi, R.E., Petrukhin, K., Chernov, I., *et al*. (1993). The Wilson disease gene is a copper transporting ATPase with homology to the Menkes disease gene. Nat. Genet. *5*, 344–350

"The Brain from Top to Bottom": The suprachiasmatic nuclei and Pineal Gland, 2015: http://thebrain.mcgill.ca/flash/a/a_11/a_11_cr/a_11_cr_hor/a_11_cr_hor.html

Thierry-Mieg, D., and Thierry-Mieg, J. (2006) AceView: a comprehensive cDNA-supported gene and transcripts annotation, Genome Biol *7*, Suppl 1:S12

Tobler, I., Gaus, S.E., Deboer, T., Achermann, P., Fischer, M., Rulicke, T., Moser, M., Oesch, B., McBride, P.A., and Manson, J.C. (1996). Altered circadian activity rhythms and sleep in mice devoid of prion protein. Nature *380*, 639-642

Tosini, G. and Fukuhara, C. (2003) Photic and circadian regulation of retinal melatonin in mammals. J. Neuroendocrinol. *15*, 364–369

Totoki, Y., Toyoda, A., Takeda, T., Sakaki, Y., Tanaka, A., Yokoyama, S., Ohara, O., Nagase, T. and Kikuno, R.F. (2005). Homo sapiens mRNA for ATPase, Cu++ transporting, beta polypeptide isoform a variant protein. NCBI GenBank Database, AB209461

Towbin, H., Staehelin, T., and Gordon, J. (1979). Electrophoretic transfer of proteins from polyacrylamide gels to nitrocellulose sheets: procedure and some applications. Proc. Natl. Acad. Sci. *76*, 4350-4354

Toyoshima, C., Nakasako, M., Nomura, H., and Ogawa H. (2000). Crystal structure of the calcium pump of sarcoplasmic reticulum at 2.6 Å resolution. Nature *405*, 647–655

Toyoshima, C., and Nomura, H. (2002). Structural changes in the calcium pump accompanying the dissociation of calcium. Nature *418*, 605–611

Tsvikovskii, R., Eisses, J.F., Kaplan, J.H., and Lutsenko S. (2002). Functional Properties of the Copper-transporting ATPase ATP7B (The Wilson's Disease Protein) Expressed in Insect Cells. J. Biol. Chem. *277*, 976-983

Tsvikoskii, R., Efremov, R.G., and Lutsenko, S. (2003) The Role of the Invariant His-1069 in Folding and Function of the Wilson’s Disease Protein, the Human Copper-transporting ATPase ATP7B. J. Biol. Chem. *278*, 13302-13308.

Tsivkovskii, R., MacArthur, B.C., and Lutsenko, S. (2001). The Lys1010 –Lys1325 Fragment of the Wilson's Disease Protein Binds Nucleotides and Interacts with the N-terminal Domain of This Protein in a Copper-dependent Manner. J. Biol. Chem. *276(3)*, 2234–2242

Tsuda, T., and Toyoshima, C. (2009). Nucleotide recognition by CopA, a Cu+-transporting P-type ATPase. Embo J. *28*, 1782-1791

Uthus, E.O. (1992). Evidency for arsenical essentiality, Environ. Geochem. Health *14(2)*, 55–58

Vanderwerf, S.M., Cooper, M.J., Stetsenko, I.V., and Lutsenko, S. (2001). Copper specifically regulates intracellular phosphorylation of the Wilson's disease protein, a human copper-transporting ATPase. J. Biol. Chem. *276*, 36289-36294

Voskoboinik, I., Greenough, M., La Fontaine, S., Mercer, J.F.B., and Camakaris, J. (2001). Functional Studies on the Wilson Copper P-Type ATPase and Toxic Milk Mouse Mutant. Biochem. Biophys. Res. Com. *281*, 966–970

Voskoboinik, I., Brooks, H., Smith, S., Shen, P., and Camakaris, J. (1998). ATP-dependent copper transport by the Menkes protein in membrane vesicles isolated from cultured Chinese hamster ovary cells. FEBS Let. *435(2-3)*, 178–182

Voskoboinik, I., Strausak, D., Greenough, M., Brooks, H., Petris, M., Smith, S., Mercer, J.F., and Camakaris, J. (1999). Functional analysis of the N-terminal CXXC metal-binding motifs in the human Menkes copper-transporting P-type ATPase expressed in cultured mammalian cells. J. Biol. Chem. *274*, 22008-22012

Wan, L., Tsai, C.H., Hsu, C.M., Huang, C.C., Yang, C.C., Liao, C.C., Wu, C.C., Hsu, Y.A., Lee, C.C., Liu, S.C., Lin, W.D., and Tsai, F.J. (2010). Mutation Analysis and Characterization of Alternative Splice Variants of the Wilson Disease Gene ATP7B. Hepatol. 52, 1662–1670

Wu, C., Allen, G.S., Cardozo, T., Stokes, D.L. (2011). The Architecture of CopA from Archeaoglobus fulgidus Studied by Cryo-Electron Microscopy and Computational Docking. Structure *19*, 1219-1232

Wyler-Duda, P. and Solioz, M. (1996). Phosphoenzyme formation by purified, reconstituted copper ATPase of *Enterococcus hirae*. FEBS Lett. *399*, 143-146

Xiao, Z., and Wedd, A.G. (2010). The challenges of determining metal–protein affinities. Nat. Prod. Rep. *27*, 768–789

Xu, C., Rice, W. J., He, W. and Stokes, D. L. (2002). A structural model for the catalytic cycle of Ca^{2+}-ATPase. J. Mol. Biol. *316*, 201–211

Xu, Y., Padiath, Q.S., Shapiro, R.E., Jones, C.R., Wu, S.C., Saigoh, N., Saigoh, K., Ptacek, L.J. and Fu, Y.H. (2005). Functional consequences of a CK1δ mutation causing familial advanced sleep phase syndrome. Nature *434*, 640–644.

Zeng, L., Miller, E.W., Pralle, A., Isacoff, E.Y., and Chang, C.J. (2006). A Selective Turn-On Fluorescent Sensor for Imaging Copper in Living Cells. J. Am. Chem. Soc. *128*, 10-11

Zhang, R., Lahens, N.F., Balance, H.I., Hughes, M.E., and Hogenesch, J.B. (2014). A circadian gene expression atlas in mammals: Implications for biology and medicine. PNAS *111(45)*, 16219–16224

Zmrzljak, U.P., Korenčič, A., Košir, R., Goličnik, M., Sassone-Corsi, P., and Rozman, D. (2013). Inducible cAMP early repressor regulates the *Period1* gene of the hepatic and adrenal clocks. J. Biol. Chem. *288(15)*, 10318–10327